LEBANESE AMERICAN UNIVERSITY

Effect of *Cinnamomum zeylanicum* and *Origanum onites* on the growth and biofilm forming ability of ESBL and non-ESBL producing *Klebsiella pneumoniae*

By

Sara Elias Mitri

A thesis

Submitted in partial fulfillment of the requirements for the degree of Masters of Science in Molecular Biology

School of Arts and Sciences

May 2020

LAU
الجامعة اللبنانية الأميركية
Lebanese American University

THESIS APPROVAL FORM

Student Name: Sara Mitri I.D. #: 201305162

Thesis Title: Effect of Cinnamomum zeylanicum and Origanum onites on the growth and biofilm formin

Program: Graduate

Department: Natural Sciences

School: Arts and Sciences

The undersigned certify that they have examined the final electronic copy of this thesis and approved it in Partial Fulfillment of the requirements for the degree of:

MS in the major of Molecular Biology

Thesis Advisor's Name: Dr. Tarek Nawas

Signature: [redacted] Date: 21 / 05 / 2020
Day Month Year

Committee Member's Name: Dr. Samira Korfali

Signature: [redacted] Date: 21 / 05 / 2020
Day Month Year

Committee Member's Name: Dr. Roy Khalaf

Signature: [redacted] Date: 21 / 05 / 2020
Day Month Year

LAU
الجامعة اللبنانية الأميركية
Lebanese American University

THESIS COPYRIGHT RELEASE FORM

LEBANESE AMERICAN UNIVERSITY NON-EXCLUSIVE DISTRIBUTION LICENSE

By signing and submitting this license, you (the author(s) or copyright owner) grants the Lebanese American University (LAU) the non-exclusive right to reproduce, translate (as defined below), and/or distribute your submission (including the abstract) worldwide in print and electronic formats and in any medium, including but not limited to audio or video. You agree that LAU may, without changing the content, translate the submission to any medium or format for the purpose of preservation. You also agree that LAU may keep more than one copy of this submission for purposes of security, backup and preservation. You represent that the submission is your original work, and that you have the right to grant the rights contained in this license. You also represent that your submission does not, to the best of your knowledge, infringe upon anyone's copyright. If the submission contains material for which you do not hold copyright, you represent that you have obtained the unrestricted permission of the copyright owner to grant LAU the rights required by this license, and that such third-party owned material is clearly identified and acknowledged within the text or content of the submission. IF THE SUBMISSION IS BASED UPON WORK THAT HAS BEEN SPONSORED OR SUPPORTED BY AN AGENCY OR ORGANIZATION OTHER THAN LAU, YOU REPRESENT THAT YOU HAVE FULFILLED ANY RIGHT OF REVIEW OR OTHER OBLIGATIONS REQUIRED BY SUCH CONTRACT OR AGREEMENT. LAU will clearly identify your name(s) as the author(s) or owner(s) of the submission, and will not make any alteration, other than as allowed by this license, to your submission.

Name: Sara Mitri

Signature: 

Date: 21/05/2020

LAU
الجامعة اللبنانية الأميركية
Lebanese American University

PLAGIARISM POLICY COMPLIANCE STATEMENT

I certify that:

1. I have read and understood LAU's Plagiarism Policy.
2. I understand that failure to comply with this Policy can lead to academic and disciplinary actions against me.
3. This work is substantially my own, and to the extent that any part of this work is not my own I have indicated that by acknowledging its sources.

Name: Sara Mitri

Signature: [redacted]

Date: 21/05/2020

Acknowledgement

First, I would like to express my genuine appreciation to my advisor Dr. Tarek Na'was. I will forever be grateful for his continuous support, motivation and guidance. It was an honor working under his supervision. I am also indebted to the committee members Dr. Samira Korfali and Dr. Roy Khalaf for their time and help.

A special thank you to Dr. Elias Akoury and Ms. Sally El Kantar who worked actively to help me in the chemistry part of my project and to Mrs. Sawsan Jabi. My appreciation also extends to my dearest friends and colleagues at LAU and for every member of the microbiology lab, especially Mr. Hrag Dilabazian for his continuous help, support and motivation and to Ms. Patil Babikian. You all made this journey an unforgettable one.

My sincere thanks also go to two special people in my life, Ms. Sara Nasr and Mr. Raed Ayoub. None of this would have been possible without you and your constant encouragement and love. I am also thankful to my MJO family and my dearest friend Ms. Gaelle Guekjian.

Last but not least, I wish to express my deepest gratitude to every member of my family; My father Elia and my mother Christine, to whom I dedicate this work, my siblings Daniel, Youhanna, Samar, Melissa, and Fadi for their love, support and encouragement and to my little niece Nour-Sara and my nephews Elia and James for their never-ending positive vibes.

Effect of *Cinnamomum zeylanicum* and *Origanum onites* on the growth and biofilm forming ability of ESBL and non-ESBL producing *Klebsiella pneumoniae*

Sara Elias Mitri

ABSTRACT

Klebsiella pneumoniae is a leading cause of a wide range of community and hospital-acquired infections. Most *K. pneumoniae* strains have acquired plasmids containing varying set of antimicrobial resistance genes, conferring resistance to nearly all available classes of antibacterials and placing this species among the most defiant pathogens to treat. An important virulence factor of *K. pneumoniae* is its ability to form biofilms, which are communities of microbes attached to an abiotic or biotic surface, including native tissues, medical implants and catheters. In fact, bacterial cells in biofilm are found to be up to 1000-fold more resistant to antibacterials as compared to planktonic cells. Hence the need for discovering alternative treatments. Using medicinal plants and/or their essential oil constituents, in order to prevent and inhibit biofilm formation, was suggested. In this study, *Cinnamomum zeylanicum* and *Origanum onites* methanolic extracts and their major essential oils, cinnamaldehyde, eugenol, thymol and carvacrol, were tested for their ability to inhibit the *K. pneumoniae* biofilm formation. Twenty-six biofilm forming clinical isolates of *K. pneumoniae* were included in this study. Of these isolates, 13 were chosen to produce extended-spectrum β-lactamases (ESBLs), while the remaining 13 were chosen to be non-ESBLs producing. These *K. pneumoniae* isolates were genetically characterized by pulsed-field gel electrophoresis. The antibacterial effects of different concentrations of cinnamon (0.2, 0.15, 0.05 g/ml) and oregano (0.2, 0.15, 0.1, 0.05 and 0.02 g/ml) methanolic extracts were then detected using the standard well diffusion assay. Sublethal concentrations of 0.02 g/ml of *Cinnamomum zeylanicum*

and *Origanum onites* methanolic extracts were later used to test for their ability to inhibit the biofilms formed by the test isolates. Both extracts displayed successful inhibition of *K. pneumoniae* biofilm formation. Gas chromatography-mass spectrometry was then employed to quantify the exact concentrations of the main essential oil constituents of the *C. zeylanicum* (cinnamaldehyde and eugenol) and *O. onites* (thymol and carvacrol) methanolic extracts. The anti-biofilm effect of these essential oils was later tested, in order to check if any of them might have been the chemical responsible for the anti-biofilm effect of the plants' extracts. Moreover, the possibility of demonstrating a synergistic anti-biofilm effect of a combination of cinnamaldehyde and eugenol and another of thymol and carvacrol was tested. The results showed a biofilm inhibitory effect in 46.15% to 62% of the *K. pneumoniae* isolates, upon exposure to the different essential oil solutions, with no synergism noted upon their combination. These natural plant-derived compounds can potentially be used in coating indwelling medical devices to prevent bacterial biofilm formation. Consequently, using them not only will prevent infections, but will also help in minimizing the emergence of antibiotic resistance among pathogens and thus aid in solving one of the most challenging health problems.

Keywords: Biofilm, Carvacrol, Cinnamaldehyde, *Cinnamomum zeylanicum*, ESBLs, Essential oils, Eugenol, *Klebsiella pneumoniae*, *Origanum onites*, Thymol.

TABLE OF CONTENTS

LIST OF TABLES

LIST OF FIGURES

LIST OF ABBREVIATIONS

AIs	Autoinducers
AMR	Antimicrobial resistance
ARGs	Antibiotic resistance genes
ATP	Adenosine triphosphate
BHI	Brain heart infusion
bla	β-lactamase
BSA	Bovine serum albumin
BSIs	Blood stream infections
C	Cinnamon
C. zeylanicum	*Cinnamomum zeylanicum*
CA	Cinnamaldehyde
CAIs	Community Acquired Infections
CA-PLA	Community-acquired pyogenic liver abscesses
CAUTIs	Catheter-associated urinary tract infections
CAZ-30	Ceftazidime (30 μg)
CDC	Centers for disease control and prevention
cKp	Classical *Klebsiella pneumoniae*
CLSI	Clinical and Laboratory Standards Institute
CNS	Central nervous system
CPD-10	Cefpodoxime (10 μg)
CPs	Capsular Polysaccharides
CR	Carvacrol
CRE	Carbapenem-resistant *Enterobacteriaceae*
CTR-30	Ceftriaxone (30 μg)
CTX-30	Cefotaxime (30 μg)
CTX-M	Cefotaxime hydrolyzing capabilities
DCs	Dendritic cells

DNA	Deoxyribonucleotide
E.coli	*Escherichia coli*
eDNA	Extracellular DNA
EDTA	Ethylenediaminetetraacetic acid
EG	Eugenol
EIs	Electron impact
EO	Essential oils
EPS	Extracellular polymeric substance
ESBLs	Extended-spectrum β-lactamases
EtBr	Ethidium bromide
Fe^{3+}	Ferric iron
GC-MS	Gas chromatography-Mass spectrometry
GI	Gastrointestinal
HAIs	Hospital Acquired Infections
HGT	Horizontal gene transfer
hvKp	Hypervirulent *Klebsiella pneumoniae*
I	Intermediate
ICU	Intensive care units
IL	Interleukin
IRFs	Interferon regulatory factors
K. pneumoniae	*Klebsiella pneumoniae*
kb	Kilo base pairs
KPC	Klebsiella *pneumoniae* carbapenemase
Lcn2	Lipocalin-2
LPS	Lipopolysaccharides
MAC	Membrane attack complex
magA	Mucoviscosity-associated gene A
MAPs	Medicinal and aromatic plants
Mb	Mega base pairs
MBLs	Metallo-β-lactamases
MDR	Multi-drug resistant

MGE	Mobile genetic elements
MGEs	Mobile Genetic Elements
MHA	Mueller-Hinton agar
MIC	Minimum Inhibitory Concentration
NDM-1	New Delhi metallo-β-lactamase
NGAL	Neutrophil gelatinase-associated lipocalin
NLRs	Nucleotide binding and oligomerization domain-like receptors
nm	Nanometers
Non-ESBLs	Non- Extended-spectrum β-lactamases
O	Oregano
O. onites	*Origanum onites*
OD	Optical density
OMPs	Outer membrane porins
PAMPs	Pathogen associated molecular patterns
PBPs	Penicillin binding proteins
PBS	1X Phosphate buffer saline
PCR	Polymerase chain reaction
PCR-RFLP	PCR restriction fragment length polymorphism
PFGE	Pulsed field gel electrophoresis
PMNs	Polymorphonuclear leukocytes
PRRs	Pattern recognition receptors
QS	Quorum sensing
R	Resistant
rmpA	Regulator of mucoid phenotype A
RND	Resistance-nodulation-division
RT	Retention Time
S	Susceptible
SD	Standard deviation
SHV	Sulfhydryl variable
SKG	SeaKem Gold
spp	Species

TBE Buffer	Tris-Borate EDTA buffer
TCP	Tissue culture plate method
TE Buffer	Tris-EDTA buffer (0.01M, pH 8)
TEM	Temoniera
TH	Thymol
TIFF	Tagged Image File format
TLRs	Toll-like receptors
TNF- α	Tumor Necrosis Factor alpha
TSA	Trypticase soy agar
TSB	Trypticase soy broth
UTIs	Urinary tract infections
VAP	Ventilator-associated pneumonia
WHO	World health organization
XbaI	Recommended restriction enzyme
XDR	Extremely drug resistant
µl	Microliters

Chapter One

Introduction

1.1. *Klebsiella pneumoniae*

1.1.1. History

In 1882, Friedländer, a German pathologist and microbiologist, isolated an encapsulated bacillus from the lungs of a patient who passed away from pneumonia. Hence, that pathogen was initially designated as *Friedlander's bacillus* (Russo & Marr, 2019). Freidländer's pneumonia is a community-acquired pneumonia affecting mainly immunocompromised individuals (Murphy & Clegg, 2012). Later in 1886, and in honor of the German bacteriologist Edwin Kleb, who was well-known for his important discoveries in medicine and extensive studies on infectious diseases, this bacterium was given the generic name of *Klebsiella* (Ali & Al-kakei, 2019).

At present, the number of validly published species of *Klebsiella* is fifteen including *Klebsiella granulomatis*, *K. michiganensis*, *K. mobilis*, *K. pneumoniae* sp. pneumoniae, *K. pneumoniae* ssp. *ozaenae*, *K. pneumoniae* sp. *rhinoscleromatis*, *K. quasipneumoniae* ssp. *quasipneumoniae*, *K. quasipneumoniae* ssp. *similipneumoniae*, *K. ornithinolytica*, *K. oxytoca*, *K. planticola*, *K. singaporensis*, *K. terrigena*, *K. trevisanii*, *K. variicola*, *K. michiganensis* and *K. quasipneumoniae*. *K. rhinoscleromatis* and *K. ozaenae* species were later reclassified as subspecies of *K. pneumoniae*. Recently, *K. ornithinolytica*, *K. planticola*, *K. terrigena* were moved to the genus *Raoultella* (Ali & Al-kakei, 2019).

Klebsiella pneumoniae and *K. oxytoca* are the clinically most important species of the genus (Podschun, Pietsch, Höller, & Ullmann, 2001; Rodrigues et al., 2019).

1.1.2. Bacterial characteristics

K. pneumoniae is a Gram-negative bacterium that belongs to the phylum Proteobacteria, class Gammaproteobacteria and to the family *Enterobacteriaceae*. This bacterium is related to other genera such as *Escherichia*, *Salmonella*, *Shigella*, and *Yersinia* (Wu, K. et al., 2009). It is important to note that *K. pneumoniae* is one of the most commonly encountered Gram-negative bacteria (Wasfi, Elkhatib, & Ashour, 2016).

It is a rod-shaped, encapsulated, non-motile, lactose-fermenting, non-spore forming and facultative anaerobic bacillus (Bachman et al., 2011). Because of the prominent polysaccharide capsule that is attached to the bacterial outer membrane, *K. pneumoniae* has a mucoid and a glistening phenotype on agar plates (Ali & Al-kakei, 2019).

1.1.3. Colonization and transmission

K. pneumoniae is ubiquitous in nature. It mainly inhabits the environment, specifically soil, sewage, surface waters and medical devices. It can also exist in a variety of plant species, insects and birds. The environment can thus act as a reservoir for human acquisition of this bacterium (Struve & Krogfelt, 2004; Wyres, Lam, & Holt, 2020).

Many studies demonstrated a similarity between *K. pneumoniae* strains that are present in the environment and the ones present in the hospital. In fact, they share similar biochemical patterns, and virulence and pathogenicity techniques (Struve & Krogfelt, 2004).

There are many possible methods of transmission of *K. pneumoniae* in the hospital environment. For instance, it can be transmitted through person-to-person contact among patients and healthcare workers (i.e., doctors and nurses), but can also be acquired from contaminated instruments and surfaces (Martin et al., 2016).

It is important to note that the carrier rate of *K. pneumoniae* is much higher among hospitalized patients as compared to that of the general community. According to Ashurst and Dawson (2019), 77% of hospitalized patients were found to have *K. pneumoniae* in

their stool, whereas only 5% to 38% of people in the community were found to have it (Ashurst & Dawson, 2019).

As such, water, food and person-to-person transmission are all vehicles for the acquisition and consequent colonization of *K. pneumoniae* to humans. Once acquired, this bacterium colonizes the mucosal surfaces in humans, where it can act either as a commensal organism or as a potential pathogen (Wyres et al., 2020). Accordingly, this bacterium can be carried asymptomatically on the skin and in the nose, oropharynx and gastrointestinal tract of healthy individuals (Holt et al., 2015).

The gastrointestinal colonization is the most frequent reservoir among these body sites. Subsequently, in healthy individuals, the detection rate of *K. pneumoniae* in stool samples is higher than its rate in the oropharynx. As a matter of fact, the rate of carriage of *K. pneumoniae* is 5 to 38% in stool samples as compared to 1 to 6% only in the nasopharynx. This is probably due to the non-optimal growth conditions of *Klebsiella* spp. on the human skin. In the hospital settings, these carrier rates increase significantly in direct proportion to the length of stay of the patient (Podschun & Ullmann, 1998).

Many factors can affect the *K. pneumoniae* colonization rate, including whether the patient is infected by a hospital-acquired or community acquired *K. pneumoniae* strain, and whether the patient has undergone a long-term antibiotic treatment. Besides, colonization can only be detected by culture when the density of the microbe surpasses a certain threshold; hence, the bacterial density of a colonizing strain has an important role in the progression to disease (Martin & Bachman, 2018).

1.1.4. From colonization to infection

Many studies have been done to discover whether the infections are caused by *K. pneumoniae* strains carried in the normal flora of the patients. These studies showed around 80% concordance between the colonizing *K. pneumoniae* strains and the infecting strain within infected patients, particularly for urinary tract infections (UTIs) and pneumonia (Martin et al., 2016). However, once the bacterium enters the body, it can display high degrees of virulence and antibiotic resistance (Wyres et al., 2020).

1.1.5. Types of infections

K. pneumoniae used to infect mainly immunocompromised individuals, but recently, and with the emergence of hypervirulent strains, even healthy and immunosufficient individuals have become susceptible to infection by this bacterium (Paczosa & Mecsas, 2016). It is noteworthy that the elderly, neonates, immunocompromised individuals and those with inserted medical devices still have a higher risk of acquiring a *K. pneumoniae* infection. This is mainly caused by the overgrowth and lack of immunological control of commensal *K. pneumoniae* strains (Wyres et al., 2020).

K. pneumoniae is the second most common Gram-negative pathogen, after *Escherichia coli* (*E. coli*). It is associated with diverse serious infections including pneumonia, UTIs, bloodstream infections (BSIs) and surgical wounds infections (Martin et al., 2016; Vading, Nauclér, Kalin, & Giske, 2018).

K. pneumoniae is one of only few Gram-negative rods that can cause primary pneumonia (Choby, Howard-Anderson, & Weiss, 2020). Species of this pathogen can also cause ventilator-associated pneumonia (VAP) in patients in intensive care units (ICUs). It was reported that 7 to 12 % of nosocomial pneumonia cases in ICUs in the United States are caused by *K. pneumoniae* (Guo et al., 2016). On the other hand, the most frequently infected site is the urinary tract, and UTIs caused by this pathogen were especially prevalent among diabetic patients (Martin & Bachman, 2018). Additionally, *K. pneumoniae* can cause catheter-associated UTIs (CAUTIs). This is mainly facilitated by the ability of this bacterium to adhere to the urinary catheters and form biofilm (Schroll, Barken, Krogfelt, & Struve, 2010). Furthermore, it is the second most common cause of Gram-negative bacteremia, after *E. coli*, especially in immunocompromised patients (Zheng et al., 2018). It is worthwhile noting, however, that 13% of all infections caused by *K. pneumoniae* are related to wound or surgical site infections (Martin & Bachman, 2018).

Even with ideal therapy, infection of the lungs by *K. pneumoniae* is found to carry a mortality rate of 30% to 50%, with a worse prognosis in the vulnerable patients' groups (Ashurst & Dawson, 2019).

1.1.6. Classical versus hypervirulent *K. pneumoniae* strains

Classical *K. pneumoniae* (cKp) and hypervirulent *K. pneumoniae* (hvKp) are mainly the two pathotypes that are posing a threat to people's health (Liu & Guo, 2019). Most cKp infections occur in hospitals' environments and long-term care facilities (Pomakova et al., 2012). CKp is an opportunistic bacterium that causes infections in immunocompromised patients (Lee et al., 2017). In contrast, hvKp is more virulent and causes highly invasive community-acquired infections (CAI), also termed hypervirulent *K. pneumoniae* infections (Feldman et al., 2019). Unlike cKp, hvKp usually causes infections in young healthy and immunocompetent individuals (Choby et al., 2020). HvKp infections can also occur in diabetic patients and among individuals of Asian descent (Pomakova et al., 2012).

Historically, *K. pneumoniae* has been traditionally considered an opportunistic pathogen that causes nosocomial infections (Struve et al., 2015). However, in the mid-1980s and 1990s, a distinctive clinical syndrome of community acquired *K. pneumoniae* infection was reported from Taiwan (Marr & Russo, 2019). Healthy patients were diagnosed with community-acquired pyogenic liver abscesses (CA-PLA) and a tendency for metastatic spread for distant sites (Feldman et al., 2019). Eventually, hvKp has become the predominant cause of liver abscesses (Yeh et al., 2007). In fact, CA-PLA account for 80% of all cases of pyogenic liver abscesses that are occurring in Taiwan and Korea (Krapp, Morris, Ozer, & Hauser, 2017). Even though the initial reports of hvKp are from the Asian Pacific Rim, recently this pathogen has emerged worldwide and an increasing number of cases are being reported from the United States, Europe, the Middle East, Africa, Australia, etc… (Shon, Bajwa, & Russo, 2013).

K. pneumoniae species have been identified as the third leading cause of healthcare-associated infections in the United States, after *Clostridium difficile* and S*taphylococcus aureus* (Magill et al., 2014). Additionally, *K. pneumoniae* was considered to be among the eight major infectious bacteria in hospitals, since it was found to be responsible for causing 3 to 7% of all nosocomial bacterial infections in the US (Horan et al., 1988; Podschun & Ullmann, 1998). The most common HAIs, caused by cKp, are pneumonia, urinary tract infections and wound infections that can headway to bacteremia

and endocarditis (Pomakova et al., 2012). Intensive care and oncology patients had a fourfold increased risk of infection (Podschun & Ullmann, 1998). One of the critical features that allowed cKp to be a highly effective healthcare-associated pathogen is its acquisition of antimicrobial resistant determinants, including extended-spectrum β-lactamases (EBSLs) and carbapenemases, making it resistant to many common classes of antibiotics (Khaertynov et al., 2018; Liu & Guo, 2019).

Many bacterial and clinical features defined hvKp and distinguished it from cKp and its traditional infections. First, the unusual sites of infections that were observed such as, pyogenic liver abscess, endophthalmitis, meningitis, bloodstream infections and necrotizing fasciitis (Marr & Russo, 2019). Second, the tendency to metastasize to distant sites including lungs, kidneys, spleen, soft-tissue, skin, eyes, pleura, prostate, bone, joints, muscle/fascia and central nervous system (CNS). Metastasis occurred in around 11 to 80% of the cases (Pomakova et al., 2012). It should be noted that metastatic spread of infection to distant sites was considered a rare characteristic for enteric Gram-negative bacilli. Third, the ability of hvKp to cause serious infections in healthy hosts (Shon et al., 2013). Diabetes and alcoholism, were found to be two risk factors that increased the chance of developing a CAI by hvKp (Piperaki, Syrogiannopoulos, Tzouvelekis, & Daikos, 2017). Fourth, hvKp is characterized by the overproduction of the capsular polysaccharide (CPS), resulting in hypermucoviscous strains (Palacios et al., 2018). Interestingly, hvKp strains used to be more susceptible to antibiotics as compared to cKp (Shon et al., 2013), this shift was probably due to the selective pressure existing in the hospital environment (Martin & Bachman, 2018). A study, done in China in 2016, revealed that only 12.6% of the hvKp strains, that caused many invasive infections, produced ESBLs (Khaertynov et al., 2018). However, with the recent worldwide propagation of mobile genetic elements (MGEs) conferring antibiotic resistance, hvKp are also becoming antibiotic resistant (Lee et al., 2017). Despite the fact that hvKp infections occur in younger individuals, hvKp infections are associated with a high mortality rate, ranging from 3 to 42% (Shon et al., 2013).

1.1.7. *K. pneumoniae* and host defenses

In order for *K. pneumoniae* to establish an infection, it has to first surpass the mechanical and chemical barriers, and escape host humoral and cellular innate immune defenses. Pathogens are usually faced by many mechanical and chemical defenses, such as, mucociliary clearance in the respiratory tract, the flow of urine along with its low pH in the genitourinary tract, peristalsis and the mucus lining of the gastrointestinal tract. In addition, the digestive enzymes, acidic pH and bile also contribute to prevent the attachment and colonization of bacteria in the gastrointestinal tract (Bengoechea & Sa Pessoa, 2019). The pathogen is then subjected to other chemical defenses, mainly the numerous soluble extracellular antimicrobial factors present in the host's serum or within tissues, such as, the complement system, collectins and antimicrobial peptides (Bengoechea & Sa Pessoa, 2019).

Once the bacterium crosses the initial barriers, it has to surmount numerous humoral and cellular innate defenses. To launch these responses, the immune cells, through the germline-encoded pattern recognition receptors (PRRs) of the host, recognize conserved molecules uniquely expressed by the pathogens, referred to as pathogen associated molecular patterns (PAMPs). Among the many distinct classes of PRRs present in mammals, the best-characterized ones belong to the Toll-like receptors (TLRs) and nucleotide binding and oligomerization domain-like receptors (NLRs) families (Regueiro et al., 2011).

Among TLRs, TLR4 are involved in the detection of lipopolysaccharides (LPS) of the pathogens. Among NLRs, NOD1 recognizes a peptidoglycan motif, referred to as g-D-glutamyl-mesodiaminopimelic acid from Gram-negative bacteria (Regueiro et al., 2011). These TLRs are expressed in innate immune cells such as macrophages and dendritic cells (DCs). In addition, some non-immune cells express these receptors such as epithelial cells and fibroblasts (Kawasaki & Kawai, 2014). Upon PAMPs recognition, TLRs initiate signal transduction pathways that lead to the activation of NF-kB, interferon regulatory factors (IRFs) or MAP kinases to regulate the expression of chemokines, cytokines and type I interferon that defend the host from microbial infection (Kawasaki & Kawai, 2014).

Among the first effector cells recruited to the infection site are the polymorphonuclear leukocytes (PMNs), also known as neutrophils, which migrate rapidly to the site of inflammation in order to protect the host and control the acute infection (Lin et al., 2004). Different mediators are engaged in this process, one of which is interleukin (IL)-17. Interleukin-17 is an important cytokine that helps in mediating an effective immune response, mainly through granulopoiesis and neutrophil recruitment. First, IL-8 and IL-23 induce the production of IL-17. Second IL-12, through the production of interferon gamma, also amplifies the expression of IL-17 (Happel et al., 2005).

The host uses many different pathways and mediators in order to control bacterial infections. However, successful pathogens have evolved many different anti-immune strategies to overcome both innate and acquired immunity. Pathogens, including *K. pneumoniae*, work on subverting the fast-acting inflammatory response in order to survive during the early stages of the infection. Hence, they will be able to avoid instant removal by the host defense and increase the chances of forming a critical population size. This is accomplished by modifying PAMPS, the bacterial cell surface molecules', such as peptidoglycan, lipid A of LPS, or flagella, that are usually detected by PRRs in order to become less recognized by the immune surveillance systems, and hence altering the host immune defenses (Finlay & McFadden, 2006; Regueiro et al., 2011).

1.1.8. Virulence of *K. pneumoniae*

Like any other bacterium, *K. pneumoniae* uses many strategies to grow and guard itself from the host immune response. The modus operandi of *K. pneumoniae* seems to be defensive instead of offensive in protecting itself against the host immune response. For instance, *Yersinia* spp. use type III secretion systems to inject toxins to inactivate the phagocytic capability of attacking immune cell. On the other hand, *K. pneumoniae* evades phagocytosis by using its virulence factors, such as the capsule, to make it more difficult for the phagocytes to bind and engulf it instead of actively suppressing the host humoral and cellular immune defenses (Paczosa & Mecsas, 2016).

Apparently, many factors are responsible for the virulence of this bacterium. Some of which include the polysaccharide capsule, lipopolysaccharides, fimbriae (sometimes referred to as pili) and siderophores (Candan & Aksöz, 2015). In addition, outer membrane porins (OMPs), efflux pumps, the enzyme urease and genes related to allantoin metabolism have been recently identified to be involved in the virulence of *K. pneumoniae*. Yet, more work needs to be done to fully comprehend the mechanisms of action and clinical significance of these latter virulence factors.

It is noteworthy, however, that there is a significant amount of heterogeneity in *K. pneumoniae* strains. Different strains express different virulence factors, which can play numerous roles in the pathogenesis of the different *K. pneumoniae* strains (Paczosa & Mecsas, 2016).

1.1.8.1. Polysaccharide capsule (CPS)

Host immune defenses usually perceive bacterial surfaces as complex structures that present many diverse antigenic targets. Bacterial pathogens work on hiding this complicated structure of proteins and carbohydrates from the immune system and PRRs recognition yet exposing adhesins and invasin molecules (Finlay & McFadden, 2006). One mechanism of masking the *K. pneumoniae* surface is to express a carbohydrate capsule. This capsule is an extracellular polysaccharide matrix that encloses *Klebsiella* spp. and is considered to be the most important virulence factor expressed by this bacterium. The composition of this capsule plays a significant role in protecting this bacterium against the host immune defenses and in enhancing its survival within the host (Piperaki et al., 2017; Struve et al., 2015).

The presence of this thick capsule protects *K. pneumoniae* from opsonization, phagocytosis, binding and internalization by macrophages, neutrophils, DCs and epithelial cells (Chung, 2016). This avoidance of bacterial binding and internalization by the immune cells limits early inflammatory signals, resulting in a less firm launching of the immune response. In fact, data shows that *K. pneumoniae* infections do not lead to an early production of cytokines (Regueiro et al., 2011). The capsule can also protect the bacterium

from the bactericidal effect of the host's serum (Chung, 2016; Piperaki et al., 2017). Moreover, this CPS acts as a protective shield against the access of host derived antimicrobial peptides. Free CPS released from *K. pneumoniae* trap these polypeptides aiming to decrease the number of antimicrobial peptides touching the bacterial cell surface (Li, B., Zhao, Liu, Chen, & Zhou, 2014). Also, another study proved that wild-type *K. pneumoniae* does not activate an immune response in airway epithelial cells (Regueiro et al., 2011). Mechanistically, the anti-inflammatory effect of this capsule is characterized by the inhibition of PRRs, mainly TLR2 and TLR4 signaling and NOD1-dependent pathways, thus obstructing IL-8 expression, which plays a role in the granulopoietic response (Li, B. et al., 2014). In addition, this capsule has the ability to impair DC maturation, hence lessen the DC-mediated production of pro-Th1 cytokines like Tumor Necrosis Factor alpha (TNF-α) and IL-12, which will lead to destructive function of immature DCs, thus impairing T-cell activation and weakening the cellular immune response. CPS will work on inhibiting all these immune defenses allowing *K. pneumoniae* to multiply in vivo more easily (Evrard et al., 2010).

For nearly a century, *Klebsiella* spp. have been grouped into different capsular (K) types that differ significantly in pathogenicity and epidemiological relevance. Since 1926, when K typing was initiated, 78 distinct capsular serotypes have been recognized based on the composition and molecular variability of their capsular polysaccharides (Brisse et al., 2013). Biochemical analyses of these capsules show that they are acidic polysaccharides normally formed of repeated subunits of three to six sugars. For instance, K21a, K36 and K50 serotypes contain di-mannose/rhamnose residues, in opposite to K2, K8 and K55 serotypes that do not contain these polysaccharides (Sahly, Keisari, & Ofek, 2009).

While classical *K. pneumoniae* strains produce a capsule that can be any of the 78 serotypes (K1 to K78), the vast majority of hypervirulent *K. pneumoniae* strains belong to serotypes K1 and K2. A study aiming to characterize hvKp strains isolated from four different continents revealed that 93% were K1 strains and the rest were K2 strains (Jun, 2018). Hypervirulent strains particularly of capsular serotypes K1 and K2 have a unique hypermucoviscous phenotype due to excess production of capsular material, forming a relatively large capsule (Piperaki et al., 2017). There are two genes responsible of

enhancing the capsule production of hvKp. The first one is the regulator of mucoid phenotype A (*rmpA*) gene and its isoform *rmpA2*, which are two plasmid-borne transcriptional regulators (Yu et al., 2007). The second is the mucoviscosity-associated gene A (*magA*), which is labeled as the capsule polymerase and is specific for K1 strains (Hunt, Wang, & Callegan, 2011). As compared to classical strains, bacteria with the hypercapsule phenotype, displayed lower levels of interaction with macrophages along with increased resistance to the different humoral defenses, such as complement killing. In addition, these strains were able to steadily escape from neutrophil-mediated intracellular killing then move to distant sites, like the liver, and cause abscess formation. Therefore, the degree of mucoidy appears to be directly correlated to the successful establishment of invasive infections (Jun, 2018; Li, B. et al., 2014).

Because of the technical complexity of the serological method of capsular typing, the difficulty in the production of the necessary reagents and other practical limitations, molecular methods have been developed in order to deduce the K type of the pathogen from genomic sequences. Polymerase chain reaction (PCR) restriction fragment length polymorphisms (PCR-RFLP) or allele-specific PCR amplification are easy to perform. However, these PCRs were essentially developed for serotypes that are frequent in community acquired liver abscess and bacteremia isolates such as K1, K2, K5, K20, K54, and K57 (Brisse et al., 2013).

The *cps* Operon contains all the genes needed for the production of the *K. pneumoniae* capsule. The *cps* gene clusters consist of genes for sugar nucleotide synthesis, capsule repeat-unit synthesis and capsular repeat-unit assembly and export which are involved in the production of the capsule (Shu et al., 2009). *K. pneumoniae cps* gene cluster harbors between 16 to 25 genes expanded on 21 to 30 kilobases (kb). The 5' end of all known *K. pneumoniae* gene clusters consist of six conserved genes (*galF, orf2, wzi, wza, wzb, and wzc*). K-antigen typing is usually done by sequencing the *wzi* locus. The *wzi* gene encodes for the outer membrane protein Wzi, which is engaged in the attachment of the CPS to the outer membrane of the bacterium. Additionally, this capsule is synthesized by the Wzy-dependent polymerization pathway. *wzi* and *wzy* genes exist in all the different capsular types of this pathogen, however, different genes sequences are associated with different K antigen types (Brisse et al., 2013; Jun, 2018).

1.1.8.2. Lipopolysaccharides (LPS)

The second virulence factor present in *K. pneumoniae* is lipopolysaccharide, also known as endotoxin. It is a major component of the outer surface of the Gram-negative cell membrane. Although the LPS structure differs widely between different pathogens, it is usually composed of a highly hydrophobic and conserved lipid A, a core polysaccharide, and the highly variable O-antigen, which is the outermost component (Hsieh et al., 2012). LPS is both an advantage and an obstruction for *K. pneumoniae* in the course of an infection. It helps in the adhesion on the bacterium to mucous layers (Huynh, Kim, & Kim, 2017) and it protects it against the host humoral defenses. On the other hand, LPS can be a robust immune activator. Usually, whenever the host organism senses the presence of lipopolysaccharides, an inflammatory cascade is released. In fact, LPS is recognized as the strongest mediator of septic shock (Ashurst & Dawson, 2019).

Yet, *K. pneumoniae* established different techniques in order to evade the host's immune defenses. For example, some strains may use their capsule to mask their LPS from detection by the immune system and mainly TLR. Studies show that K1, K10 and K16 are some of the serotypes that can mask their LPS, in contrast to the K2 strains that cannot (Merino, Camprubi, Alberti, Benedi, & Tomas, 1992). On the other hand, *K. pneumoniae*, like many other pathogens, tries to modify its LPS to a form that is no longer recognizable by certain immune receptors in order to escape its clearance by the immune system (Opoku-Temeng, Kobayashi, & DeLeo, 2019).

The outermost part of the LPS structure is the O-antigen, which is a polymer of repeating oligosaccharide units. The *wb* gene cluster, previously known as *rfb*, encodes the O-antigen biosynthesis enzymes. The variation in composition and sequence of the sugar monomers has led to the identification of nine *K. pneumoniae* O-antigen clusters, associated to serotypes O1, O2, O2ac, O3, O4, O5, O7, O8 and O12 (Follador et al., 2016; Opoku-Temeng et al., 2019). The seroepidemiology of this bacterium showed that the most prevalent O serotypes for human-host associated isolates are O1, O2 and O3, with O1 being the dominant serogroup in human infections (Follador et al., 2016). Additionally, the length of O antigens affects bacterial survival. Strains expressing full-length O antigens or "smooth LPS" are resistant to complement mediated killing, whereas the ones

that lack or express truncated O chains or "rough LPS" are susceptible to complement-mediated killing. O antigens have the ability to bind and sequester components of the complement system or else prevent their binding to the bacterial surface thus making the microbe resistant to complement-mediated killing (Opoku-Temeng et al., 2019). The O antigen protects against the binding of C1q to the cell surface and hence inhibiting the activation of the classical pathway and the formation of the membrane attack complex (MAC, C5b-C9). Therefore, *K. pneumoniae* with smooth LPS phenotypes obstruct the formation of the MAC on the surface of the bacteria, because the O-antigen bind C3b far away from the bacterial membrane and revoking pore formation (Merino et al., 1992; Opoku-Temeng et al., 2019). Finally, the lack of O antigen could make this bacterium sensitive to complement-mediated killing in the bloodstream hence making the *K. pneumoniae* strain less virulent (Evrard et al., 2010).

The lipid A portion of bacterial LPS is encoded by the *lps* gene cluster. Usually, the lipid A of Gram-negative bacteria is a potent ligand for TLR4. However, certain strains of *K. pneumoniae* demonstrated noticeable plasticity in their lipid A structure. They modified their structure to a degree that is not recognized by the host cells. Modified lipid A does not activate host innate defenses, including resistance to antimicrobial peptides, hence rendering these *Klebsiella* strains more virulent (Finlay & McFadden, 2006; Llobet et al., 2015).

Finally, it is worth noting that the capsule and the lipopolysaccharides of *K. pneumoniae* are not produced independently of each other. The formation of one of these two structure can affect the presence and amount of the other (Clegg & Murphy, 2016).

1.1.8.3. Fimbriae

Frequently pathogens presenting surface capsules, such as *K. pneumoniae*, have filamentous adhesins like fimbriae. These fimbriae can project through the capsule and attach to the host receptors while keeping the bacterial surface hidden (Finlay & McFadden, 2006). Since these fimbriae are stretchable and flexible, *Klebsiella* spp. are capable of reducing the impact of the aqueous and gaseous flushes in the urethra and

respiratory tract respectively, and hence remain attached to host cells. Additionally, due to these fimbriae, some *K. pneumoniae* strains are very sticky and can attach to medical devices (Chen, F. et al., 2011). Type 1 and 3 fimbriae are the most important adhesive structures that have been described as pathogenicity factors in *K. pneumoniae*. These fimbriae facilitate the adherence to epithelial and immune cells as well as to abiotic surfaces. Furthermore, KPF-28 adhesin and Kpc fimbriae are other adhesive structures that were also reported to be present in *K. pneumoniae*, they assist in the adhesion of the bacterium to host cells and colonization of tissues (Wu, C., Huang, Fung, & Peng, 2010).

Type 1 fimbriae are thin, rigid, thread-like protrusions located on bacterial cell surfaces. They are found on most of the members of the *Enterobacteriaceae* family and are expressed in around 90% of *K. pneumoniae* isolates (Murphy, Mortensen, Krogfelt, & Clegg, 2013). Type 1 fimbriae are encoded on *fim* gene cluster, which contain all the genes required for the structure and assembly of these fimbriae. This fimbrial appendage is made up mainly of repeating FimA subunits, which constitute the majority of the structure (Murphy et al., 2013). In addition to this, an adhesin molecule FimH is located at the tip of the fimbriae and is responsible for the adhesive properties of type 1 fimbriae. Hence, through FimH, type 1 fimbriae lengthen beyond the capsule and mediate *K. pneumoniae* adhesion to mannose-containing glycoproteins that are located on many mammalian host tissues, in particular the surfaces of the urinary tract (Schembri, Blom, Krogfelt, & Klemm, 2005). Therefore, the expression of type 1 fimbriae enables *Klebsiella* spp. to attach and colonize the epithelial cells of the urogenital tract leading to the initial establishment of a urinary tract infection (UTI) and to the formation of biofilm in the bladder. Since type 1 fimbriae are not expressed neither in the lungs nor in the gastrointestinal (GI) tract, thus these fimbriae have no effect on the ability of *K. pneumoniae* to infect the lungs or colonize the intestines (Schembri et al., 2005; Schroll et al., 2010).

The second type of fimbriae present in *K. pneumoniae* is type 3 fimbriae. These helix-like filaments are characterized as 2-4 nm wide and 0.5-2 μm long appendages (Schembri et al., 2005). These fimbriae are encoded by the *mrkABCD* gene cluster, which may be chromosome or plasmid borne. The helical fimbrial shaft is encoded by *mrkA*. Besides, the adhesive subunit is located at the tip of the fimbriae and is encoded by *mrkD*

(Murphy & Clegg, 2012). This adhesive subunit facilitates the binding of the bacteria to extracellular proteins such as collagen molecules. Furthermore, they mediate bacterial attachment to many types of cells including the renal tubular cells, the basolateral surfaces of tracheal epithelial cells, components of basement membranes of lung tissues. In contrast to type 1 fimbriae, type 3 fimbriae are "mannose-resistant" and hence they do not bind mannose molecules. Accordingly, type 3 fimbriae assist *K. pneumoniae* in causing respiratory tract infection and have an accessory role in urinary tract infections (Chen, F. et al., 2011). It should be noted, however, that type 3 fimbriae play an important role in *K. pneumoniae* biofilm formation on abiotic surfaces, in addition to surfaces covered with host-derived extracellular matrix proteins (Murphy et al., 2013).

1.1.8.4. Siderophores

Since iron is an essential nutrient for a vast majority of pathogens, these organisms employ a strategy to acquire iron from the host organism, so that they can survive and spread during mammalian infections. The predominant technique used by many bacteria of the *Enterobacteriaceae* family is through the secretion of siderophores. Siderophores are small iron-chelating molecules that display a higher affinity for iron than host transport proteins do (Gomes et al., 2018). After being secreted by the bacteria, siderophores bind ferric iron (Fe^{3+}) with an affinity ten times higher than that of the host's iron acquisition proteins, transferrin or lactoferrin. Siderophores can also scavenge the iron from the environment. Afterwards, the iron-bound siderophores are imported to the bacterium through the outer membrane receptors, and iron is released by different mechanisms (Lawlor, O'Connor, & Miller, 2007). Iron chelation by siderophores could have major effects on host cells, since iron has important roles in different cellular processes, including oxygen metabolism, deoxyribonucleotide (DNA) replication and many cellular reactions (Holden, Breen, Houle, Dozois, & Bachman, 2016).

Four different iron-chelating molecules have been identified in *K. pneumoniae*: enterobactin, yersiniabactin, salmochelin and aerobactin. Every strain can encode several siderophores. Each siderophore contributes to the pathogen virulence in a different way.

Enterobactin is a catecholate siderophore that has the highest affinity for iron (Lam et al., 2018). It is expressed in both classical and hypervirulent *K. pneumoniae* strains. Hence, it is considered the primary siderophore-mediated iron uptake system in *K. pneumoniae*. Eventually, enterobactin has a higher affinity for Fe^{3+} compared to transferrin and lactoferrin, so it can easily scavenge iron from the host. Once formed, the enterobactin-Fe^{3+} complex is imported into the bacterium (Gomes et al., 2018). Enterobactin helps *Klebsiella* spp. in colonization of and dissemination from the lungs. One way of defense used by the host against *K. pneumoniae* infections is the secretion of lipocalin-2 (Lcn2) in order to counter the effect of enterobactin. The innate immune protein lipocalin-2 is also known as neutrophil gelatinase-associated lipocalin (NGAL). Lcn2 has many antibacterial abilities and it is secreted by different cell types such as neutrophils and epithelial cells (Holden et al., 2016). In response to *K. pneumoniae* infection, the host increases the transcription of Lcn2 in the respiratory tract. Lcn2 inhibits the growth of this pathogen by binding and deactivating some of the secreted siderophores, hence preventing bacteria from scavenging the host's iron and finally inhibiting the growth of *K. pneumoniae*. Moreover, increase in the production of lcn2 in the host, leads to an increase in neutrophil recruitment to the site of infection, through the secretion of the chemokine IL-8. Subsequently, in the presence of lnc2, *K. pneumoniae* strains that produce enterobactin solely are cleared (Bachman et al., 2011).

Accordingly, successful pathogens do not depend only on enterobactin for iron acquisition. For instance *K. pneumoniae* usually produce other siderophores such as yersiniabactin, salmochelin and aerobactin that are not subject to lipocalin-2 binding (Bachman, Miller, & Weiser, 2009). Unlike enterobactin, yersiniabactin, salmochelin and aerobactin are much more expressed in hypervirulent *K. pneumoniae* strains. Besides, hypervirulent strains have the ability to produce more siderophores compared to non-virulent strains, which may increase their virulence and pathogenesis (Piperaki et al., 2017).

The second type of siderophore is the phenolate siderophore yersiniabactin. Eighteen percent of the classical *K. pneumoniae* strains and 90% of the hypervirulent *K. pneumoniae* strains express yersiniabactin. It has been reported that this siderophore type is over expressed during lung infections and they help *K. pneumoniae* in maintaining

respiratory infections and causing pneumonia (Bachman et al., 2011). Nevertheless, yersiniabactin is unable to promote growth of *K. pneumoniae* in the presence of serum transferrin. Therefore, *Klebsiella* strains that produce only this siderophore are not able to disseminate from the lungs into the blood, mainly because transferrin is present in plasma (Bachman, Lenio, Schmidt, Oyler, & Weiser, 2012).

The third siderophore type present in *K. pneumoniae* is a glycosylated derivative of enterobactin, known as salmochelin. Plasmid-borne genes encode salmochelin. This large plasmid is not present in most of the classic *K. pneumoniae* strains, a reason why salmochelin is present in only about 2 to 4% of cKp strains. In contrast, salmochelin is much more prevalent in hypervirulent *K. pneumoniae* strains (Jun, 2018; Russo et al., 2014). Due to steric hindrance, salmochelin is not neutralized by lipocalin-2, hence it can enhance *K. pneumoniae* colonization of the nasopharynx (Lam et al., 2018).

The fourth siderophore produced by *Klebsiella* strains is a hydroxamate siderophore called aerobactin. Compared to the other three siderophore types, aerobactin has the lowest affinity for free Fe^{3+} (Lawlor et al., 2007). Like salmochelin, the gene encoding this siderophore is located, in some strains, on a large 200 to 220 kb virulence plasmid that does not exist in most cKp strains. This is why, aerobactin is found in only about 7 to 18% of cKp isolates, but it is present in 93 to 100% of the hvKp strains (Russo et al., 2014). Even though this siderophore is not present in all hypercapsulated strains, the presence of this siderophore is often accompanied with a hypercapsule. Therefore, the presence of aerobactin seems to be a defining trait for hvKp (Li, G., Sun, Zhao, & Sun, 2019).

1.2. *K. pneumoniae* and antimicrobial agents

1.2.1. History of the development of antimicrobial agents and emergence of resistant bacteria

The clinical introduction of antimicrobial agents for the treatment of human infections greatly influenced life on earth. It all started in 1910; when Paul Ehrlich synthesized the first antimicrobial agent in the world to treat syphilis. Later in 1935, Gerhard Domagk and a group of researchers developed a sulfonamide called Prontosil (Saga & Yamaguchi, 2009). Due to the extensive use of Prontosil, the only available and effective antibiotic in the market then, sulfa drug resistance developed (Aminov, 2010). Later, Alexander Fleming discovered penicillin in 1928, but in the 1940s and shortly after the antibiotic came into clinical use, resistance to penicillin started appearing (Saga & Yamaguchi, 2009). During the subsequent two decades, researchers developed a number of new antibiotics, leading to a golden age of antimicrobial chemotherapy between 1950s and 1970s (Aminov, 2010). The overuse, the underuse, and the misuse of antibacterial agents lead to the development of antibiotic resistance in bacteria (Kim, Jo, Chukeatirote, & Ahn, 2016). This increasing clinical incidence of antibiotic resistance is now recognized as a worldwide crisis (Kumar, V. et al., 2011) and the treatment of infections is now considered a major problem (Türkel, Yıldırım, Yazgan, Bilgin, & Başbulut, 2018).

Many factors contributed in the spread of antibiotic resistance, such as, the inappropriate use of antibiotics in the hospitals, the lack of new antimicrobial agents, and finally the transfer of resistance from the now spread resistant microorganisms (Pendleton, Gorman, & Gilmore, 2013). The antimicrobial resistance (AMR) crisis in the hospital setting is driven by the ESKAPE pathogens, which are *Enterococcus faecium*, *Staphylococcus aureus*, *Klebsiella pneumoniae*, *Acinetobacter baumannii*, *Pseudomonas aeruginosa* and *Enterobacter spp*. (Bialek-Davenet et al., 2014). These ESKAPE organisms are environmental and commensal bacteria that lead to opportunistic infections in immunocompromised or hospitalized individuals. Due to their AMR, they have the ability to escape the biocidal actions of antibiotics and to develop resistance to multiple antibiotics (Founou, Founou, & Essack, 2018). Currently around 70% of the pathogens that are responsible for nosocomial infections are resistant to at least one of the most

commonly used drugs for treatment, and some organisms are even resistant to all available antibiotics (Türkel et al., 2018).

Under this antibiotic selective pressure, bacteria are accumulating antibiotic resistance genes (ARGs) by forming new mutations and acquiring successful multiresistant plasmids and transferable genetic elements, leading to the formation of multidrug-resistant (MDR) and extremely drug resistant (XDR) strains with a "super resistome" (Navon-Venezia, Kondratyeva, & Carattoli, 2017). Successful bacterial strains work on effectively disseminating their antibiotic resistance traits. This spread can occur either vertically to their daughter cells, or horizontally, by donating their mobile genetic elements (MGEs), like plasmids and transposons, to other strains, species or genera (Ferreira et al., 2019). The accumulation of many resistance determinants in one bacterial strain can lead to the appearance of pan resistant strains that are untreatable with almost all available antibiotic agents (Wyres & Holt, 2018). In addition, clinical wastes establish the ideal pool for the exchange of resistance genes between hospital and community bacteria, because colonized and infected patients can spread the antibiotic-resistant bacteria they are carrying, along with the active antimicrobial compounds, through their excreta (Sakkas, Bozidis, Ilia, Mpekoulis, & Papadopoulou, 2019).

1.2.2. Emergence of antibiotic resistance in *K. pneumoniae*

1.2.2.1. Introduction

Studies suggest that *K. pneumoniae* has a more diverse DNA composition, greater AMR gene diversity, more plasmid carriage and a wider ecological dispersal than other Gram-negative opportunistic pathogens. The presence of *K. pneumoniae* in different organisms' microbiomes, including humans, increased its exposure to antibiotics and its contact with other nosocomial pathogens, thus enhancing the amplification and spreading of acquired AMR genes (Wyres & Holt, 2018). Most *K. pneumoniae* strains have acquired additional genetic traits and have evolved toward increased levels of antibiotic resistance, rendering this species among the most challenging pathogens to treat (Sakkas et al., 2019). Eventually, many *K. pneumoniae* strains ended up carrying multiple plasmids that contain different sets of AMR genes, resulting in resistance to almost all available classes of

antibiotics (Wyres & Holt, 2016). This resulted in *K. pneumoniae* being responsible for numerous outbreaks in health care settings, leading to high morbidity and mortality rates (Brisse et al., 2013).

1.2.2.2. *K. pneumoniae* genome in progression to disease

K. pneumoniae genomes are usually highly diverse and differ between strains. The core genome, which is shared between almost more than 95% of the isolates, consist of around 2000 genes. However, the accessory genome that differs between the isolates consists of approximately 3500 genes, chosen from a large pool of more than 30,000 gene (Wyres & Holt, 2016). The accessory genome includes chromosomally encoded and plasmid-encoded genes, which code for various ARGs and mechanisms, reducing the susceptibility of this pathogen to many antibiotics. These accessory genes can be obtained through horizontal gene transfer (HGT) between different bacterial species. This diversity between *K. pneumoniae* strains resulted in variable metabolic capacity between the strains, which potentially supplemented them with an additional ecological range thus providing more opportunities for genetic exchange (Martin & Bachman, 2018). Soil was an ideal setting for AMR genes exchange from the environmental or zoonotic pathogens to human bacteria (Pendleton et al., 2013).

Moreover, the mean GC content of *K. pneumoniae* core genes is 58%, while the GC content of the accessory genes is between 20% to 70%. This could indicate that they originated from a taxonomically varied group of donors, hence suggesting that this bacterium received DNA from a broad range of HGT partners (Wyres & Holt, 2018). In fact, analysis of the lowest common ancestor of *K. pneumoniae* has showed more than 20 distinct genera as DNA donors, including other *Enterobacteriaceae* members in addition to other groups such as *Acinetobacter*, *Streptomyces*, *Vibrio*, *Burkholderia*, etc… (Kumar, V. et al., 2011). Additionally, the elevated plasmid load of *K. pneumoniae* with many replicon types is another evidence that this pathogen captured plasmid-borne material from diverse donors present in different niches and can transmit these distinct plasmids to other recipients in human and animal-associated niches (Wyres & Holt, 2018). A more direct evidence for this inter-species HGT in *K. pneumoniae* was presented by comparing

carbapenem-resistant *Enterobacteriaceae* in the healthcare environment. Eventually, the same ward or patient showed identical or highly similar carbapenemase encoding plasmids and transposons, from *K. pneumoniae*, *E. coli*. *Citrobacter freundii* and other species (Wyres & Holt, 2016). This interspecies and intraspecies transmission of, plasmids and insertion elements, is facilitated by the close genetic association of members of the family *Enterobacteriaceae* (Kumar, V. et al., 2011).

It is noteworthy that several new mobile AMR genes, such as carbapenem-resistance genes (KPC), OXA-48 and NDM-1, were first discovered in *K. pneumoniae* before their spreading to other clinically relevant Gram-negative bacteria. Combining all of these factors together shows that this pathogen is a key amplifier and spreader of many important AMR genes (Wyres & Holt, 2016).

K. pneumoniae harbors many resistance mechanisms against the different classes of antibiotics. First, the release of antibiotic inactivating enzymes such as the extended-spectrum β-lactamases, oxacillinases and metallo-β-lactamases that can degrade β-lactam antibiotics. Particularly, several enzymes target and cleave the chemical bonds, such as amides and esters, that are present in antibiotics. Second, mutations of antibiotic target sites. Third, modification in membrane proteins and membrane permeability. Fourth, activation of efflux pump systems, which belong to the resistance-nodulation-division (RND) family, and can actively force out charged and amphiphilic antibiotics including such as fluoroquinolones, aminoglycosides and β-lactams . Fifth, alteration of metabolic pathways (Kim et al., 2016).

1.2.3. β-lactam antibiotics and emergence of ESBLs in *K. pneumoniae*

1.2.3.1. β-lactams

β-lactam antibiotics are the dominant class of antibiotics used for the treatment of bacterial infections (Ierardi et al., 2017). There are hundred different β-lactams. These antibiotics are classified into different groups based on their structure. Penicillins, cephalosporins, carbapenems and monobactams are the most clinically important β-lactams (Palzkill, 2013). The β-lactams class of antibiotics is mainly characterized by

possessing a four-membered β-lactam ring, in the common structure, that acts as a substrate for the transpeptidase target enzymes. β-lactams inhibit a set of transpeptidase enzymes, also known as penicillin binding proteins (PBPs), that play a major role in the synthesis of the peptidoglycan layer of the bacterial cell wall (Gharrah, Mostafa El-Mahdy, & Barwa, 2017; Palzkill, 2013). Since the peptidoglycan layer is the outermost components of the bacterial cell wall, hence it is essential for the integrity of the cell wall structure. Interfering with the peptidoglycan synthesis will lead to osmotic instability or autolysis, causing modification in the surface morphology and structure of the bacteria, finally leading to the death of the bacteria. This describes the mechanism behind the antimicrobial effect of β-lactam antibiotics (Ierardi et al., 2017).

Unfortunately, these β-lactams can be deactivated. There are several mechanisms used by *K. pneumoniae* to acquire resistance to these antibiotics. First, the production of β-lactamases, followed by reducing permeability and then expulsion by efflux pumps (Türkel et al., 2018) The principal mechanism of resistance to oxyimino-cephalosporins in ESKAPE pathogens, is the production of extended-spectrum β-lactamases (ESBLs) enzymes (Founou et al., 2018).

1.2.3.2. Genetic basic of resistance

ESBLs production is one of the most predominant antibiotic resistance mechanisms in Gram-negative bacilli (Ojdana et al., 2014). This resistance usually depends on the expression of β-lactamase (*bla*) genes, which may be located on transferable elements including plasmids and transposons (Cantón, González-Alba, & Galán, 2012).

Historically, in 1960s the first two mobile β-lactamase resistant genes, $bla_{\text{SHV-1}}$ and $bla_{\text{TEM-1}}$, were identified in Gram-negative bacteria causing penicillin resistance. *K. pneumoniae* usually have Sulfhydryl variable (SHV)-1 as part of their core genome hence they are intrinsically resistant to ampicillin. In fact, ampicillin resistance is a hallmark of *K. pneumoniae* species. Other β-lactamases, including Temoniera (TEM)-1 are part of their accessory genome (Gharrah et al., 2017; Martin & Bachman, 2018). TEMs and SHVs

plasmids were found to be active against penicillins and narrow spectrum cephalosporins, like cefazolin or cephalothin, but did not hydrolyze higher generation cephalosporines with oxyimino side chains, particularly ceftazidime, ceftriaxone, cefotaxime or cefepime (Padmini, Ajilda, Sivakumar, & Selvakumar, 2017).

Due to the increasing prevalence of ampicillin-hydrolyzing β-lactamases in Gram-negative pathogens, mainly in *Enterobacteriaceae*, third generation cephalosporins gained extensive clinical use in the early 1980s (D'Andrea, Arena, Pallecchi, & Rossolini, 2013). After launching these third generation cephalosporins for clinical use, ESBLs genes encoding resistance to these antibiotics began to appear. In 1985, the first extended-spectrum β-lactamase (ESBL) gene $bla_{\text{SHV-2}}$ was identified in *K. pneumoniae*. Also, $bla_{\text{TEM-3}}$ (1984) and bla_{CMY-1} (1989), other plasmid-mediated ESBL variants, were also reported for this pathogen before their spreading into other Gram-negative pathogens (Wyres & Holt, 2018).

Later, the plasmid encoding the CTX-M ESBL genes, bla_{CTX-M}, became the most prevalent in environmental bacterial isolates (Chong, Shimoda, & Shimono, 2018). CTX-M are much more active against cefotaxime and ceftriaxone than ceftazidime (Zeynudin et al., 2018). CTX-M ESBLs were first detected in late 1989 in *E.coli*, in a newborn ear exudate, and then in early 1990s in *K. pneumoniae* (Mazzariol, Bazaj, & Cornaglia, 2017). Since CTX-M enzymes have disseminated rapidly, they are now among the most prevalent ESBLs worldwide (D'Andrea et al., 2013). A study proved that around 100, 96, and 84% of ESBL producing *K. pneumoniae* isolates harbored *CTX-M-15*, *SHV*, and *TEM* genes respectively (Gharrah et al., 2017).

In the 1990s newer groups of antimicrobials known as the carbapenems and fluoroquinolones were introduced. It was noted then that these carbapenems were resistant to CTX-M enzymes (D'Andrea et al., 2013). However soon after they were found, resistance genes called carbapenamases started to appear in different organisms, with *K. pneumoniae* playing a major role. Eventually, *qnrA* and *qnrB*, the two mobile quinolone resistance genes, were first recognized in 1998 in a *K. pneumoniae* isolate (Tamang et al., 2008).

Eventually, many *K. pneumoniae* strains expressed ESBLs and carbapenemases simultaneously. These strains are considered, by the World Health Organization (WHO), as a critical public health threat (Bialek-Davenet et al., 2014).

1.3. *K. pneumoniae* biofilm formation

1.3.1. Introduction

K. pneumoniae is well known for its ability to form a biofilm as one of its important virulence factors, allowing it to attach to biotic and abiotic surfaces (Nirwati et al., 2019). A biofilm is a structured community of microbial cells that are embedded in a self-produced extracellular matrix and attached to a surface and to each other (Thieme et al., 2019).

In most biofilms, bacterial cells make up around 10% of the total biofilm mass, while the matrix account for the rest 90% (Flemming & Wingender, 2010). The matrix is the extracellular material and it is mainly produced by the microorganisms themselves. It consists of a combination of different types of biopolymers, including polysaccharides, proteins and extracellular DNA (eDNA) and it known as extracellular polymeric substance (EPS) (Desai, Sanghrajka, & Gajjar, 2019). Hence, the EPS surround the cells in a biofilm and constitute their immediate environment. This matrix forms the scaffold for the three dimensional architecture of biofilm and is responsible for the cohesion in the biofilm and its adhesion to surfaces (Flemming & Wingender, 2010).

1.3.2. EPS composition and function

The major portion of the EPS are the exopolysaccharides. They are heteropolysaccharides consisting of a combination of charged and neutral sugar residues and are secreted by the microorganism to the surrounding environment. Exopolysaccharides also contain inorganic and organic substituents that affect their biological and physical properties. Exopolysaccharides are responsible of the mechanical stability of the biofilm. It is noteworthy that these polysaccharides can differ between

strains of the same species. Alginate is one of the most studied polysaccharides and are involved in biofilm formation. A study showed that bacterial mutants that cannot synthesize exopolysaccharides are severely compromised or incapable of forming biofilms, hence their importance in biofilm formation (Bellich et al., 2018).

The matrix also contain significant amounts of proteins. Numerous extracellular enzymes were detected in biofilms. Some of them are involved in the degradation of biopolymers within a biofilm. The enzymes' substrates include water-soluble polymers such as polysaccharide, proteins and nucleic acids, plus water-insoluble polymers such as cellulose and lipids, in addition to other organic particles that are trapped in the EPS matrix. Hence, these enzymes make the matrix an external digestive system that can break down biopolymers and provide carbon and energy sources to the biofilm cells. The detachment and dispersal of sessile, or adherent, bacteria from biofilms also requires enzymes (Rabin et al., 2015). The matrix also contains structural or non-enzymatic proteins such as lectins, also known as the cell surface-associated and extracellular carbohydrate-binding proteins, that participate in the development and stabilization of the polysaccharide matrix network and set up a link between the bacterial cell surface and extracellular EPS. Additionally, other cell surface proteins, including pili and fimbriae, participate in the initial attachment to surfaces and in interacting with other components of the biofilm matrix (Fong & Yildiz, 2015).

Mattick *et al*. (2002) proved that the extracellular DNAs (eDNAs) are actively secreted and are not only leftovers from lysed cells. DNase I could prevent *K. pneumoniae* biofilm formation. Therefore, eDNAs have an important role in biofilm formation and particularly biofilm attachment. In the initial attachment, the negative charge of eDNAs works as repulse force. However, when the distance between the bacterial cells and the surface increases, to few nanometers, eDNAs interact with receptors on the surface to facilitate adhesion. Hence, they could function as an intercellular connector. In addition, and also due to their negative charge, eDNAs chelate metal cations and some positively charged antibiotics (Okshevsky, Regina, & Meyer, 2014; Whitchurch, Tolker-Nielsen, Ragas, & Mattick, 2002).

Lipids and surfactants are the hydrophobic molecules existing in the biofilm matrix. These hydrophobic properties of the EPS were attributed to substituents such as polysaccharide-linked methyl and acetyl groups, which helps in the adhesion of microorganisms to hydrophobic surfaces. Biosurfactants, promote the initial formation of microcolonies on a surface. Finally, water is by far the largest component of the matrix. The EPS matrix present a highly hydrated environment that dries slower that its environment, thus protecting the biofilm cells against variations in water potential and desiccation (Flemming & Wingender, 2010).

The extracellular polymeric substance also encloses and immobilizes microbial aggregates. These biopolymers are the reason behind the macroscopic appearance of a biofilm, they are also referred to as slime. EPS keeps biofilm cells in close proximity hence allowing interactions and cell to cell communication and then formation of a synergistic microbial consortium. The matrix keeps all the components of lysed cells including DNA, which may be an important reservoir of genes, leading to horizontal gene transfer between bacterial isolates. Due to competition in the confined space of the EPS matrix, there is a constant adaptation of population fitness, favoring polymer producers at the expense of non-producers. It is interesting to note that this EPS matrix varies greatly between different biofilms, depending on the bacteria present, the shear forces experienced, the availability of nutrients and the temperature (Flemming & Wingender, 2010; Ramos-Vivas et al., 2019).

1.3.3. Advantages of biofilm formation

Many bacteria can switch between the planktonic form, which is the free-living bacteria, and the sessile form, which is the attached form (Surgers, Boyd, Girard, Arlet, & Decré, 2019). The planktonic bacteria usually have high cell growth and reproduction rates. However, the biofilm state seems to be the natural predominant state of bacteria. There are several benefits for bacteria within biofilms when compared to planktonic bacteria. Eventually, biofilm formation has been an important stage in the pathogenesis of many bacterial infections (Singla, Harjai, & Chhibber, 2013). First, biofilms protect enclosed bacterial cells against the host immune system along with adequate antibiotic

therapy, leading to treatment failure, recurring infection and increased mortality and morbidity (Thieme et al., 2019). In addition, biofilms reduce the bacterial growth rate, lead to the development of persister cells and increase the probability of genetic exchange (Surgers et al., 2019). Sessile bacteria can tolerate many environmental challenges such as UV exposure, acid exposure, dehydration and salinity and metal toxicity (Hall-Stoodley, Costerton, & Stoodley, 2004).

1.3.4. Biofilm infections and medical biomaterials

Growing in biofilm enhances the survival of microorganisms in the healthcare settings and inside patients, augmenting the probability of causing nosocomial infections (Ramos-Vivas et al., 2019). In fact, biofilms play a role in up to 60% to 80% of chronic human infections (Abdi-Ali, Mohammadi-Mehr, & Agha Alaei, 2006). The high capacity of *K. pneumoniae* to form a biofilm and hence to colonize tissues and biomaterials is a main factor contributing to the development of hospital-acquired infection (Guilhen et al., 2019).

The medical devices' surfaces serve as a substrate for biofilm formation. This was noted first in the early 1980s, when electron microscopy showed bacteria deposited on the surface of indwelling medical devices, including cardiac catheters and intravenous pacemakers (Hall-Stoodley et al., 2004). Implant-associated biofilms cause infection and disturb the normal functioning of the device on which they form (Nandakumar, Chittaranjan, Kurian, & Doble, 2013). The extent of biofilm formation and the severity of the infection vary depending on the location of the biomaterial, the physio-chemical properties of the medical device surface and the duration of the implant. At some point during their hospitalization, up to 50% of the patients will be catheterized. This will severely increase the patients' possibility of colonization by bacteria, which occurs in 5–10% of the patients at each day of catheterization (Stahlhut, Struve, Krogfelt, & Reisner, 2012).

K. pneumoniae are able to form biofilms on implant devices, including catheters and endotracheal tubing and then colonizing human tissues. According to Alcántar-Curiel

et al. (2013), 80% of the *K. pneumoniae* were able to form biofilms on glass or plastic surfaces (Alcántar-Curiel et al., 2013). At first *K. pneumoniae* forms biofilms of single or multiple species, but with the increase of implant duration they certainly develop into a multispecies biofilms (Nandakumar et al., 2013).

Indwelling urinary catheters are still commonly used in daily hospital urological practices. The presence of an indwelling urinary catheter provides an inert surface for bacterial attachment and hence enhancing microbial colonization and biofilm development (Djeribi, Bouchloukh, Jouenne, & Menaa, 2012). Nosocomial catheter-associated urinary tract infections (CAUTIs) are the most recurrent complication associated with these devices. *K. pneumoniae* is one of the frequent microorganisms that cause CAUTIs (Stahlhut et al., 2012). In chronic conditions, such as urolithiasis, biofilms play a major role in the persistence and recurrence of an infection (Ramos-Vivas et al., 2019).

1.3.5. Process of biofilm formation

Biofilm formation proceeds as a regulated developmental sequence composed of five stages (Hall-Stoodley et al., 2004), as illustrated in figure 1.

Bacteria approaching a biotic or an abiotic surface is a prerequisite for biofilm formation. As the bacterium comes nearer to the surface, several attractive and repulsive forces, come into play. At 10 to 20 nm from the surface, the bacterial surface negative charges are repelled by the negative charges of most environmental surfaces. However, attractive van der Waals forces can overcome this repulsion between the bacteria and the surface. Additionally, fimbriae and flagella help in the mechanical attachment of the bacteria to the surface (Rabin et al., 2015).

Stages one and two of the process are identified by a loose association of the free floating microorganisms with the surface followed by a robust adhesion (Wang, Wilksch, Strugnell, & Gee, 2015). The initial reversible attachment depends on electrostatic, van der Waals and other nonbonded forces of attraction between the bacteria and the surface. Whereas in the irreversible attachment cell surface hydrophobicity and surface

projections, such as fimbriae and pili, play an important role. Afterwards, the bacteria start forming a monolayer and start secreting the extracellular matrix, which will aggregate in the slime layer, leading to an irreversible attachment and formation of a base film (Nandakumar et al., 2013).

Stages three and four include the aggregation of the bacterial cells into microcolonies and subsequent growth and maturation. Once the first layer of the biofilm is established, bacteria of the same or different species are recruited to the biofilm from the bulk fluid. The biofilm develops from a thin flat layer into a mushroom-shaped or tower-shaped structure (Hall-Stoodley et al., 2004). In a thick biofilm, containing more than 100 layers, bacteria are organized depending on their metabolism and aero tolerance; hence, anaerobic bacteria will be located in deeper layers avoiding O_2. During biofilm maturation, the trapped bacteria secrete more proteins, polysaccharide, DNA, and other biofilm scaffolds into the biofilm. The presence of fluid filled channels in the mature biofilm guarantees the transport of nutrients to all the bacterial cells inside the film, especially the ones located at the bottom (Rabin et al., 2015).

Stage five is the last stage of biofilm formation. It is characterized by the detachment and dispersal of bacterial cells as planktonic cells, which will potentially initiate a new cycle of biofilm formation at new niches, leading to systemic infection (Rabin et al., 2015). Many factors contribute to induce the dispersion of bacterial cells, such as, increased fluid shear, nutrient starvation, intense competition or outgrown populations. Dispersal could occur in the whole biofilm or just part of it. There are three different biofilm dispersal strategies. First, swarming dispersal in which individual bacterial cells are released from a microcolony into the bulk fluid or the surrounding surfaces. Second, clumping dispersal, in which whole aggregates, containing biofilm cells surrounded by EPS, are shed from biofilm as clumps or emboli. Third, surface dispersal in which whole biofilms move across surfaces (Hall-Stoodley et al., 2004). These biofilm-dispersed cells have unique properties, that differ from planktonic and sessile bacteria. These cells are metabolically active and have enhanced colonization abilities. In addition, these cells have the capacity to rapidly form large microcolonies and to escape the immune system. Particularly, *K. pneumoniae* dispersed cells could impair phagosome maturation (Guilhen et al., 2019).

It is noteworthy that *K. pneumoniae* biofilms have demonstrated a heterogeneous nature, with the bacteria present on the peripheral areas of a biofilm, showing a higher activity as compared to the ones situated in the middle of the consortium (Ribeiro, Cardoso, Cândido, & Franco, 2016).

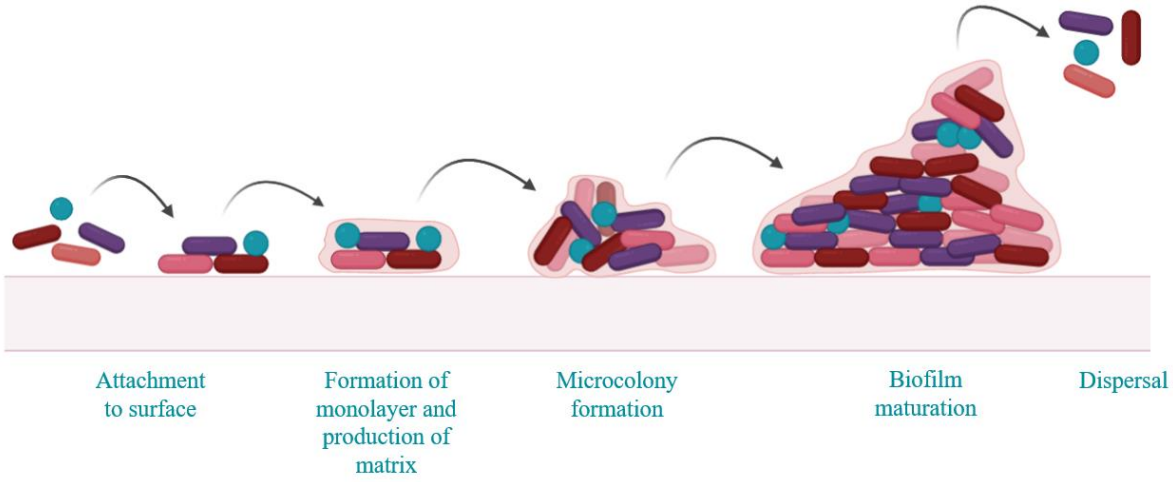

Figure 1: Steps of biofilm formation.

1.3.6. Factors influencing biofilm formation

Three important factors could affect biofilm formation: the nature of the bacterium, the host and the surface properties of the material on which the biofilm will form.

First, in the adhesion stage, the type of the adhesins secreted by the colonizing organisms and that are involved in the biofilm formation could affect the adhesion process and hence could lead to the restriction of the whole process (Desai et al., 2019). In addition, cell-to-cell communication inside the biofilm can affect the maturation stage of the biofilm. Cell-to-cell communication between bacterial cells is usually regulated by quorum sensing (QS). QS appears to be mediated by small chemical signaling molecules named pheromones or autoinducers (AIs). When the bacterial cell density increases and becomes above a threshold concentration, bacteria secrete these AIs. When produced, these pheromones are capable of performing a cell density-dependent regulation of bacterial gene expression, hence influencing bacterial adhesion and motility, transport, stress response and EPS synthesis, which are all intrinsically engaged in biofilm

formation. The intracellular release of AI-2 regulatory molecules, in *K. pneumoniae*, contributes to biofilm formation (Balestrino, Haagensen, Rich, & Forestier, 2005; Ribeiro et al., 2016).

Second, the host state generally can contribute to the biofilm formation and infection, especially in immunocompromised patients. Also, predisposing factors such as the existence of indwelling medical devices or the presence of other systemic diseases including diabetes mellitus, chronic renal failure, etc… will most definitely increase the odds of acquiring a biofilm-associated infection. On the other hand, after adhering to a surface, bacterial cells gain access to the host binding molecules, such as the components of blood plasma, fibrinogen, fibronectin and host extracellular matrix. Eventually, host factors can act as mediators in the adhesion of the bacterium, by providing specific and non-specific sites for bacterial adhesins' binding. This will increase the density of bacteria tremendously within 24 hours (de Avila, de Molon, Vergani, de Assis Mollo, Jr, Francisco, & Salih, 2014; Nandakumar et al., 2013).

Third, the surface characteristics of the implant, including its hydrophobicity and roughness, in addition to its chemical composition and design also greatly affect the attachment of bacteria and hence biofilm formation and the thickness of the biofilm (de Avila et al., 2014).

1.3.7. *K. pneumoniae* virulence factors function in biofilm formation

As it was already mentioned, adhesins located on the bacterial surface play an important role in the attachment of the bacteria to biotic and abiotic surfaces. Particularly, fimbriae type 1 and type 3 are present on *K. pneumoniae* surface. In addition to their role in surface attachment and biofilm formation, they also play a role in inter-bacterial aggregation. Both types of fimbria-encoding operons, are found in and expressed by nearly all *K. pneumoniae* strains in biofilm state (Desai et al., 2019). These fimbriae are not only important in the initial step of biofilm formation, but they also play a role during biofilm maturation (Ribeiro et al., 2016). In *K. pneumoniae* type 3 fimbriae play a role in maintaining the fluidity of the CPs. This is done by decreasing hydrogen-bonding

interconnection between the CPs molecules. This fluidity is important for good cell adhesion to surfaces and well-organized biofilm formation in these *Klebsiella* spp. (Wang et al., 2015). The absence of type 1 and type 3 fimbriae attenuates the ability of *K. pneumoniae* to form biofilm (Stahlhut et al., 2012).

Polysaccharide capsules also play a significant role in biofilm formation (Balestrino, Ghigo, Charbonnel, Haagensen, & Forestier, 2008). They protect *K. pneumoniae* from stressful environmental conditions including detergents, dryness and attacking the host immune system. Additionally, they can affect the architecture of *K. pneumoniae* biofilms (Ribeiro et al., 2016).

Interestingly, *K. pneumoniae* biofilm dispersed cells and sessile cells down-regulate the expression of all siderophores encoding genes. Suggesting that these cells down regulate yersiniabactin, enterobactin, salmochelin and aerobactin expression in order to hide from the host immune system and escape any strong proinflammatory response (Guilhen et al., 2019).

1.3.8. Biofilm antibiotic resistance

One of the resistance mechanisms used by bacteria, including *K. pneumoniae*, to endure the presence of antimicrobial agents, is the formation of biofilms embedded in an EPS matrix (Surgers et al., 2019). In fact, biofilm cells are up to 1000-fold more resistant to antibiotics than planktonic cells (Cepas et al., 2019). Therefore, the presence of biofilms drive the failure of antimicrobial treatments (Fu et al., 2018) The bactericidal dose of the different antibiotics specified by the Clinical and Laboratory Standards Institute (CLSI) method for free-floating bacteria is ineffective on bacteria present in biofilms (Singla et al., 2013). Eventually, if we compare the doses needed to eradicate sessile bacteria as compared to planktonic ones, in the same environment, much higher concentrations of antibiotics are needed to kill sessile bacteria (Thieme et al., 2019). *K. pneumoniae* biofilms comprising antibiotic resistant strains are much more tolerant to biocidal agents as compared to antibiotic susceptible isolates (Ribeiro et al., 2016). Resistance usually varies

between one specie and another and even between different strains of the same species. Many mechanisms explain this variation.

The first reason behind antibiotic resistance of a biofilm is the permeability barrier created by the EPS matrix. The matrix composition will lead to limited penetration of some antimicrobial agents, and dilution to sublethal doses of others, such as bleach, superoxides, metals and immunoglobulins, before reaching all of the single bacterial cells inside the biofilm (Singla et al., 2013). Alginate, an important polysaccharide present in the EPS, also plays an important role in rendering antibiotics ineffective against bacteria (Abdi-Ali et al., 2006).

Second, the limited nutrient supply to the cells that are embedded deep within the biofilms, lead to a decrease in the metabolic activity of these bacterial cells. The presence of bacterial cells in this stationary phase dormancy and their slow growth leads to resistance to many classes of antibiotics (Abdi-Ali et al., 2006). Since antibiotics work by disrupting different microbial mechanisms, hence they need some degree of cellular activity to become effective. For instance, β-lactams usually kill cells by interrupting the synthesis of their cell wall. During dormancy, β-lactam antibiotics will not be able to inhibit bacterial cells within the biofilm, this process is known as phenotypic tolerance. In addition, penicillin-binding proteins are rarely expressed in dormant microorganisms. Therefore, piperacillin, for example, will be unable to inhibit biofilm cells (Singla et al., 2013).

One percent of the bacterial cell population in any biofilm is composed of persister cells. Persisters downregulate the biosynthetic genes and their growth rate is almost zero. They slowly absorb any compound and hence can tolerate the toxic effects of antibiotics. Once the antibiotic stress is removed, persister cells will reactivate into infectious particles leading to recurrence of the infection (Rabin et al., 2015).

The direct proximity between bacterial cells inside a biofilm, increases the chances of horizontal gene transfer between the isolates. Eventually, the high cell density biofilms have a high concentration of DNA, which paves the way for transformation to other susceptible strains thus leading to increased antibiotic resistance inside the biofilm (Nandakumar et al., 2013).

It was reported that older biofilms have the ability to resist higher antimicrobial agent concentrations. This is due to the higher amount of EPS present in older biofilms. Thus, the age of the biofilm also influences the success or the failure of a therapeutic regimen. Therefore, early initiation of the antibiotic treatment of biofilm forming bacteria is essential (Singla et al., 2013).

Finally, it should be noted that acquiring antimicrobial resistance in many Gram-negative bacterial species can enhance biofilm formation. However, if we compare MDR strains to non multidrug resistant strains we can notice that MDRs do not have higher biofilm production ability (Cepas et al., 2019).

1.4. Medicinal plants

1.4.1. Introduction

Ethnobotany and medicinal plants are a main source of new medications and may prove valuable as alternatives to usual drugs (Al-Mariri & Safi, 2014). Currently, more than 80% of the world's population use traditional plant-based medications to treat different health problems and diseases. The WHO reported that the majority of the global population rely on plant-based herbal medications for treating different illnesses (Prabuseenivasan, Jayakumar, & Ignacimuthu, 2006). In fact, more than 9000 native plants have been identified for their curative medicinal properties (Swamy, Akhtar, & Sinniah, 2016).

Medicinal and aromatic plants (MAPs) synthesize a huge collection of secondary metabolites called phytochemicals. These phytochemicals are not necessary for the plant's physiological functions, but they are used to protect them from microbial pathogens. Many of these bioactive compounds have confirmed their prospects as antimicrobials, including essential oils (EO) (Borges, Abreu, Malheiro, Saavedra, & Simõe, 2013).

Essential oils are multifarious mixtures of volatile compounds that are obtained from plant materials including flowers, buds, leaves, bark, etc… They are aromatic in nature. Their special odor and bioactive characteristics depend on their chemical constituents that belong to many chemical families such as aldehydes, phenols, ketones,

alcohols, terpenes and esters. It is noteworthy, that the chemical analysis of EOs of specific plants, shows that they contain mainly 2 to 3 major, highly concentrated, constituents accounting for 20 to 70% while the other constituents exist in trace amounts (Swamy et al., 2016).

For a long time, these aromatic oils have been used in food preservation, pharmaceuticals and medicine (Al-Mariri & Safi, 2014). EOs are deemed as potential therapeutic agents for a variety of diseases including cardiovascular diseases, cancer, diabetes, Alzheimer's and inflammatory diseases (Swamy et al., 2016). Additionally, these volatile oils appear to have antibacterial, antioxidant, insecticidal, antifungal and antiviral properties (Prabuseenivasan et al., 2006).

Each bioactive compound displays a different mechanism of antimicrobial action towards bacteria. These complex processes are mediated by a sequence of biomedical reactions in the microbial cell. The complexity of these antimicrobial mechanisms rendered the emergence of bacterial resistance more difficult. Generally, EOs increase bacterial cell membrane permeability, resulting in proton gradient depletion and hence disturbance of adenosine triphosphate (ATP) synthesis (Zodrow, Schiffman, & Elimelech, 2012). Also, since EOs are lipophilic they can cross the plasma membrane and interact with intra-organelle sites or intracellular proteins (Özkan & Erdoğan, 2011).

1.4.2. Cinnamon (*Cinnamomum zeylanicum*)

Cinnamon is one of the ancient spices (Chen, P., Sun, & Ford, 2014). Around 250 different cinnamon species have been identified, with trees being dispersed in Asia, Australia and Pacific Islands (Mallavarapu & Rao, 2007). The bark of the different cinnamon species was popular in traditional and modern medicines. In addition, it was used as a flavoring agent in food, beverages and chewing gums (Rao & Gan, 2014).

Cinnamomum zeylanicum belongs to the genus *Cinnamomum* of the plant family *Lauracaeae*. It grows wide in India, Sri Lanka, Madagascar and Indochina (Unlu, Ergene, Unlu, Zeytinoglu, & Vural, 2010). The aromatic essential oils are the source of the flavor and aroma of cinnamon. The higher their EO's content, the stronger the flavor.

Traditionally, cinnamon and the different cinnamon extracts, independently of the species, were used for the treatment of many health conditions (Chen, P. et al., 2014). For example, they were reported to help in the treatment of diabetes, headaches, digestive disorders, common cold and respiratory tract infections. They also, were found to reduce the risk of colon cancer, prevent bleeding, increase tissue regeneration and raise the uterus blood circulation (Chen, P. et al., 2014; Prabuseenivasan et al., 2006; Rao & Gan, 2014).

Numerous therapeutic actions were also attributed to the cinnamon essential oils including antibacterial, antifungal, antidiabetic, anticancer, and antioxidant activities (Unlu et al., 2010). A study done to test the activity of 21 essential oils, including cinnamon oil, clove oil, lemon oil, rosemary oil, etc… against *K. pneumoniae*, *E. coli*, *Proteus vulgaris*, *Pseudomonas aeruginosa*, *Bacillus subtilis* and *S. aureus*, showed that among all the analyzed oils, cinnamon essential oils had the most potential antibacterial properties (Prabuseenivasan et al., 2006). Another studies showed that *C. zeylanicum* inhibited effectively many microorganisms, including Gram-positive bacteria, Gram-negative bacteria and even yeasts, as it was able to inhibit *S. aureus*, *Streptococcus* spp., *Enterococcus* spp., *K. pneumoniae*, *E. coli*, *Yersinia enterocolitica*, *Proteus* spp., *Listeria* spp. and *Candida* spp (Al-Mariri & Safi, 2014; Unlu et al., 2010).

1.4.3. Oregano (*Origanum onites*)

Origanum onites belongs to the genus *Origanum* of the plant family *Lamiaceae* (Ozkan, Baydar, & Erbas, 2010). The different species of oregano are commonly found in the Mediterranean countries. So the *O. onites* distribution area is limited to a small region of the Mediterranean island Sicily, in the southern part of Greece, and most importantly in Turkey (Spyridopoulou et al., 2019). In fact, Turkey is a very important gene center for the family *Lamiaceae* and *O. onites* is dominant in the northwest of Turkey (Coskun et al., 2008). *O. onites* is considered on the top of the list of commercial *Origanum* spp. of Turkey, sold under the commercial name of “Turkish oregano” (Kaskatepe et al., 2017). Oregano has been used in the production of spices, herbal teas, beverages and folk drugs in Turkey (Ozkan et al., 2010). Oregano’s spice properties are known to be due to its volatile and aromatic compounds; its essential oils (Milovanović et al., 2009).

Oregano is well known to have many medicinal properties. It was reported to reduce blood cholesterol and glucose levels and to help in resolving gastrointestinal problems. In addition, many oregano extracts proved to have an antiproliferative activity against cancer cells, mainly colon cancer cells, in vitro. They were also used as menstrual regulators, cough suppressants and diuretics (Kaskatepe et al., 2017; Spyridopoulou et al., 2019). Furthermore, oregano was reported to have antibacterial, antiparasitic, antifungal and antioxidant activities, these activities were attributed to the major essential oils constituents of the plant (Coskun et al., 2008; Özkan & Erdoğan, 2011). These essential oils were also used topically to reduce limb pain in rheumatism (Kaskatepe et al., 2017). In fact, oregano's essential oils were found to possess strong bactericidal activity against many pathogens, including *K. pneumoniae*, *S. aureus*, *P. aeruginosa*, *Y. enterocolitica*, *Shigella sonnei*, *Salmonella* Typhi and others (Swamy et al., 2016).

1.5. Aim of the study

Currently, the increased prevalence of antimicrobial resistance and the scarcity of effective treatments are the most important public health threats. The huge increase of multi-drug resistant bacterial infections and their high mortality rate, indicate that the golden era of antibiotics can be followed by the era of no antibiotic (Sakkas et al., 2019). Hence, the high demand for finding antimicrobial compounds that will not lead to the spread on ARGs (Zodrow et al., 2012).

Since it is accepted that the best strategy for the eradication of bacterial biofilms is by the prevention of their development (Borges et al., 2013), this study was devised to find natural compounds that are capable of preventing the biofilm formation by *K. pneumoniae*.

The main focus of this study was directed towards testing the ability of the major essential oils constituents of the two plants: Cinnamon (*Cinnamomum zeylanicum*) and oregano (*Origanum onites*), to inhibit the biofilm forming ability of *K. pneumoniae*. Subsequently, the essential oils with the highest anti-biofilm effect were tested for any synergistic effect to prevent the *K. pneumoniae* biofilm formation.

Chapter Two

Materials and Methods

2.1. Source of bacterial isolates

In this study, 26 *Klebsiella pneumoniae* bacterial isolates were used. These clinical strains were provided by the Clinical Microbiology Laboratory of the Lebanese American University Medical Center – Rizk Hospital (LAUMC-RH).

Table 1: *Klebsiella pneumoniae* clinical isolates used in this study.

Strain's name	Accession number	Strain's name	Accession number
KP1	427	**KP14**	74
KP2	1097	**KP15**	111
KP3	1333	**KP16**	2265
KP4	4429	**KP17**	4314
KP5	4590	**KP18**	4396
KP6	4677	**KP19**	7958
KP7	4769	**KP20**	7995
KP8	4982	**KP21**	9153
KP9	5188	**KP22**	9182
KP10	8118	**KP23**	11010
KP11	9368	**KP24**	11091
KP12	9468	**KP25**	11418
KP13	91190	**KP26**	12385

2.2. Processing of bacterial isolates

All the bacterial isolates were identified using standard microbiological procedures (Mohammed, Seid, Gebrecherkos, Tiruneh, & Moges, 2017). The identity of the isolates was reconfirmed using the Api20E test kits according to the manufacturer's instructions (Biomerieux, Marcy-L'Étoile, France).

2.3. Detection of extended-spectrum β-lactamases (ESBLS)

2.3.1. Antimicrobial susceptibility testing

Antimicrobial susceptibility testing, to detect ESBLs, was done by the standard Kirby-Bauer disk diffusion method as recommended by the Clinical Laboratory Standards Institute (CLSI) guidelines (CLSI, 2013). The following antibiotic discs were used, azteronam (30 μg), ceftriaxone (30 μg), cefpodoxine (10 μg), cefotaxime (30 μg), ceftazidime (30 μg).

The inoculum was prepared by mixing fresh colonies grown on a Trypticase soy agar (TSA) agar plates to a 0.9% saline solution (Sodium Chloride solution) and adjusting it to 0.5 McFarland standard turbidity. Within 15 minutes, a sterile cotton swab was dipped into the bacterial suspension, was rotated many times and pressed promptly against the inside wall of the tube, above the fluid level and used in seeding the dried surface of a 25 mm Mueller-Hinton agar (MHA) plate. For even distribution, the swab was rubbed gently over the whole surface two more times at an angle of 60°C. After 3 to 5 minutes, antibiotic discs were applied and pressed gently over the surface, using forceps, to ensure complete contact with the MHA surface. The discs were distributed evenly. At the center of the plate cefpodoxime (CPD-10) was placed, 15 mm out from the edge of CPD-10 to the left ceftazidime (CAZ-30) was placed, 15 mm to the right side ceftriaxone (CTR-30) was put, 15 mm downwards azteronam (AZT-30) was located and 15 mm to the left, of AZT-30, cefotaxime (CTX-30) was positioned. The plates were then inverted and incubated at 35°C for 18 to 24 hours. After incubation, the diameters of the zones of inhibition around each antibiotic disc, whenever present, were measured from three different directions and then averaged. The zone diameters were then compared to the CLSI guidelines tables,

interpreting if the bacterial strains were susceptible (S), intermediate (I), or resistant (R) to the used antibiotics (CLSI, 2013; Cockerill et al., 2013; Kumar, D., Singh, Ali, & Chander, 2014).

2.4. Pulsed field gel electrophoresis for DNA fingerprinting

The genetic relatedness of the 26 *Klebsiella* isolates, was analyzed via PFGE fingerprinting using XbaI restriction enzyme (Thermo Fisher Scientific, MA, USA), 1% SeaKem Gold (SKG) agarose gel and lambda ladder 170-3635 (Bio-Rad Laboratories, Inc, CA, USA) according to a modified CDC protocol (Centers for Disease Control and Prevention, 2013). Electrophoresis was performed on Bio-Rad Laboratories CHEF DR-III system (Bio-Rad Laboratories, Inc, CA, USA) under the conditions set for *Klebsiella pneumoniae* strains (Centers for Disease Control and Prevention, 2013). Gels were stained with ethidium bromide (EtBr), and imaged on Chemidoc XRS (Bio-Rad Laboratories, Inc, CA, USA), the gel were then analyzed.

2.4.1. Preparation of agarose plugs

At first, TE Buffer was prepared by adding 2 ml of 0.5 M EDTA (pH 8) and 10 ml of 1 M Tris (pH 8). The solution was then diluted, with sterilized water, to 1000 mL. Then, the 1% SeaKem Gold agarose plugs were prepared by mixing 0.50 g of SeaKem Gold agarose and 50 ml TE Buffer. Using a microwave, the solution was heated, in 30 seconds intervals, until it becomes completely clear.

Next, the Cell Suspension Buffer was prepared by mixing 200 ml of 0.5 M EDTA (pH 8) and 100 ml of 1 M Tris (pH 8). The solution was then diluted, with sterile water, to 1000 ml. 2 ml of Cell Suspension Buffer were transferred to small tubes, labeled for each sample number. Using a sterile swab, add sufficient bacterial colonies to the Suspension Buffer to give an absorbance reading of 0.8 to 1.0 in the Spectrophotometer at 610 nanometers (nm).

2.4.2. Casting plugs

For each strain, 400 µl adjusted cell suspension and 20 µl of Proteinase K (20 mg/ml stock) were added to a labeled 1.5 ml microcentrifuge tube and mixed gently with a pipette tip. 400 µl melted 1% SeaKem Gold agarose was then added to each tube. The solution was again pipetted up and down gently. 200 µl of the solution was immediately dispensed in disposable sterile plug molds.

2.4.3. Lysis of cells in agarose plugs

The Cell Lysis Buffer was prepared by adding 100 ml of 10 % Sarcosyl (N-Lauroylsarcosine, Sodium salt), 100 ml of 0.5 M EDTA (pH 8) and 50 ml of 1 M Tris (pH 8). 5 ml of the Lysis Buffer were then transferred to different conical tubes onto which 25 µl Proteinase K stock solutions (20 mg/ml) were added. Using a spatula, the plugs were removed carefully from the plug mold and were placed into their properly labeled conical tubes. The plugs were incubated overnight, for about 16 h, in a 42°C shaker incubator with constant and vigorous agitation at 140 rpm.

2.4.4. Washing of agarose plugs after cell lysis

The conical tubes were removed from the shaking incubator. The lysis buffer was carefully poured out of the conical tubes. 10 to 15 ml preheated sterile water (42°C) were then added to each tube. Next, the conical tubes were shaken at 140 rpm in a 42°C incubator for 10 to 15 minutes. This step was repeated twice. Water from the plugs was poured off and the plugs were next washed with 10 to 15 ml of preheated (42°C) TE buffer and were left to shake in the incubator at 140 rpm for 10 to 15 minutes. This step was repeated three times.

2.4.5. Restriction digestion of DNA in agarose plugs

The restriction enzyme master mix for the 15 plugs was then prepared by adding 2595 µl sterile water, 300 µl 10X Restriction Buffer (Tango Buffer), 30 µl BSA (10mg/ml) and 75 µl XbaI (10U/ µl). 2 to 2.5 mm wide plug slice from each sample were cut and transferred to 1.5ml microcentrifuge tubes containing 200 µl of the master mix. The microcentrifuge tubes were incubated in a water bath at 40°C for 4 hours.

2.4.6. Casting an agarose gel

From a 10X TBE buffer stock, 2.2 L of 0.5X Tris-Borate EDTA Buffer (TBE), needed for the gel and the electrophoresis running buffer, were prepared. Next, 1% SKG agarose was prepared by mixing 1.5 g agarose with 150 ml 0.5X TBE. The solution was heated and mixed gently until the agarose was completely dissolved. The 13 restricted plug slices were removed from the water bath. The plugs and the lambda ladders were then placed evenly at the ends of the 15 comb wells. The 150 ml agarose was poured into the gel form and bubbles were removed.

2.4.7. Electrophoresis conditions for *K. pneumoniae*

The electrophoresis conditions used consisted of an initial switch time of 5 s and a final switch time of 40 s. A gradient of 6 V/cm was used. The gels were electrophoresed for 22 hours.

2.4.8. Staining the gel

The EtBr solution was prepared by diluting 40 µl of ethidium bromide stock solution (10 mg/ml) with 400 ml sterile water.

After the electrophoresis run was over, the gel was stained in the EtBr solution for 30 to 40 min in a covered container while rotating gently on a rocker. Then, the gel was destained in 500 ml sterile water for 20 min.

2.4.9. Gel imaging and analysis of patterns

The gel image was then captured with UV light on Chemidoc XRS (Bio-Rad Laboratories, Inc, CA, USA).

2.5. Detection of biofilm formation

The ability of the study isolates to form biofilms, was done using a modified procedure of the tissue culture plate method (TCP) introduced by Hassan *et al.* (2011). Each *Klebsiella* isolate was collected from fresh brain heart infusion (BHI) plates and inoculated in 20 ml of trypticase soy broth (TSB) with 1% glucose, to match the turbidity of a 0.5 McFarland standard. The TSB broths were incubated at 35°C for 24 h. Then after incubation, 200 µl of each TSB inoculum were pipetted in 96 well flat-bottomed tissue culture plates (Corning, NY, USA). For every *Klebsiella* isolate, a column of empty wells served as a negative control. The 96 well plates were incubated at 35°C for 24 h. After incubation, the contents of all the wells were removed by gentle tapping. The wells were then washed with 200 µl 1X phosphate buffer saline (PBS) to remove the free floating bacteria. Staining of the bacterial biofilms adherent to the wells was done by 0.1% crystal violet for about 15 min. A final wash with 200 µl PBS was done to remove the excess stain. The plates were then kept aside for drying. The optical densities (ODs) of the stained adherent biofilms were then measured using Varioskan Flash microplate ELISA plate reader (Thermo Fisher Scientific, Waltham, MA, USA) at 570 nm (Hassan et al., 2011).

2.6. Natural extracts

2.6.1. Source of the natural products used in the study

Cinnamon powder (*Cinnamomum zeylanicum*) and oregano (*Origanum onites*) were bought from, a well-known herb store in Hamra Street - Beirut. Both plants were imported from Turkey. Cinnamon was harvested in December, whereas oregano was harvested in March.

2.6.2. Preparation of the plants' methanolic extract solutions

200 g of cinnamon (C) and 200 g of oregano (O) were weighed and then grinded. Each of the plants' powders were mixed with a 1000 ml solution of 80% methanol (80 methanol: 20 distilled water) in two Erlenmeyer flasks. Both extracts had a concentration of 0.2 g/ml. The solutions were placed in the orbital shaker for 1 week at 42^{o}C and 80 rpm. C and O methanolic extracts were then filtered in Corning disposable plastic vacuum filters, with 0.22 µm pore size (Corning, NY, USA). Both extracts were stored in a dark container and placed in the refrigerator for further testing (Afroz et al., 2020; Keyrouz, Abou Raji El Feghali, Jaafar & Nawas, 2017).

2.6.3. Well diffusion assay to check the antimicrobial effect of the methanolic extracts

From freshly streaked TSA plates, inoculums in 0.9% saline, were prepared to a turbidity equivalent to a 0.5 McFarland standard, for the 26 *Klebsiella* isolates. Using a cork borer, a 10.5 mm well was pierced in the middle of the, 25 mm thick, MHA plates and filled with 200 µl of the different extract concentrations. The MHA plates were then incubated, bottom side up, for 24 h at 35^{o}C. The next day, the zones of inhibition around the wells, if present, were measured in three different angles and the readings averaged (Keyrouz, Abou Raji El Feghali, P, Jaafar, & Nawas, 2017).

For the cinnamon methanolic extract, 3 different concentrations were tested: 0.2 g/ml, 0.15 g/ml and 0.05 g/ml. Whereas for the oregano methanolic extract, 5 different concentrations were tested: 0.2 g/ml, 0.15 g/ml, 0.1 g/ml, 0.05 g/ml and 0.02 g/ml.

2.6.4. Effect of the two natural extracts on biofilm formation

Cinnamon and oregano methanolic extracts were prepared each with a concentration of 0.02 g/ml.

To test the effect of C and O extracts on biofilm formation, the tissue culture plate method was also used. 200 µl, of the 0.02 g/ml C solution and 0.02 g/ml O solution, were

pipetted to the different 96 well flat-bottomed tissue culture plates and left to dry in the incubator at 35ºC for 3 days, under aseptic conditions. After drying, 200 µl of the TSB inoculums of the 26 *Klebsiella* isolates were added to the 96 well-plates. For every isolate, the inoculum was added in a set of empty wells and in another set of wells containing dried sample extract. The following steps were described previously in section 2.5 (Detection of biofilm formation): Incubation for 24 h, emptying the plates, washing with PBS, staining with crystal violet, washing with PBS and finally drying the plates and reading the ODs at 570 nm (Ismail, Hneini, & Nawas, 2019).

Every isolate was placed in four columns of the 96 well plate. The first column was considered a negative control and was left empty, the second was filled with the methanolic extract alone, the third contained the extract and the bacteria together, while the fourth contained only the bacterial isolate as a positive control.

This experiment was repeated three times for every extract and the mean ± SD was reported for each.

2.6.5. Sources of the major essential oils of the tested plants

The major essential oil constituents of cinnamon and oregano, as reported in the literature, were purchased. Cinnamaldehyde (CA) and eugenol (EG) were the two major essential oil constituents of the *C. zeylanicum* methanolic extract. Thymol (TH) and carvacrol (CR) were the two major essential oils constituents of the *O. onites* methanolic extract. These four chemicals were purchased from Sigma-Aldrich (Sigma-Aldrich, Inc) in liquid or solid state and were stored in a dark place in the refrigerator.

2.6.6. GC-MS of the *C. zeylanicum* and *O. onites* methanolic extracts

The major essential oil constituents of cinnamon and oregano were obtained from the literature. Then, Gas Chromatography-Mass Spectrometry (GC-MS) was done to identify the presence of these essential oils (EO) in the 0.02 g/ml prepared methanolic extracts and specify their concentrations.

2.6.6.1. Instrument and method set up

All measurements were carried out using the Shimadzu GC Thermo Scientific™ TSQ 9000™ triple quadrupole GC-MS/MS system equipped with the Thermo Scientific™ TRACE™ 1310 GC with SSL Instant Connect™ SSL module and Thermo Scientific™ TriPlus™ RSH autosampler (Thermo Fisher Scientific, MA, USA).

1 µl of each sample solution was injected in a splitless mode. The carrier gas Helium was used in the constant flow mode at 6 ml/min. The chromatographic oven temperature was programmed as follows: 50 °C maintained for 5 min then raised to 250 °C (15 °C/min) and held for 5 min at 250 °C. The transfer line temperature was maintained at 250 °C. Total analysis of the sample took 28 min. Moreover, the mass spectrometer operated in the EI mode at 70 eV. The MS ion source temperature was kept at 220 °C. The SRM scan mode was used with a transition setup automatically build-up by the AutoSRM software.

Diluted solutions of the four essential oils, cinnamaldehyde, eugenol, thymol and carvacrol were prepared. Each compound was dissolved in pure methanol (concentration =1000 ppm) and diluted before analysis. 1 µL of each EO were analyzed in the GC-MS and the retention time (RT) for each compound was reported (Chen, A. & Huebschmann, 2008).

The GC is composed of a column preserved inside an oven. In the heated injection port, the mixture is flash vaporized. The different components of the sample pass through the column by the carrier gas, helium, which is considered the mobile phase. It carries the sample through the stationary phase, which is coated onto the capillary column's inner wall. Depending on the vapor pressures of the analytes, such as the EOs and the methanolic extracts, they are vaporized and pushed through the stationary phase. These analytes interact differently with the stationary phase because of their different chemical and physical properties and hence they elute from the column at different RTs. All the constituents are then introduced into the MS. In this phase, the components are ionized and fragmented by the Electron impact (EI) method. In EI, sample molecules are bombarded by an energetic beam of electrons. These electrons hit a molecule and knock an electron out of it, making the molecule positively charged. This ionizing collision

passes some energy to the molecule, which could be enough to cause the fragmentation of the ion. The large quantity of ion fragments with different masses characterize the intact molecule. The mass spectrum will contain the resulting plots of relative intensity versus mass-to-charge ratio. Different libraries are present to help in the analysis of EI mass spectra and identify these unknown compounds (Emwas, Al-Talla, Yang, & Kharbatia, 2015; Kristo, 2012).

2.6.6.2. Quantification of the analytes

Calibration curves were used to quantify the actual content of CA, EG, TH and CR in the extracts. Using the same GC-MS conditions, five different concentrations of each compound were prepared (0.125 ppm, 0.25 ppm, 0.5 ppm, 0.75 pm and 1 ppm). For each concentration, CA was mixed with EG and TH with CR and the mixtures were run for analysis. A linear graph was drawn for every mixture of essential oils representing peak area values versus the concentration of the EO. Later, the cinnamon methanolic extract was diluted and analyzed in the GC-MS. The peaks that appeared at the retention times specific for cinnamaldehyde and eugenol were detected and quantified. The areas of these peaks were measured and hence the concentrations of these compounds in the extract were deduced. The same was done for the oregano methanolic extract and its essential oil constituents thymol and carvacrol (Craig, Fields, & Simpson, 2014).

2.6.7. Preparation of the six different essential oil solutions and testing for an anti-biofilm effect

2.6.7.1. Preparation of the four essential oils' solutions

The CA methanolic solution was prepared by adding 12.271 µl of the original stock solution to 99.987 ml of methanol. The EG methanolic solution was prepared by adding 0.34 µl of the original stock solution to 99.99 ml of methanol. The TH methanolic solution was prepared by mixing 36.25 mg of the original stock powder and 100 ml of methanol. While the CR methanolic solution was prepared by adding 25.26 µl of the original stock solution to 99.975 ml of methanol.

2.6.7.2. Preparation of the two essential oils mixtures for testing for any synergistic effect.

Two different solutions were prepared for testing for any synergistic effect, the first containing CA and EG and the second containing TH and CR.

Before preparing the two mixtures, four new stock solutions, with a concentration of 0.02 g/ml each, were prepared for all the EOs including CA, EG, TH and CR. These 0.02g/ml solution were then used for the preparation of the mixtures.

To prepare the CA+EG mixture, 643 µl of CA stock solution and 18.125 µl of EG stock solution were added to 99.338 ml methanol solution. In addition, to prepare the TH+CR mixture, 1.8125 ml of TH stock solution and 1.2325 ml of CR were mixed with 96.95 ml of methanol.

2.6.7.3. Testing the ability of the four essential oils to inhibit the *K. pneumoniae* biofilm formation and checking the possibility of a synergistic effect of the two essential oils mixtures

The same procedure described in section 2.6.4. (Effect of the natural extracts on biofilm formation) was used here. However, there was a difference in the contents of the wells. The first column of the 96 tissue culture plates, was considered a negative control and was left empty, the second was filled with the EOs solutions (CA, EG, TH or CR) or the two mixtures (CA+EG or TH+CR), the third contained the EOs solutions and the bacteria together, while the fourth contained only the bacterial isolate and served as a the positive control.

These experiments were also repeated three times for every EO solution and the mean ± SD was reported for each.

2.7. Statistical analysis

The statistical analysis of the data was performed using GraphPad Prism Prism 8 (San Diego, CA, USA). The p-values were calculated using t-tests. A p-value less than 0.05 was considered significant. Significant differences were reported, with * indicating a p-value: $0.01 < p < 0.05$, ** indicating a p-value: $0.001 < p < 0.01$, *** indicating a p-value: $0.0001 < p < 0.001$, and **** indicating a p-value: $p < 0.0001$.

Chapter Three

Results

3.1. Detection of extended-spectrum β-lactamases

The 26 clinical isolates were tested for their expression of β-lactamases as per the CLSI standard procedure (CLSI, 2013). As shown in Table 2 and figure 2 (KP2), 13 of the isolates were susceptible to at least four out of the five β-lactam antibiotics used and are called the non-ESBL isolates, while the other 13 isolates, the results of which appear in Table 3 and figure 2 (KP24), were resistant to almost all of the β-lactam antibiotics and are called the ESBL isolates.

Table 2: Antimicrobial susceptibility testing for the *K. pneumoniae* isolates (Non-ESBLs). For each antibiotic disc, the diameter of the zone of inhibition was measured. The diameters were then compared to the CLSI guidelines. S: indicating that the isolate was susceptible to this antibiotic, I: intermediate and R: resistant.

Isolates	Aztreonam (AZT-30)	Ceftriaxone (CTR-30)	Cefpodoxime (CPD-10)	Cefotaxime (CTX-30)	Ceftazidime (CAZ-30)
KP1	S	S	S	S	S
KP2	S	S	S	S	S
KP3	S	S	S	S	S
KP4	S	S	S	I	S
KP5	S	S	S	S	S
KP6	S	S	S	S	S
KP7	S	S	S	S	S
KP8	S	S	S	S	S
KP9	S	S	S	S	S
KP10	S	S	S	I	S
KP11	S	S	S	S	S
KP12	S	S	S	S	S
KP13	S	S	S	I	S

Table 3: Antimicrobial susceptibility testing for the *K. pneumoniae* isolates (ESBLs). For each antibiotic disc, the diameter of the zone of inhibition was measured. The diameters were then compared to the CLSI guidelines. S: indicating that the isolate was susceptible to this antibiotic, I: intermediate and R: resistant.

Isolates	Aztreonam (AZT-30)	Ceftriaxone (CTR-30)	Cefpodoxime (CPD-10)	Cefotaxime (CTX-30)	Ceftazidime (CAZ-30)
KP14	R	R	R	R	R
KP15	R	R	R	R	R
KP16	S	R	R	R	R
KP17	R	R	R	R	R
KP18	R	R	R	R	R
KP19	R	R	R	R	R
KP20	R	R	R	R	R
KP21	S	R	R	R	I
KP22	R	R	R	R	R
KP23	R	R	R	R	R
KP24	R	R	R	R	R
KP25	R	R	R	R	R
KP26	R	R	R	R	R

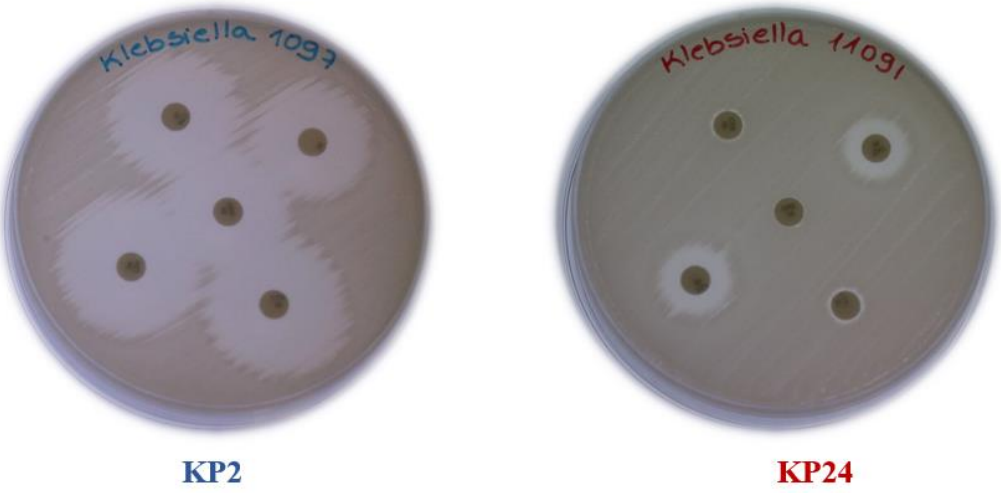

Figure 2: Antibiograms of KP2 and KP24 isolates. KP2 is a non-ESBL isolate and KP24 is an ESBL isolate.

3.2. Pulse-field gel electrophoresis runs of non-ESBLs and ESBLs *K. pneumoniae* isolates

To determine the degree of relatedness among the different strains of *K. pneumoniae* PFGE was done according to the CDC protocol (Centers for Disease Control and Prevention, 2013). The PFGE gel patterns are presented in figure 3 for the non-ESBL isolates and in figure 4 for the ESBLs.

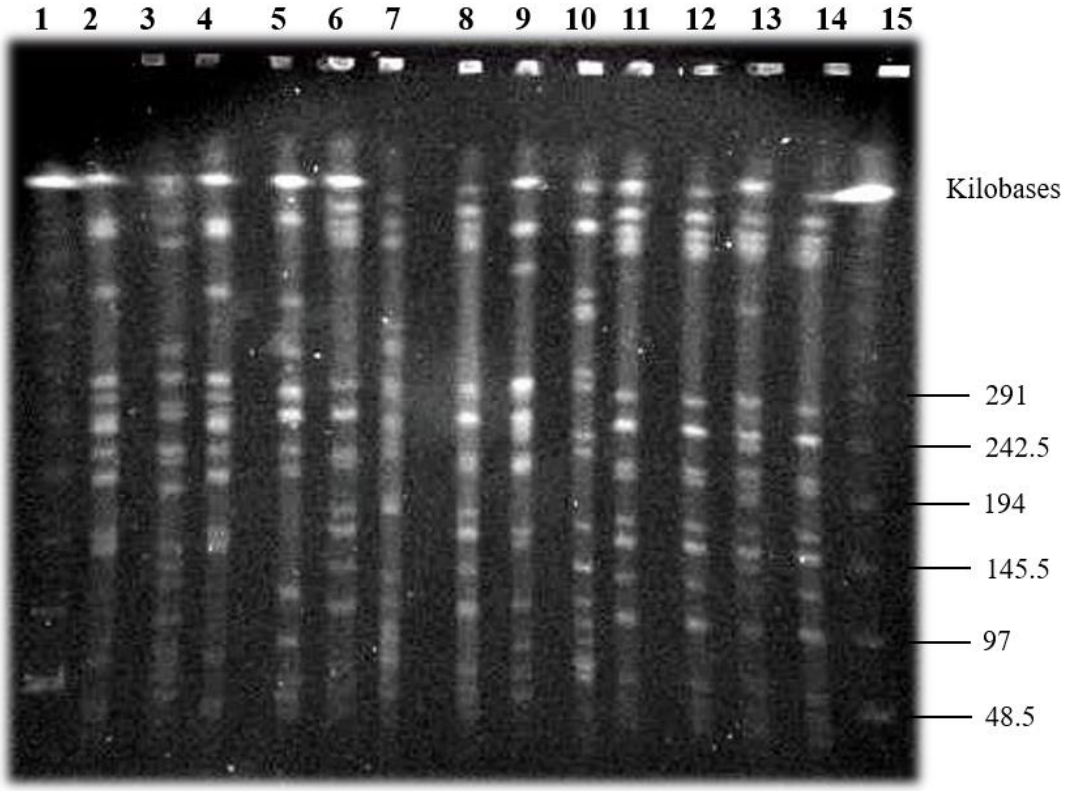

Figure 3: PFGE pattern of XbaI-cleaved genomic DNAs of non-ESBL *K. pneumoniae* clinical isolates. Lanes 1 and 15 represent the lambda ladder. Lane 2 till lane 14 represent KP1 to KP13 isolates respectively.

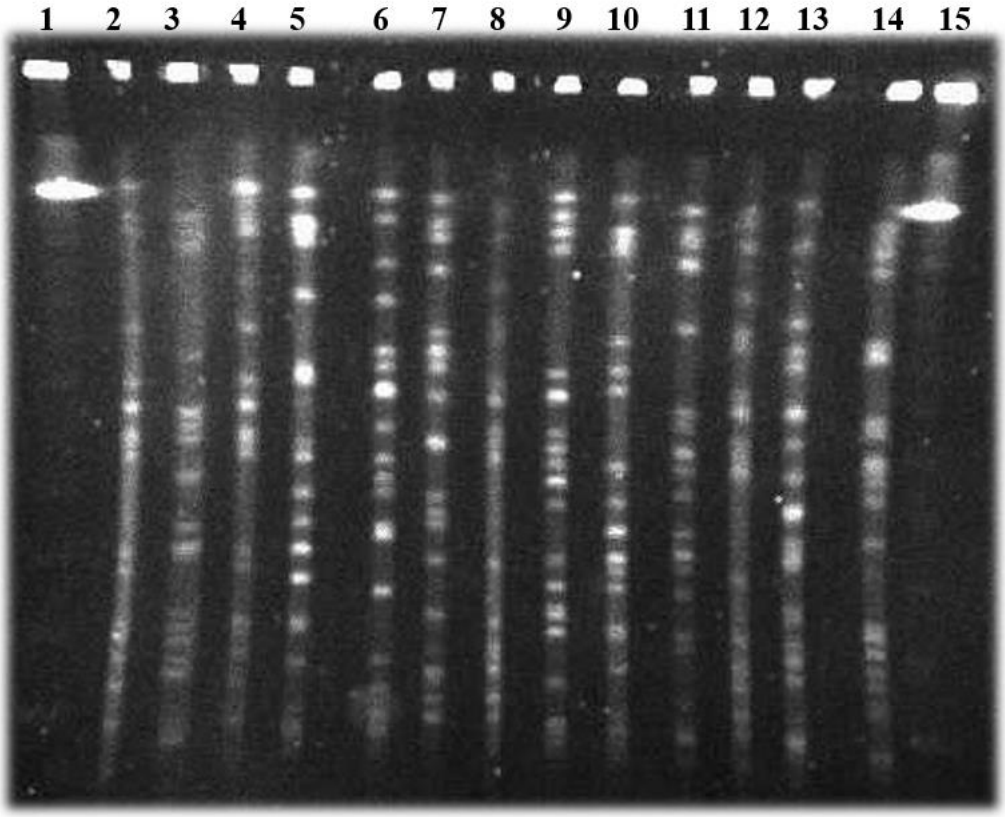

Figure 4: PFGE pattern of XbaI-cleaved genomic DNAs of ESBL *K. pneumoniae* clinical isolates. Lanes 1 and 15 represent the lambda ladder. Lane 2 till lane 14 represent KP14 to KP26 isolates respectively.

Figure 3 shows that isolates KP1 and KP3; KP5 and KP7; K10, K11, K12 and KP13 have similar and close genetic patterns, revealing identical profiles. Hence, the similar isolates could be part of an outbreak, originating for the same environment. Whereas ESBL isolates, in figure 4, show different separation profiles and thus they are considered genetically unrelated bacterial strains.

3.3. Detection of biofilm formation among *K. pneumoniae* isolates

The 26 bacterial isolates were chosen to be biofilm formers. The tissue culture plate method (described in section 2.5) was used to confirm that the chosen isolates were

biofilm producing *K. pneumoniae* strains. The ability of the chosen non-ESBL and ESBL isolates to form biofilm are shown respectively in figures 5 and 6.

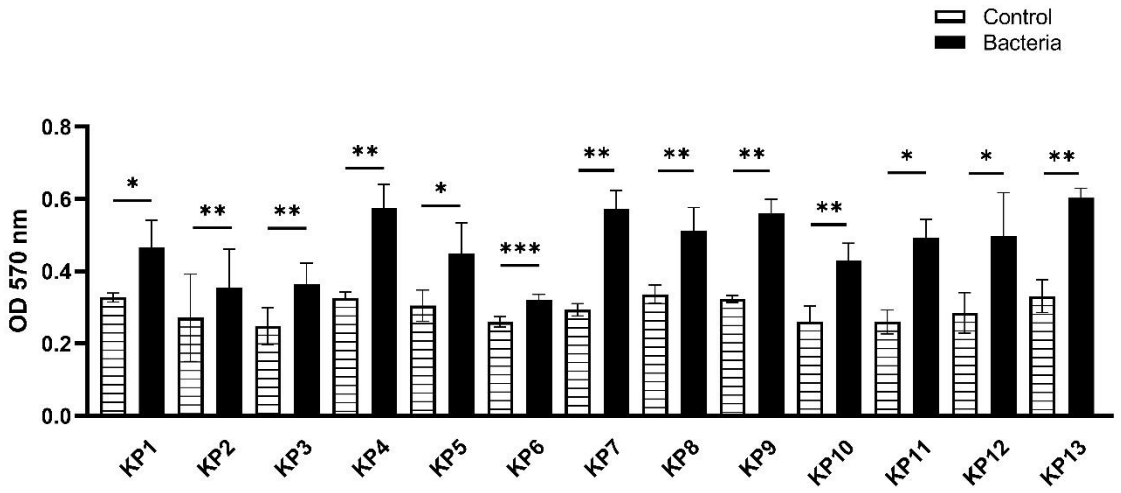

Figure 5: Biofilm formation by non-ESBL *K. pneumoniae* isolates. The values of OD_{570} are represented as means ± standard deviations (SDs) of 3 independent trials (n=3). The P values were obtained by one-tailed paired *t* test with *p* value ≤ 0.05 considered statistically significant.

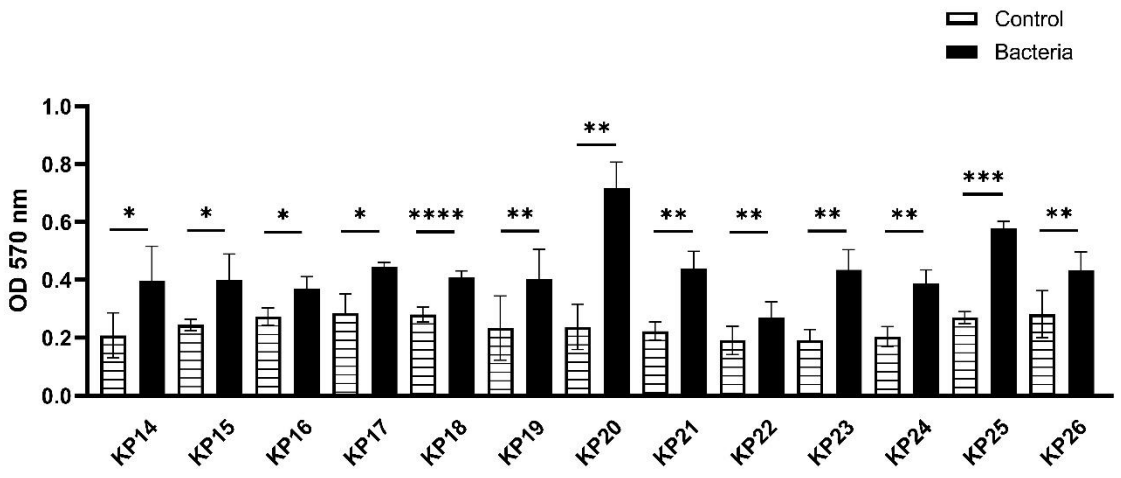

Figure 6: Biofilm formation by ESBL *K. pneumoniae* isolates. The values of OD_{570} are represented as means ± SDs of 3 independent trials (n=3). The P values were obtained by one-tailed paired *t* test with *p* value ≤ 0.05 considered statistically significant.

3.4. Antimicrobial effect *C. zeylanicum* and *O. onites* methanolic extracts

The standard well diffusion assay (Keyrouz et al., 2017) was used to determine the minimum inhibitory concentration (MIC) of the cinnamon and oregano methanolic extracts. As shown in Table 4 and figure 7, a concentration of 0.05 g/ml *C. zeylanicum* extract was able to inhibit the growth of non-ESBL and ESBL *Klebsiella* isolates. Whereas, as shown in Table 5 and figure 8, a concentration of 0.02 g/ml *O. onites* extract was able to inhibit the growth of non-ESBL and ESBL *Klebsiella* isolates.

Table 4: Inhibition zone diameters of 10 *K. pneumoniae* isolates at different concentrations of *C. zeylanicum* methanolic extract. For each concentration (0.2 g/ml, 0.15 g/ml and 0.05 g/ml), the diameter of the zone of inhibition was measured. The well diameter was 10.5 mm. Absolute methanol was used as a control. C: Cinnamon methanolic extract.

Isolates	Zone of inhibition (mm)			
	Control	C 0.2 (g/ml)	C 0.15 (g/ml)	C 0.05 (g/ml)
KP1	0	16	15	0
KP2	0	16.167	15	0
KP4	0	15	13.67	0
KP10	0	15	14	0
KP13	0	15	14	0
KP14	0	16.67	16	0
KP15	0	17	15	0
KP17	0	17	16	0
KP24	0	17	15.5	0
KP25	0	15.33	14	0

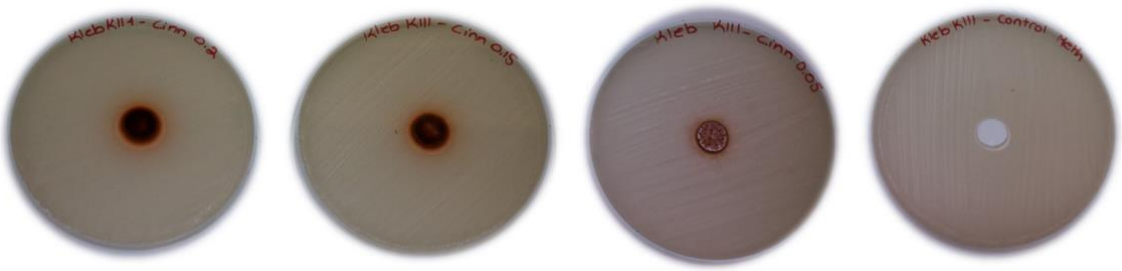

Figure 7: Antimicrobial activity of *C. zeylanicum* methanolic extract. Three different concentrations of the extract were used: 0.2 g/ml, 0.15 g/ml and 0.05 g/ml. Absolute methanol was used as a control.

Table 5: Inhibition zone diameters of 10 *K. pneumoniae* isolates at different concentrations of *O. onites* methanolic extract. For each concentration (0.2 g/ml, 0.15 g/ml, 0.1 g.ml, 0.05 g/ml and 0.02 g/ml), the diameter of the zone of inhibition was measured. The well diameter was 10.5 mm. Absolute methanol was used as a control. O: Oregano methanolic extract.

Isolates	Zone of inhibition (mm)					
	Control	O 0.2 (g/ml)	O 0.15 (g/ml)	O 0.1 (g/ml)	O 0.05 (g/ml)	O 0.02 (g/ml)
KP1	0	16	16	15	13.83	0
KP2	0	16	15	14.5	14.167	0
KP4	0	15.33	15	14.5	14	0
KP10	0	16	15	15	15.33	0
KP13	0	16	16	15	13.33	0
KP14	0	16	16	15	13.33	0
KP15	0	16.33	16	16	14.33	0
KP17	0	16	15.67	15	14.67	0
KP24	0	15.67	15	15	13.1667	0
KP25	0	16.67	16	14.67	15	0

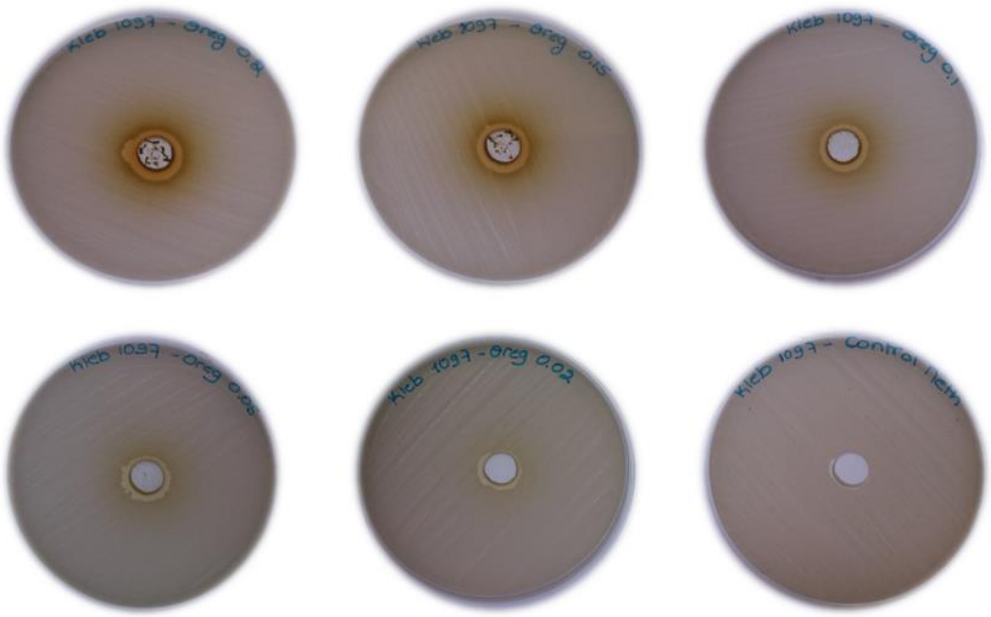

Figure 8: Antimicrobial activity of *O. onites* methanolic extract. Five different concentrations of the extract were used: 0.2 g/ml, 0.15 g/ml, 0.1 g/ml, 0.05 g/ml and 0.02 g/ml. Absolute methanol was used as a control.

3.5. Effect of the two natural extracts on biofilm formation

The anti-biofilm effect of cinnamon and oregano extracts, using a sub-inhibitory concentration of 0.02 g/ml for both solutions, was tested (procedure described in section 2.6.4). Comparing the OD values of the cinnamon extract (2nd bar, figure 9 and 10) and the OD values of *Klebsiella* isolates' biofilm alone with the OD values of the biofilm produced by the isolates in the presence of cinnamon revealed that cinnamon was able to minimize the biofilm formed by the 26 *K. pneumoniae* isolates.

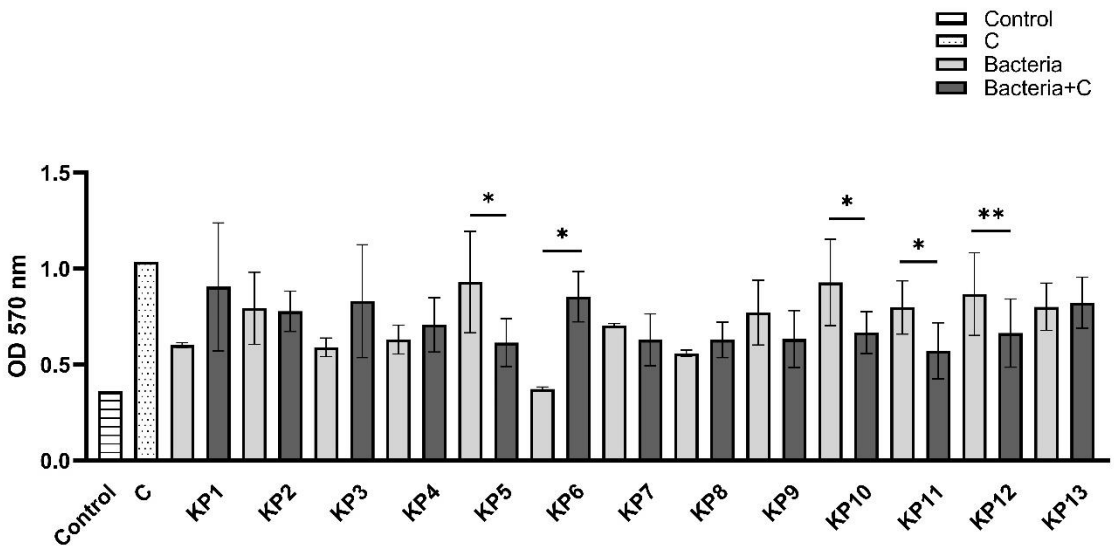

Figure 9: The effect of *C. zeylanicum* methanolic extract on the biofilm formation of non-ESBL *K. pneumoniae* isolates. The values of OD_{570} are represented as means ± SDs of 3 independent trials (n=3). The P values were obtained by one-tailed paired *t* test with *p* value ≤ 0.05 considered statistically significant. C: Cinnamon methanolic extract.

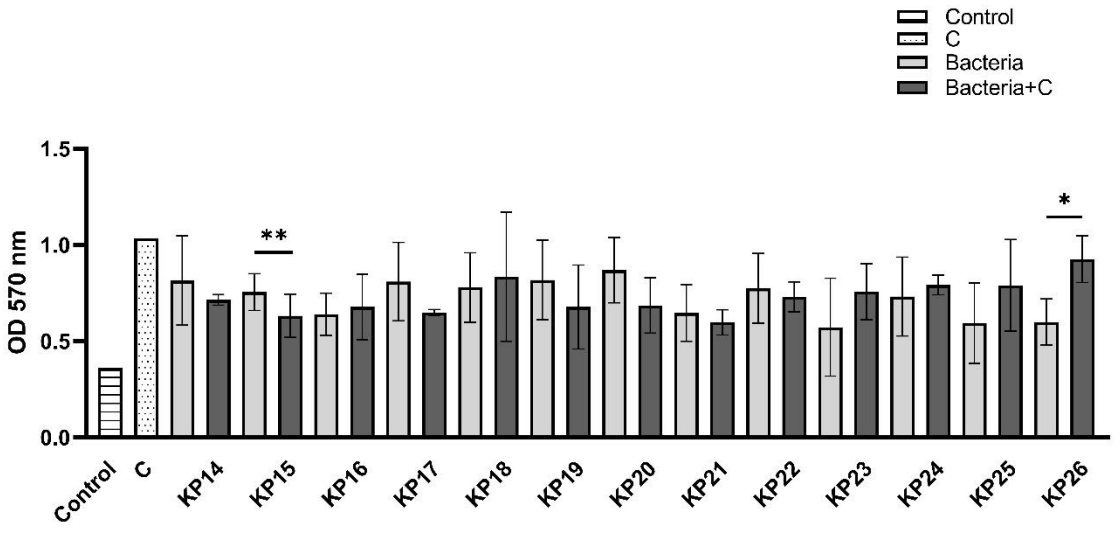

Figure 10: The effect of *C. zeylanicum* methanolic extract on the biofilm formation of ESBL *K. pneumoniae* isolates. The values of OD_{570} are represented as means ± SDs of 3 independent trials (n=3). The P values were obtained by one-tailed paired *t* test with *p* value ≤ 0.05 considered statistically significant. C: Cinnamon methanolic extract.

On the other hand, Comparing the OD values of the oregano extract (2nd bar, figures 11 and 12) and the OD values of *Klebsiella* isolates' biofilm alone with the OD values of the biofilm produced by the isolates in the presence of oregano, revealed that oregano was able to minimize the biofilm formed by the 26 *K. pneumoniae* isolates.

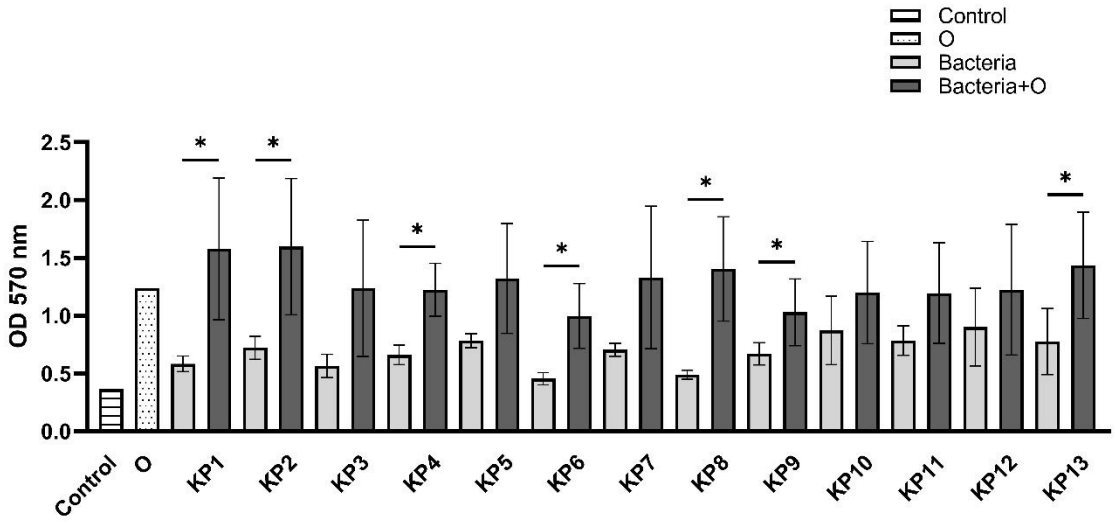

Figure 11: The effect of *O. onites* methanolic extract on the biofilm formation of non-ESBL *K. pneumoniae* isolates. The values of OD_{570} are represented as means ± SDs of 3 independent trials (n=3). The P values were obtained by one-tailed paired *t* test with *p* value ≤ 0.05 considered statistically significant. O: Oregano methanolic extract.

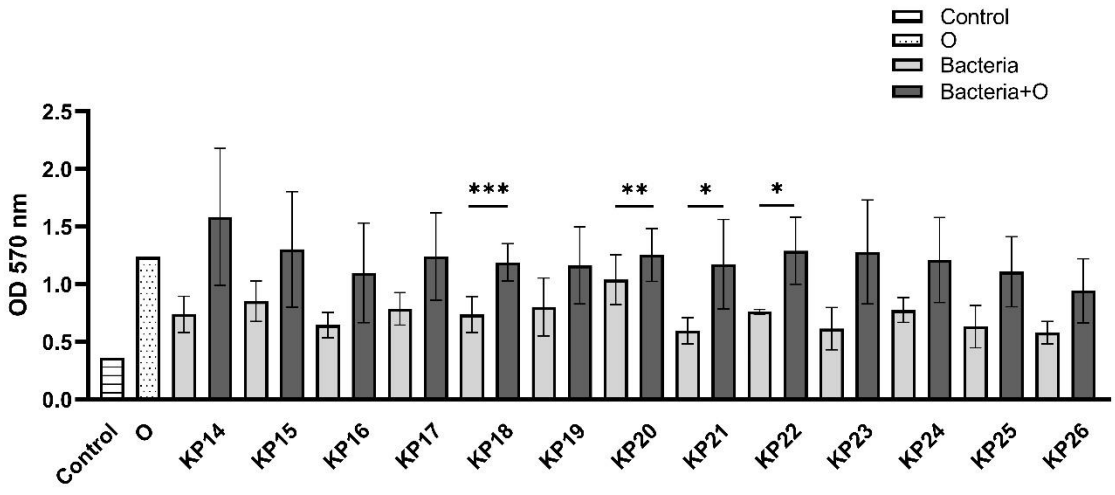

Figure 12: The effect of *O. onites* methanolic extract on the biofilm formation of ESBL *K. pneumoniae* isolates. The values of OD_{570} are represented as means ± SDs of 3 independent trials (n=3). The P values were obtained by one-tailed paired *t* test with *p* value ≤ 0.05 considered statistically significant. O: Oregano methanolic extract.

3.6. Gas chromatography-mass spectrometry of *C. zeylanicum* and *O. onites* methanolic extracts

GC-MS was done to quantify the exact concentrations of the main essential oil constituents, of cinnamon and oregano, in the prepared methanolic extracts. The essential oils were run in the GC-MS and their retention times were determined (Table 6). Five dilutions (0.125 ppm, 0.25 ppm, 0.5 ppm, 0.75 ppm and 1ppm) of CA and EG mixture and TH and CR mixture were run in the GC-MS in order to draw the calibration curves, represented in figure 13 and figure 14, and quantify the exact concentration of these essential oils in the methanolic extracts (Table 7). Diluted samples of cinnamon and oregano methanolic extracts (25 times and 50 times dilutions respectively) were analyzed in the GC-MS, and their chromatograms are shown in figure 15 and figure 16.

Table 6: Retention time of the essential oil constituents of *C. zeylanicum* and *O. onites*.

Methanolic extract	Chemical Compound	Retention Time (min)
Cinnamomum zeylanicum	Cinnamaldehyde	9.455
	Eugenol	10.245
Origanium onites	Thymol	9.56
	Carvacrol	9.66

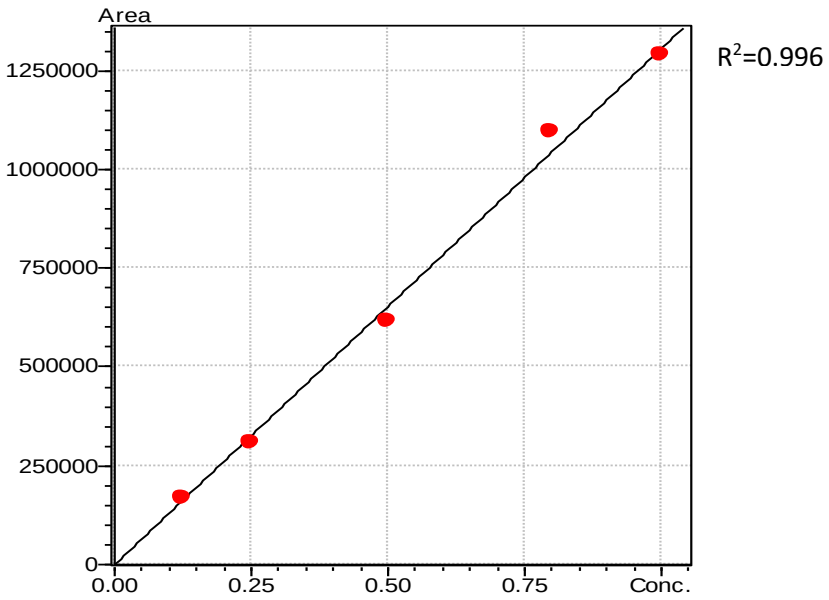

Figure 13: Standard curve for CA and EG chemicals, by GC-MS. It represents the plot area of the peaks versus the concentration of the two EOs in ppm.

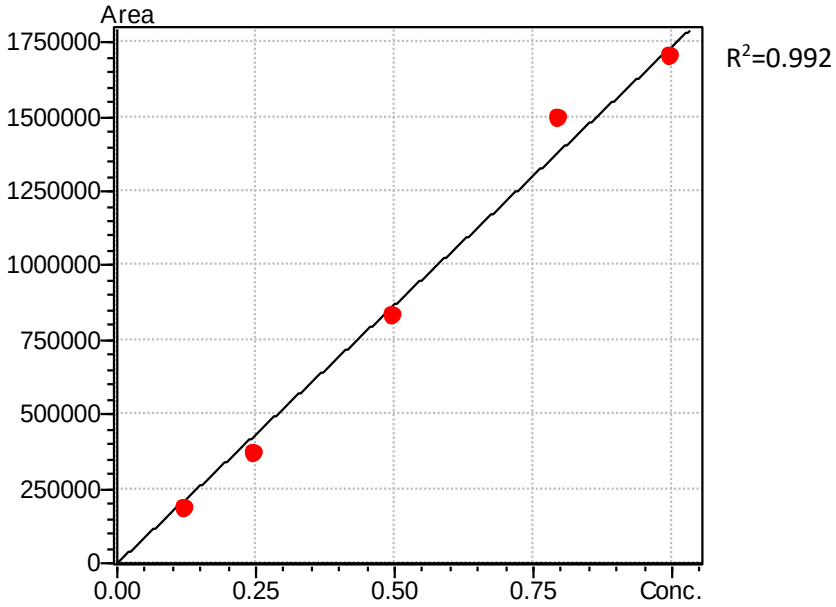

Figure 14: Standard curve for TH and CR chemicals, by GC-MS. It represents the plot area of the peaks versus the concentration of the two EOs in ppm.

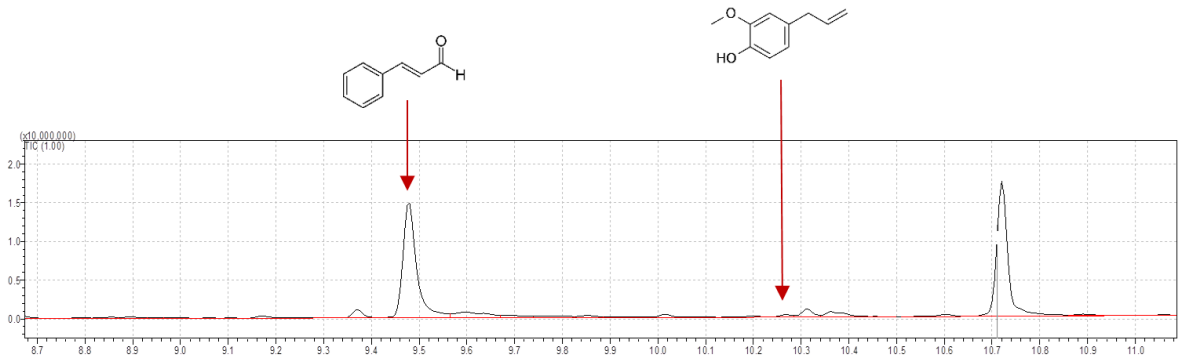

Figure 15: GC-MS chromatogram of methanolic extract of *Cinnamomum zeylanicum*. Peak 1 at 9.455 min assures the presence of CA. Peak 2 at 10.245 min confirm the presence of EG.

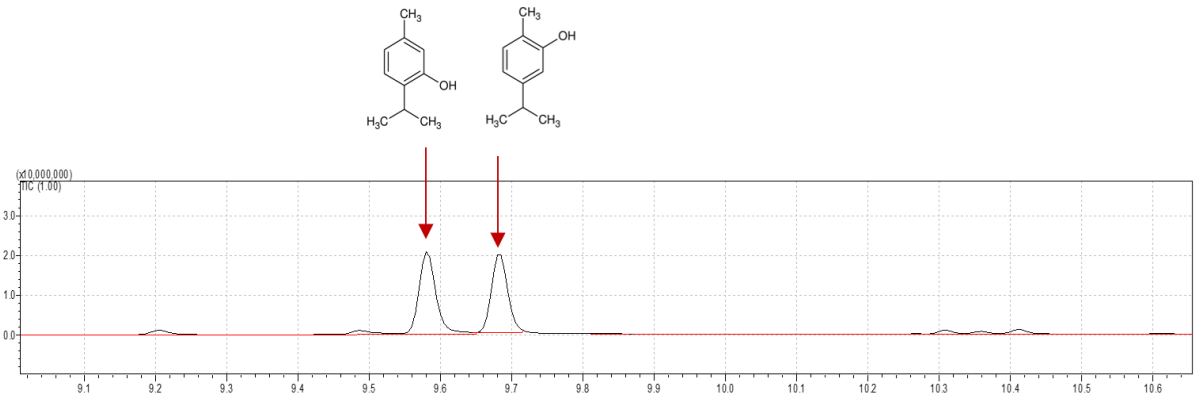

Figure 16: GC-MS chromatogram of methanolic extract of *Origanum onites.* Peak 1 at 9.56 min assures the presence of TH. Peak 2 at 9.66 min confirm the presence of CR.

Table 7 shows that the *C. zeylanicum* methanolic extract contained 0.643% cinnamaldehyde and 0.018125% eugenol. Whereas, the *O. onites* methanolic extract contained 1.8125% thymol and 1.2315% carvacrol.

Table 7: Concentrations and percentages of the essential oil constituents in *C. zeylanicum* and *O. onites* methanolic extracts, as elucidated by GC-MS.

Methanolic extract	Chemical Compound	Concentration (ppm)	Concentration (g/ml)	Percentage in methanolic extract
Cinnamomum zeylanicum	Cinnamaldehyde	5.144	0.1286	0.643
	Eugenol	0.145	0.003265	0.018125
Origanium onites	Thymol	7.25	0.3625	1.8125
	Carvacrol	4.93	0.2465	1.2325

3.7. Anti-biofilm effect of the major essential oil constituents of *C. zeylanicum* and *O. onites* methanolic extracts

The four main essential oils were then tested to check if any of them had an anti-biofilm effect on the *K. pneumoniae* isolates and may have been responsible for the anti-biofilm effect of the plants' extracts. Figure 17 shows that the biofilms formed by 9 out of the 13 *K. pneumoniae* non-ESBL isolates were reduced after the addition of cinnamaldehyde (KP2, KP3, KP5, KP6, KP7, KP9, KP10, KP11 and KP12). While, as is clear from figure 18, the biofilms formed by 6 out of the 13 *K. pneumoniae* ESBL isolates were also reduced after the addition of cinnamaldehyde (KP14, KP15, KP16, KP17, KP18 and KP20).

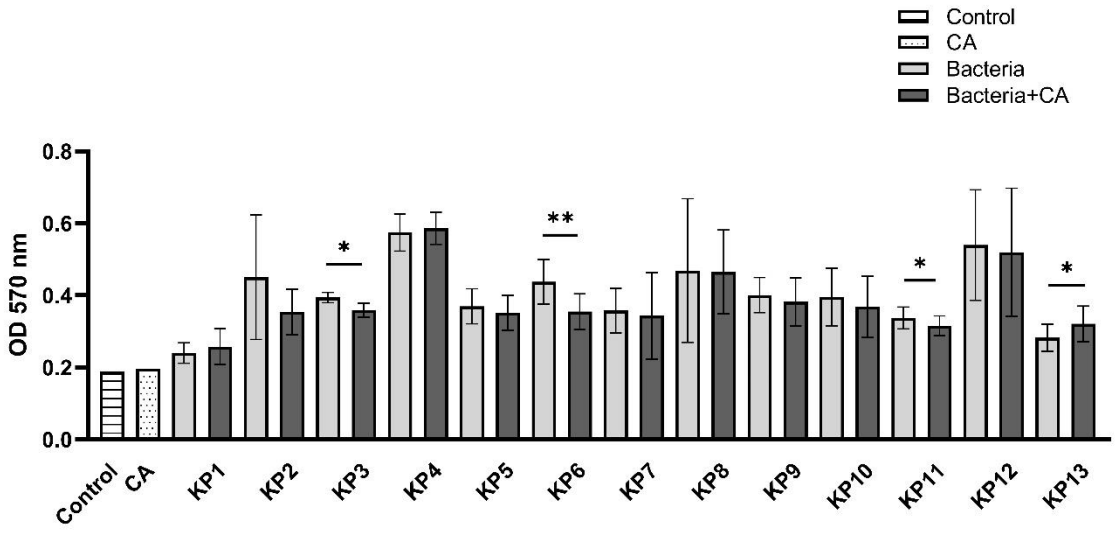

Figure 17: The effect of cinnamaldehyde (CA) on the biofilm formation of non-ESBL *K. pneumoniae* isolates. The values of OD_{570} are represented as means ± SDs of 3 independent trials (n=3). The P values were obtained by one-tailed paired *t* test with *p* value ≤ 0.05 considered statistically significant.

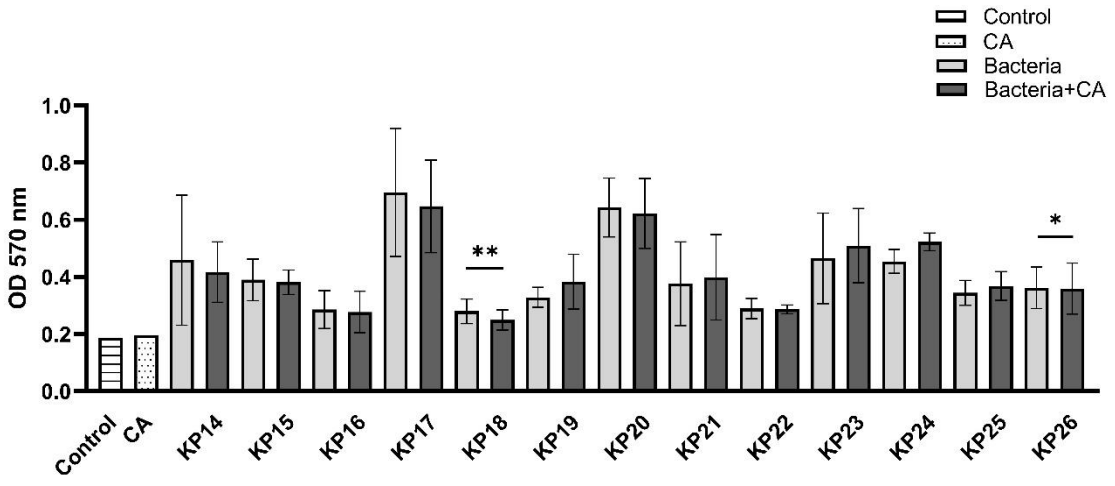

Figure 18: The effect of cinnamaldehyde (CA) on the biofilm formation of ESBL *K. pneumoniae* isolates. The values of OD_{570} are represented as means ± SDs of 3 independent trials (n=3). The P values were obtained by one-tailed paired *t* test with *p* value ≤ 0.05 considered statistically significant.

After testing the effect of eugenol, it is evident from figure 19 that the biofilms formed by 6 out of the 13 *K. pneumoniae* non-ESBL isolates were reduced after the addition of eugenol (KP2, KP5, KP6, KP9, KP10 and KP11). Figure 20 shows that the biofilms formed by 7 out of the 13 *K. pneumoniae* ESBL isolates were also reduced after the addition of eugenol (KP14, KP15, KP17, KP20, KP21, KP23 and KP26).

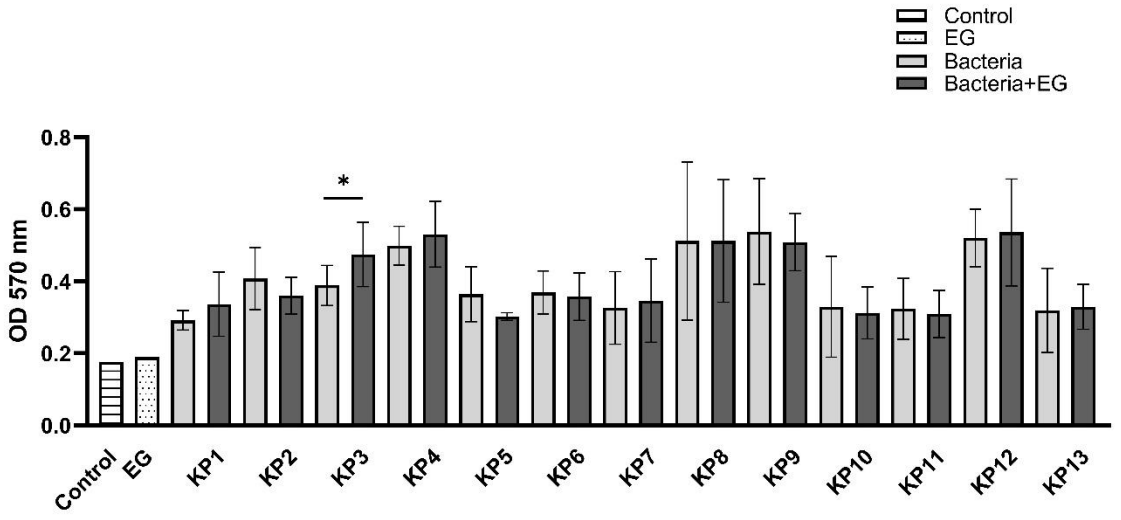

Figure 19: The effect of eugenol (EG) on the biofilm formation of non-ESBL *K. pneumoniae* isolates. The values of OD_{570} are represented as means ± SDs of 3 independent trials (n=3). The P values were obtained by one-tailed paired *t* test with *p* value ≤ 0.05 considered statistically significant.

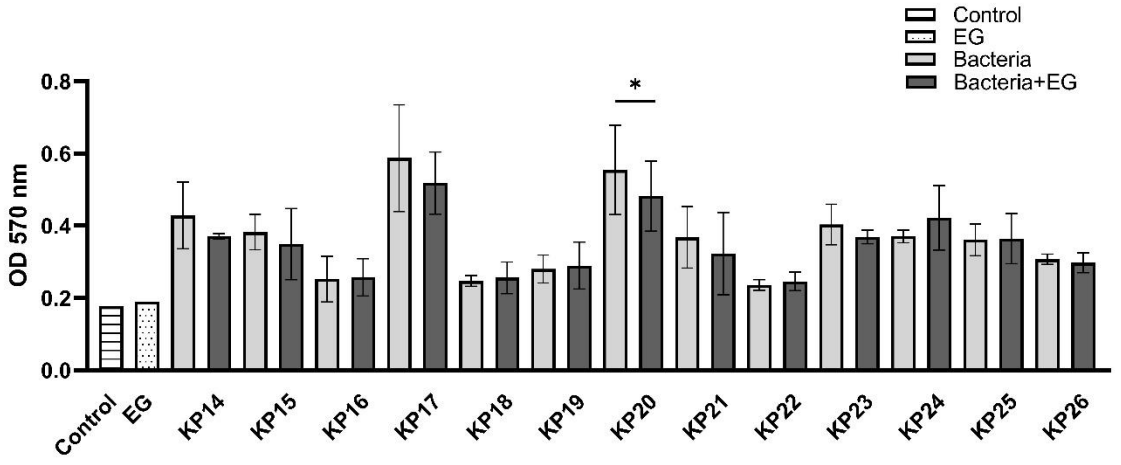

Figure 20: The effect of eugenol (EG) on the biofilm formation of ESBL *K. pneumoniae* isolates. The values of OD_{570} are represented as means ± SDs of 3 independent trials (n=3). The P values were obtained by one-tailed paired *t* test with *p* value ≤ 0.05 considered statistically significant.

Figure 21 shows that the biofilms formed by 7 out of the 13 *K. pneumoniae* non-ESBL isolates were reduced after the addition of thymol (KP3, KP5, KP6, KP8, KP9, KP11 and KP12), whereas figure 22 shows that the biofilms formed by 5 out of the 13 *K. pneumoniae* ESBL isolates were reduced after the addition of thymol (KP17, KP18, KP19, KP20 and KP21).

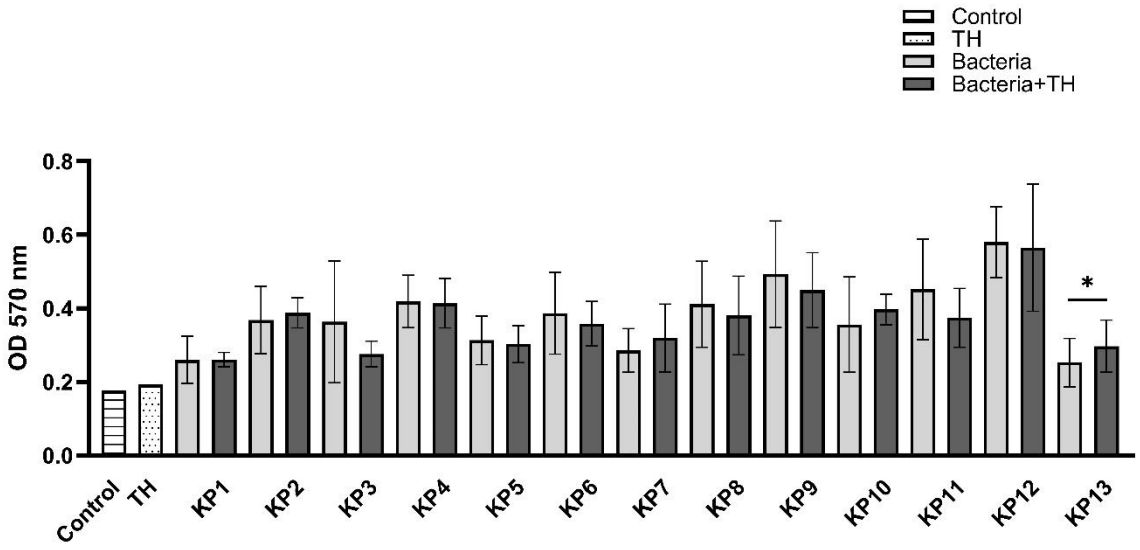

Figure 21: The effect of thymol (TH) on the biofilm formation of non-ESBL *K. pneumoniae* isolates. The values of OD_{570} are represented as means ± SDs of 3 independent trials (n=3). The P values were obtained by one-tailed paired *t* test with *p* value ≤ 0.05 considered statistically significant.

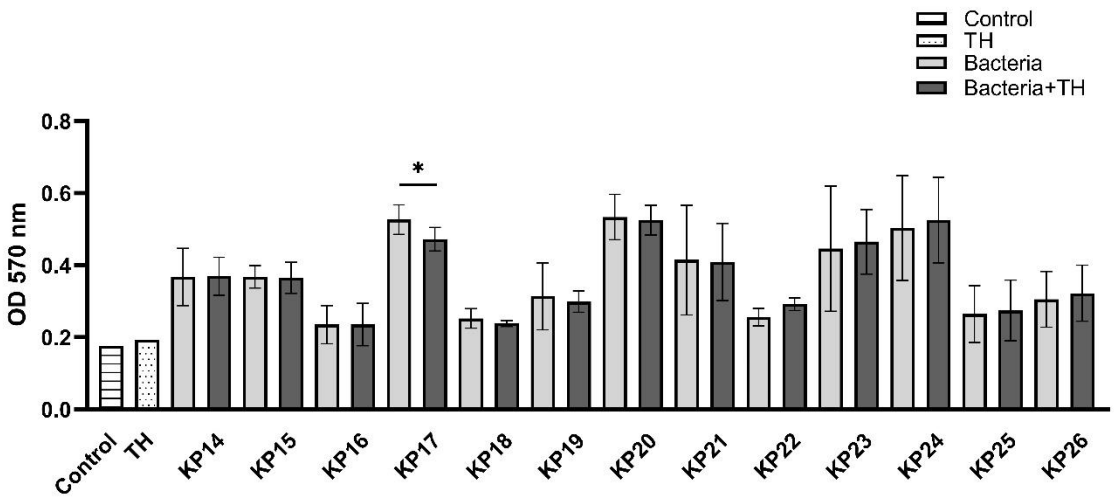

Figure 22: The effect of thymol (TH) on the biofilm formation of ESBL *K. pneumoniae* isolates. The values of OD_{570} are represented as means ± SDs of 3 independent trials (n=3). The P values were obtained by one-tailed paired *t* test with *p* value ≤ 0.05 considered statistically significant.

When the fourth essential oil, carvacrol, was tested, and as figure 23 shows, the biofilms formed by 5 out of the 13 *K. pneumoniae* non-ESBL isolates were reduced (KP2, KP3, KP5, KP8 and KP11). Figure 24 shows that the biofilms formed by 7 out of the 13 *K. pneumoniae* ESBL isolates were also reduced after the addition of carvacrol (KP14, KP15, KP19, KP20, KP23, KP24 and KP26).

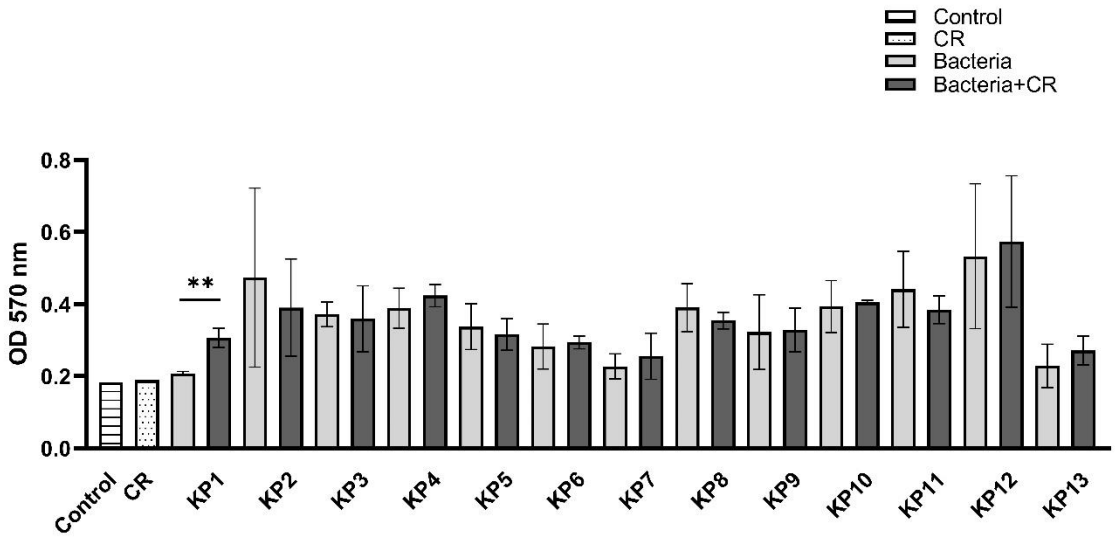

Figure 23: The effect of carvacrol (CR) on the biofilm formation of non-ESBL *K. pneumoniae* isolates. The values of OD_{570} are represented as means ± SDs of 3 independent trials (n=3). The P values were obtained by one-tailed paired *t* test with *p* value ≤ 0.05 considered statistically significant.

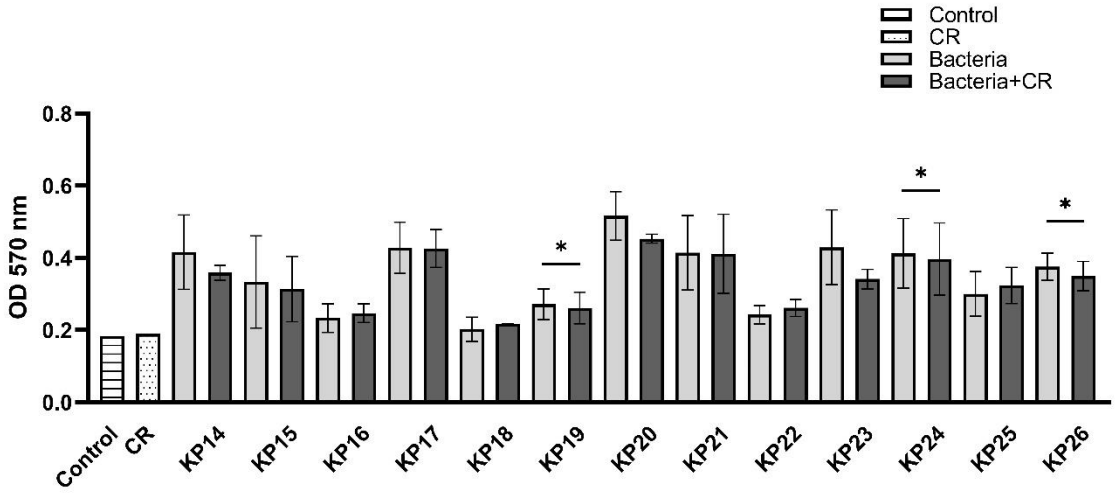

Figure 24: The effect of carvacrol (CR) on the biofilm formation of ESBL *K. pneumoniae* isolates. The values of OD_{570} are represented as means ± SDs of 3 independent trials (n=3). The P values were obtained by one-tailed paired *t* test with *p* value ≤ 0.05 considered statistically significant.

3.8. Synergistic effect of the effective essential oils

The possibility of a synergistic anti-biofilm effect of cinnamaldehyde and eugenol mixture and thymol and carvacrol mixture was determined by the TCP method. Figure 25 shows that the biofilms formed by 9 out of the 13 *K. pneumoniae* non-ESBL isolates were reduced after the addition of the cinnamaldehyde and eugenol mixture (KP1, KP3, KP5, KP6, KP8, KP9, KP10, KP12 and KP13), while figure 26 shows that the biofilms formed by 7 out of the 13 *K. pneumoniae* ESBL isolates were also reduced after the addition of the cinnamaldehyde and eugenol mixture (KP16, KP17, KP18, KP21, KP23, KP24 and KP26).

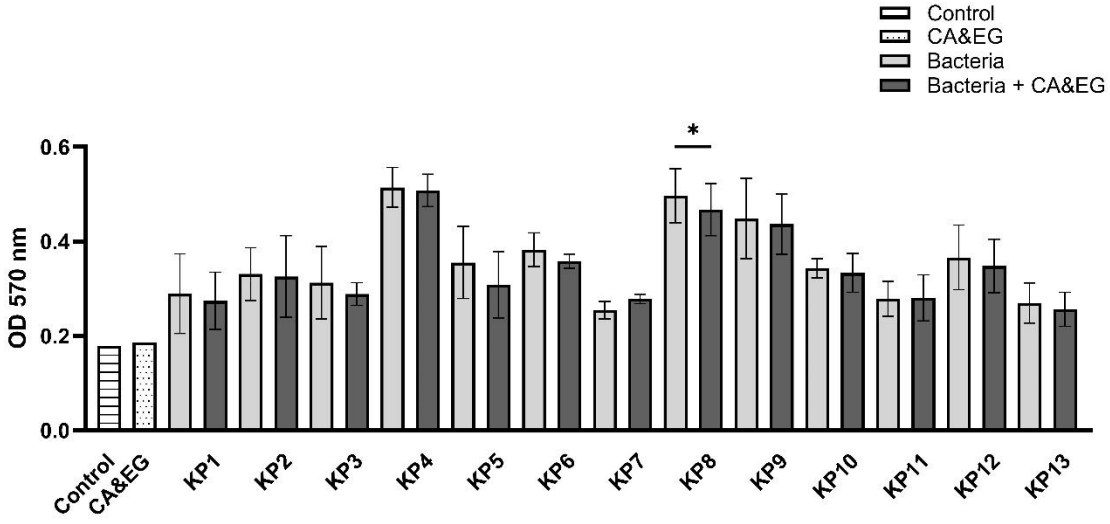

Figure 25: The effect of cinnamaldehyde and eugenol (CA&EG) mixture on the biofilm formation of non-ESBL *K. pneumoniae* isolates. The values of OD_{570} are represented as means ± SDs of 3 independent trials (n=3). The P values were obtained by one-tailed paired *t* test with *p* value ≤ 0.05 considered statistically significant.

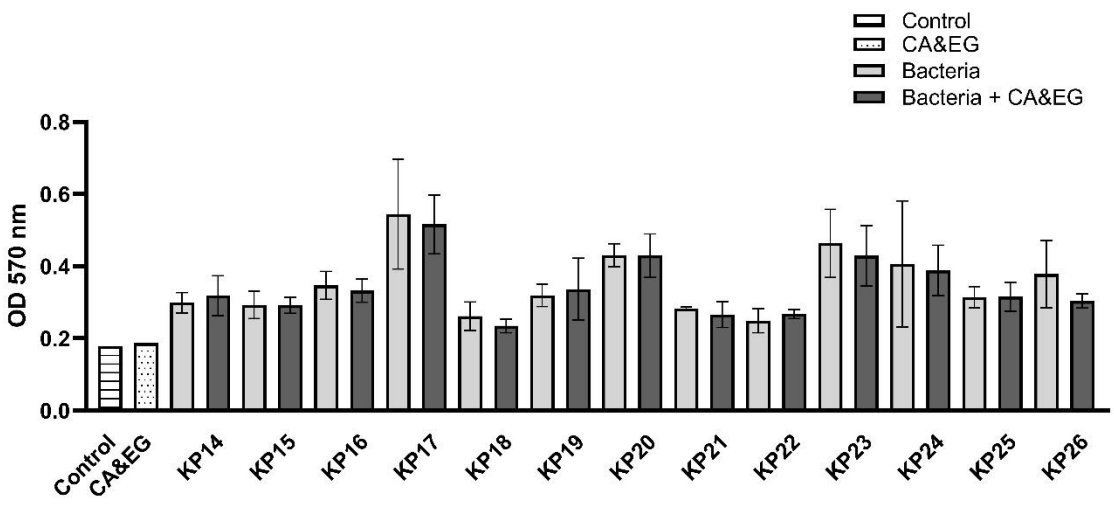

Figure 26: The effect of cinnamaldehyde and eugenol (CA&EG) mixture on the biofilm formation of ESBL *K. pneumoniae* isolates. The values of OD_{570} are represented as means ± SDs of 3 independent trials (n=3). The P values were obtained by one-tailed paired *t* test with *p* value ≤ 0.05 considered statistically significant.

On the other hand, figure 27 shows that the biofilms formed by 10 out of the 13 *K. pneumoniae* non-ESBL isolates was reduced after the addition of the thymol and carvacrol mixture (KP2, KP3, KP4, KP5, KP6, KP7, KP9, KP10, KP11 and KP12), whereas, figure 28 shows that the biofilms formed by 5 out of the 13 *K. pneumoniae* ESBL isolates were also reduced after the addition of the thymol and carvacrol mixture (KP17, KP19, KP21, KP23 and KP26).

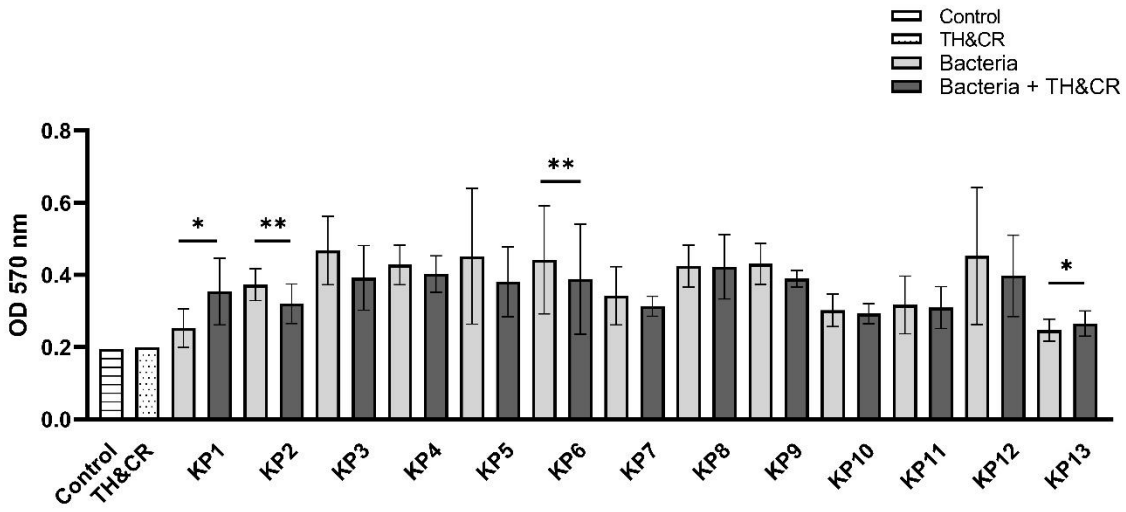

Figure 27: The effect of thymol and carvacrol (TH&CR) mixture on the biofilm formation of non-ESBL *K. pneumoniae* isolates. The values of OD_{570} are represented as means ± SDs of 3 independent trials (n=3). The P values were obtained by one-tailed paired *t* test with *p* value ≤ 0.05 considered statistically significant.

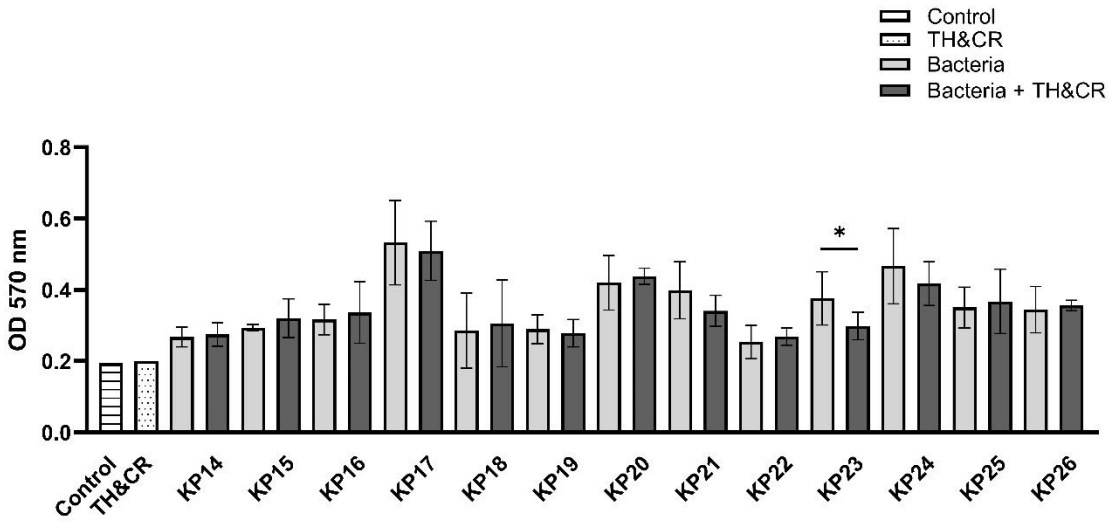

Figure 28: The effect of thymol and carvacrol (TH&CR) mixture on the biofilm formation of ESBL *K. pneumoniae* isolates. The values of OD_{570} are represented as means ± SDs of 3 independent trials (n=3). The P values were obtained by one-tailed paired *t* test with *p* value ≤ 0.05 considered statistically significant.

Finally, all the *Klebsiella* isolates that showed a reduced ability to form biofilms, due to the effect of each of the six essential oils solutions, were grouped together to check for the overall positive effect on biofilm inhibition. Figure 29 shows that the inhibition of *Klebsiella* biofilm formation by all the essential oils was statistically significant.

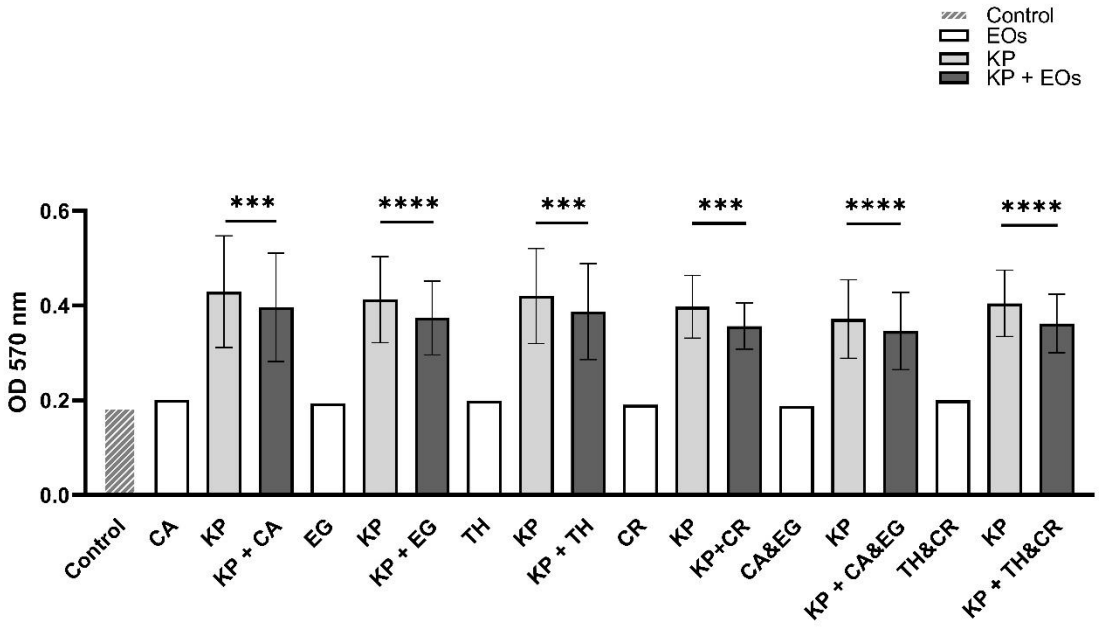

Figure 29: Overall biofilm inhibition of *K. pneumoniae* isolates by the different essential oil solutions. This graph include all the isolates that showed reduced biofilm formation upon addition of the essential oil solutions. The values of OD_{570} are represented as means ± SDs. The P values were obtained by one-tailed paired *t* test with *p* value ≤ 0.05 considered statistically significant. EOs: Essential oils, KP: *K. pneumoniae* isolates, KP+EOs: *Klebsiella* isolates and the essential oils.

Chapter Four

Discussion

Infectious diseases are a primary cause of death in the United States and worldwide. In the US, nosocomial infections alone cause around 60,000 to 90,000 deaths per year. In fact, about 80% of these hospital-acquired infections are caused by bacteria emerging from biofilms (Zodrow et al., 2012). A significant proportion of these nosocomial infections is caused by the Gram-negative rod: *Klebsiella pneumoniae*. One major virulence factor of *K. pneumoniae* is its ability to form a thick biofilm, enabling this pathogen to attach to biotic and abiotic surfaces, including native tissues, catheters and medical implants (Seifi et al., 2016). The overuse and abuse of antimicrobial agents, used for the treatment of infections, led to the emergence of antibiotic resistance, rendering many classes of antibiotics ineffective. Biofilm-embedded bacterial cells are, known to be, highly resistant to antibiotics, hence causing infections that are hard to eradicate (Zodrow et al., 2012). Due to this increasing emergence of antibiotic resistance, there is a high demand for antimicrobial agents that will not cause the spread of resistance genes (Kaskatepe et al., 2017). Plants and herbal products have always been of interest to researchers in medicine and the drug industry. Up till date, it is estimated that 80% of people worldwide use traditional medicines to treat their ailments. Many species of the plant kingdom are known to contain a diversity of phytochemicals that have medicinal values including antimicrobial properties (Mallhi et al., 2014). Since preventing the formation of biofilms is the best strategy for preventing infections caused by serious bacterial pathogens (Borges et al., 2013), this study aimed to find natural products and phytochemicals that can play a role in the control of the biofilm formation of *K. pneumoniae*.

The methanolic extract of *C. zeylanicum* is known to have strong antibacterial and antifungal properties (Hameed, Altameme, & Mohammed, 2016). Studies showed that the cinnamon essential oils had a strong inhibitory effect on different *E. coli* strains, with a

power surpassing that of the antibiotic streptomycin (Jamila et al., 2018). In this study, the *C. zeylanicum* methanolic extract presented an antimicrobial effect against *K. pneumoniae* isolates at concentrations of 0.2 g/ml and 0.15 g/ml (**Table 4** and **Figure 7**). However, at a concentration of cinnamon of 0.05 g/ml, the growth of *K. pneumoniae* was not affected and did not show an inhibition zone around the well (**Table 4** and **Figure 7**). Hence, any concentration of the cinnamon extract of 0.05 g/ml or below was considered as sub-inhibitory to the growth of the organism. On the other hand, the *O. onites* methanolic extract inhibited *K. pneumoniae* growth at 0.2 g/ml, 0.15 g/ml, 0.1 g/ml and 0.05 g/ml, but not at 0.02 g/ml (**Table 5** and **Figure 8**). A previous study done by Askun *et al*. (2009) had shown that the MIC of *O. onites* methanolic extract on *K. pneumoniae* was 10240 µg/mL (Askun, Tumen, Satil, & Ates, 2009), which was higher than the MIC of the extract used in this study. The biological activities and antimicrobial properties of these two plants were mainly due to their essential oils (Borges et al., 2013), hence these EOs are considered to be potential new antibacterial agents (Prabuseenivasan et al., 2006).

The sub-inhibitory concentrations of 0.02 g/ml, of both the cinnamon and oregano methanolic extracts, proved to have an anti-biofilm effect against the *K. pneumoniae* isolates of this study. Figures 9, 10, 11 and 12 show that after coating the 96 well plates with cinnamon or oregano, the *Klebsiella* isolates formed reduced size biofilms. The biofilm formation ability by both the non-ESBL (figure 9 and 11) and the ESBL (figure 10 and 12) isolates was inhibited. Different studies demonstrated that the antimicrobial properties of phytochemicals can affect not only planktonic bacteria but also bacterial biofilm formation and maturation. For instance, *Cinnamon cassia* EOs were able to affect the adhesion, biofilm formation, swimming motility and quorum sensing of *E. coli* (Borges et al., 2013). Another study also demonstrated the ability of cinnamon EOs to totally inhibit the biofilm formation of *Acinetobacter* strains at a sublethal dose (Szczepanski & Lipski, 2014). Additionally, oregano EOs were able to inhibit biofilm formation of *S. aureus* and *S. epidermidis* isolates, but at higher concentrations than the ones needed to inhibit planktonic bacteria (Kerekes et al., 2015).

The chemical composition and functional groups of essential oils are known to affect their biological activities and their power is related to their main constituents (Borges et al., 2013). Different species of plants have varying chemical constituents of

essential oils (Swamy et al., 2016). Different publications reported varying percentages of the chemical constituents of the cinnamon and oregano essential oils. The EOs of *C. zeylanicum* were reported to contain between 75 and 90% cinnamaldehyde, about 3 to 8% eugenol and 3 to 8% cinnamyl acetate (Jamila et al., 2018; Unlu et al., 2010). Whereas the *O. onites* EOs were reported to contain mainly between 36 to 84% carvacrol, 15 to 52% linalool and around 11.6% thymol (Kaskatepe et al., 2017). Many factors can affect the amounts of these constituents including the harvest period, the geographical location of the plant, its stage of maturity, the climate and the soil condition (Faleiro, 2011; Ozkan et al., 2010). This is why GC-MS was done to identify the specific concentration of the major essential oils in the *C. zeylanicum* and *O. onites* methanolic extracts used in this study.

The GC-MS technique has a broad field of applications, most importantly combining the characteristics of GC and MS in order to mainly separate and analyze multicomponent samples including essential oils, solvents and hydrocarbons (Hadi & Hameed, 2017). The GC-MS, for instance, was able to facilitate the detection and quantification of hundreds of metabolites present in one plant extract (Kopka, Fernie, Schauer, Willmitzer, & Lisec, 2006). Identifying the major active compounds of plants helps in understanding their therapeutic potential (Iordache, Culea, Gherman, & Cozar, 2009). In addition, such information helps in discovering the real significance of the folk remedies and in revealing new sources of economic phytochemicals for synthesizing different chemical substances (Hadi & Hameed, 2017). The development of GC-MS rendered the identification of the minor constituents of essential oils possible (Mallavarapu & Rao, 2007).

GC-MS works on introducing the essential oils, then separating and detecting them. The time from the injection of the EOs or extracts to their elution from the GC column into the detector is referred to as the retention time (RT). Table 6 shows that CA is the first chemical to elute from the column after 9.455 minutes of the injection, followed by TH at 9.56 min, CR at 9.66 min and finally EG at 10.245 min.

After analyzing five different concentrations of every chemical tested, at the same GC-MS conditions, standard curves for CA and EG (**Figure 13**) and for TH and CR (**Figure 14**) were drawn. The standard curves of the four essential oils illustrated in figure

13 and figure 14 show the peaks' areas corresponding to the different concentrations. The area of the peak is proportional to the concentration of the essential oils.

When the GC-MS of the cinnamon and oregano methanolic extracts were run, chromatograms were generated. These are graphs created by the computer to represent all the signals generated by the elution of the analytes. The X-axis presented the RT while the Y-axis assessed the intensity of the signal to quantify the constituents of the sample injected (Hameed et al., 2016). The analysis of figures 15 and 16 revealed the presence of CA and EG in the cinnamon extract and the presence of TH and CR in the oregano extract, in varying amounts. This was noted by the presence of several peaks in each chromatogram at different times and with different areas under the peaks.

Moreover, the more the concentration of the essential oils in the extract, the bigger was the signal obtained (Hameed et al., 2016). This was presented in figure 15, showing that the CA peak is much higher than EG peak which was compatible with their concentrations in the sample. Eventually, it was found that the concentration of CA in the cinnamon methanolic extract was 0.1286 g/ml as compared to the concentration of EG which was 0.003265 g/ml **(Table 7)**. This was compatible with a study done by Hameed *et al.* in 2016, which showed that cinnamaldehyde is the most prevalent essential oil in the bark of *C. zeylanicum* (Hameed et al., 2016). The same was denoted in the chromatogram of oregano methanolic extract showing that TH was present in the sample more than CR, with 0.3625 g/ml and 0.2465 g/ml concentrations respectively **(Table 7)**. A study done by Milovanović *et al.* (2009), showed that even with using low concentration of the oregano essential oils, the abundant compounds, including thymol and carvacrol, showed the largest areas compared to the other compounds' peaks. The investigators also reported that the peaks of the two isomeric compounds, TH and CR, were satisfactorily separated and showed a difference between their RTs (Milovanović et al., 2009), which is compatible with the results obtained in this study as is clear in figure 16.

Eugenol, carvacrol, and thymol are phenolic compounds, whereas cinnamaldehyde is an aliphatic aldehyde (Di Pasqua et al., 2007). The concentrations of the essential oils presented in table 7 were used to test for their anti-biofilm effect against *K. pneumoniae* isolates of this study. As presented in figure 17 and 18, CA was able to reduce the biofilm

formation of 69.23% of the non-ESBL *Klebsiella* isolates and 46.15% of the ESBLs isolates. Hence, cinnamaldehyde was able to inhibit the biofilm formation of 57.69% of all the *K. pneumoniae* isolates used in this study. According to the results reported by Zodrow *et al.* (2012), CA also inhibited the *S. aureus* biofilm formation successfully (Zodrow et al., 2012). Cinnamaldehyde is reported to act by altering the lipid profile and structure of the bacterial cell membrane, increasing its surface area and penetrating to the periplasm to deeper parts of the bacterium (Di Pasqua et al., 2007).

Eugenol was previously reported to inhibit or reduce the formation of the biofilms of *S. aureus* and *E.coli* on stainless steel surfaces (Millezi et al., 2019). In this study, eugenol reduced the biofilm formation of 46.15% of the non-ESBL *K. pneumoniae* isolates (**Figure 19**) and 53.85% of the ESBL isolates (**Figure 20**). In total, eugenol was able to inhibit the biofilm formation of 50% of the tested *K. pneumoniae* isolates.

On the other hand, thymol was able to reduce the biofilm formation of 53.85% of the non-ESBL *K. pneumoniae* isolates (**Figure 21**) and 38.46% of the ESBL isolates (**Figure 22**). Thus, a total of 46.15% of the biofilms formed by the *Klebsiella* strains in this study were inhibited by thymol. Moreover, carvacrol was able to inhibit the biofilm formation of 38.46% of the non-ESBL isolates (**Figure 23**) and 53.85% of the ESBL isolates (**Figure 24**); hence inhibiting the biofilm formation of 46.15% of all the *K. pneumoniae* isolates. Since thymol, carvacrol, and eugenol are hydrophobic molecules, they can interfere with the phospholipid bilayer membrane of bacteria, increasing the cell membrane permeability and disrupting its integrity, hence, leading to a leakage of ATP, nucleic acids and ions (Faleiro, 2011). Carvacrol and thymol were also reported to control the growth of dual-species biofilm of *S. aureus* and *Salmonella enterica* serovar Typhimurium in the initial growth phase (Borges et al., 2013; Szczepanski & Lipski, 2014). They also were able to reduce the biofilm formation of many *S. aureus, S. epidermidis, S. enterica* strains at sub-inhibitory concentrations (Kerekes et al., 2015). Carvacrol was also reported to inhibit the early phases of biofilm formation preventing the establishment of mature biofilms. It was also noted to interfere with the development of the biofilm made by *P. aeruginosa* (Sharifi-Rad et al., 2018).

Testing for a synergistic anti-biofilm effect between the two major essential oils of each extract was then attempted. A solution containing both CA and EG, at concentrations equal to those in the cinnamon plant extract, was prepared. The same was done for TH and CR. The results showed that the biofilm formation of 69.23% of the non-ESBL isolates was inhibited by CA and EG together (**Figure 25**) and that of 53.85% of the ESBL isolates was inhibited by the mixed solution of CA and EG (**Figure 26**). Whereas, the biofilm formation of 76.92% of the non-ESBL *K. pneumoniae* isolates was inhibited by TH and CR mixture (**Figure 27**) as compared to 38.46% of the ESBL isolates (**Figure 28**). In summary, the biofilm formation of 62% of all the *K. pneumoniae* isolates was inhibited by the CA and EG mixture and 57.69% by the TH and CR mixture. Since synergism is reported when the effect of the combined chemicals is found to be higher than the sum of their distinct effects (Faleiro, 2011), then it would not be possible to report that neither CA and EG mixed solution nor that of TH and CR demonstrated any synergistic effect. However, it is clear that the overall anti-biofilm effect of the essential oils whenever they were combined together, was higher than their individual effects.

Figure 29 demonstrates the overall biofilm inhibition of the *K. pneumoniae* isolates, that was affected by any of the six different essential oil solutions; All the reported inhibition results were statistically significant. It was noted that, in this study, however, that there was no substantial difference between the effects of the chosen EOs on the non-ESBL *Klebsiella* isolates as compared to the ESBL isolates **(figure 30).**

Under the effect of the tested EOs, both the non-ESBLs and ESBLs isolates showed a reduced ability to form biofilms. Moreover, it is worth noting that the biofilm formation ability of the four *Klebsiella* isolates, KP1, KP8, KP13 and KP24, which was not affected by the CA or EG alone, was inhibited when the two EOs were mixed together, suggesting that whenever these EOs are present simultaneously they affect multiple regulatory pathways related to biofilm formation, or together are capable of exhibiting a stronger effect. The same was manifested for the isolates KP4, KP7 and KP10 whose biofilm formation ability was not affected by neither TH nor CR, but was inhibited by their mixture.

It was also noted that the biofilm formation ability of some isolates (KP1, KP13 and KP16), was affected by the cinnamon EOs but not by the oregano EOs, while others (KP4 and KP19), showed a biofilm inhibition when treated with the oregano EOs and not with cinnamon EOs. This suggests that these two extracts and their EOs inhibit *K. pneumoniae* biofilms by targeting different regulatory pathways controlling biofilm formation.

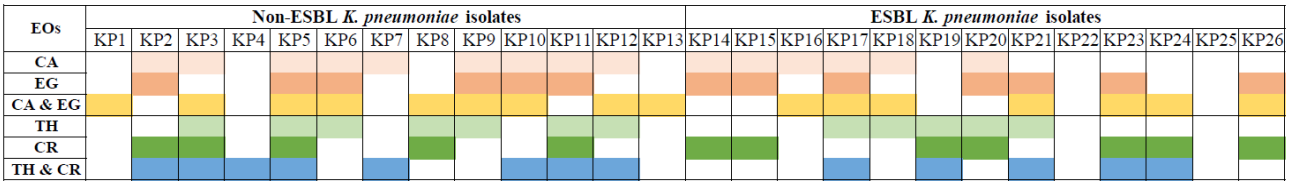

Figure 30: Summary representation of the anti-biofilm effect of EOs against all *K. pneumoniae* isolates. Colored boxes represent the inhibition of biofilm formation of *K. pneumoniae* isolates by the tested essential oils. EOs: Essential oils, CA: Cinnamaldehyde, EG: Eugenol, CA&EG: Cinnamaldehyde and eugenol mixture, TH: Thymol, CR: Carvacrol, TH&CR: Thymol and carvacrol mixture.

It is believed that many possible factors led to the variation between the percentage effects of the essential oils on the *K. pneumoniae* isolates and thus to the statistical significance of the biofilm formation inhibition. Variations between the OD_{570} values of the triplicate assays appeared in some of the *Klebsiella* isolates (**Table A1 to Table A18**). First, an increased incubation period for any inoculated 96 well-plate, could have led to a diminished supply of fresh nutrients to the bacteria, which may have stimulated bacterial detachment from the surface and hence less crystal violet staining (Merritt, Kadouri, & O'Toole, 2011). Second, in addition to the incubation time, inocula preparation according to the 0.5 McFarland turbidity standard, could vary between the replicates, hence, slightly affecting the biofilm formed by the isolate being tested (Kwasny & Opperman, 2010). Third, the repeated washings of the plates may have caused disruption of the biofilms (Roy, Tiwari, Donelli, & Tiwari, 2018). Fourth, in the TCP method, no growth of the bacterial isolate could be easily mistaken for an inability of attachment and biofilm

formation (Merritt et al., 2011). Fifth, a high number of sub-culturing of the *K. pneumoniae* isolates all through the study may have been accompanied by some mutations that could have affected the degree of biofilm formation.

The tested essential oils of this study led to the reduction of biofilm formation in a number of *Klebsiella* isolates, indicating that other chemical components of cinnamon and oregano could be playing a role in the total inhibition of *K. pneumoniae* biofilm formation. In fact, trace constituents, of the extracts and their essential oils, could have had a significant effect. The interaction between all the secondary constituents could lead to a total inhibition of the biofilm production (Jamila et al., 2018). Therefore, other essential oil constituents of the *C. zeylanicum* and *O. onites* should be quantified and tested for a probable anti-biofilm effect on different *K. pneumoniae* strains.

This study showed that natural plant-derived chemical compounds, such as cinnamaldehyde, eugenol, thymol and carvacrol, are promising alternatives for synthetic molecules in the inhibition of biofilm formation. Around 46.15% to 62% of the *K. pneumoniae* isolates, used in this study, manifested a reduction in their biofilm formation after exposure to these essential oils. Hence, coating biomaterials with these essential oils could help in the prevention of early stages of biofilm formation on catheters and other indwelling prosthetic devices, thus decreasing the risk of biofilm-associated infections in patients with indwelling devices. These natural products are inexpensive, more specific and most importantly nontoxic and exhibit less evolutionary pressure on microorganisms (Afroz et al., 2020). Therefore, using these natural products for prevention of infections will help in reducing the emergence of antibiotic resistance among pathogens and thus aid in solving one of the most challenging health problems.

References

Abdi-Ali, A., Mohammadi-Mehr, M., & Agha Alaei, Y. (2006). Bactericidal activity of various antibiotics against biofilm-producing pseudomonas aeruginosa. *International Journal of Antimicrobial Agents, 27*(3), 196-200. doi:10.1016/j.ijantimicag.2005.10.007

Afroz, N., Hoq, M. A., Jahan, S., Islam, M. M., Ahmed, F., Shahid-Ud-Daula, A., & Hasanuzzaman, M. (2020). Methanol soluble fraction of fruits of annona muricata possesses significant antidiarrheal activities. *Heliyon, 6*(1), e03112.

Alcántar-Curiel, M. D., Blackburn, D., Saldaña, Z., Gayosso-Vázquez, C., Iovine, N., De la Cruz, Miguel A, & Girón, J. A. (2013). Multi-functional analysis of klebsiella pneumoniae fimbrial types in adherence and biofilm formation. *Virulence, 4*(2), 129-138.

Ali, A. M., & Al-kakei, S. N. (2019). Virulence factors genotyping of klebsiella pneumoniae clinical isolates from baghdad. *Reviews in Medical Microbiology, 30*(1), 36-46. doi:10.1097/MRM.0000000000000151

Al-Mariri, A., & Safi, M. (2014). In vitro antibacterial activity of several plant extracts and oils against some gram-negative bacteria. *Iranian Journal of Medical Sciences, 39*(1), 36-43. Retrieved from https://www.ncbi.nlm.nih.gov/pubmed/24453392

Aminov, R. I. (2010). A brief history of the antibiotic era: Lessons learned and challenges for the future. *Frontiers in Microbiology, 1*, 134. doi:10.3389/fmicb.2010.00134

Ashurst, J. V., & Dawson, A. (2019). *Klebsiella pneumonia. in StatPearls [internet]*. StatPearls Publishing.

Askun, T., Tumen, G., Satil, F., & Ates, M. (2009). Characterization of the phenolic composition and antimicrobial activities of turkish medicinal plants. *Pharmaceutical Biology, 47*(7), 563-571. doi:10.1080/13880200902878069

Bachman, M. A., Lenio, S., Schmidt, L., Oyler, J. E., & Weiser, J. N. (2012). Interaction of lipocalin 2, transferrin, and siderophores determines the replicative niche of klebsiella pneumoniae during pneumonia. *mBio, 3*(6) doi:10.1128/mBio.00224-11

Bachman, M. A., Miller, V. L., & Weiser, J. N. (2009). Mucosal lipocalin 2 has pro-inflammatory and iron-sequestering effects in response to bacterial enterobactin. *PLoS Pathogens, 5*(10), e1000622. doi:10.1371/journal.ppat.1000622

Bachman, M. A., Oyler, J. E., Burns, S. H., Caza, M., Lépine, F., Dozois, C. M., & Weiser, J. N. (2011). *Klebsiella pneumoniae yersiniabactin promotes respiratory*

tract infection through evasion of lipocalin 2 American Society for Microbiology. doi:10.1128/IAI.05114-11

Balestrino, D., Ghigo, J., Charbonnel, N., Haagensen, J. A., & Forestier, C. (2008). The characterization of functions involved in the establishment and maturation of klebsiella pneumoniae in vitro biofilm reveals dual roles for surface exopolysaccharides. *Environmental Microbiology, 10*(3), 685-701.

Balestrino, D., Haagensen, J. A., Rich, C., & Forestier, C. (2005). Characterization of type 2 quorum sensing in klebsiella pneumoniae and relationship with biofilm formation. *Journal of Bacteriology, 187*(8), 2870-2880.

Bellich, B., Lagatolla, C., Tossi, A., Benincasa, M., Cescutti, P., & Rizzo, R. (2018). Influence of bacterial biofilm polysaccharide structure on interactions with antimicrobial peptides: A study on klebsiella pneumoniae. *International Journal of Molecular Sciences, 19*(6), 1685. doi:10.3390/ijms19061685

Bengoechea, J. A., & Sa Pessoa, J. (2019). Klebsiella pneumoniae infection biology: Living to counteract host defences. *FEMS Microbiology Reviews, 43*(2), 123-144. doi:10.1093/femsre/fuy043

Bialek-Davenet, S., Criscuolo, A., Ailloud, F., Passet, V., Jones, L., Delannoy-Vieillard, A., . . . Brisse, S. (2014). Genomic definition of hypervirulent and multidrug-resistant klebsiella pneumoniae clonal groups. *Emerging Infectious Diseases, 20*(11), 1812-1820. doi:10.3201/eid2011.140206

Borges, A., Abreu, A., Malheiro, J., Saavedra, M. J., & Simõe, M. (2013). *Biofilm prevention and control by dietary phytochemicals*

Brisse, S., Passet, V., Haugaard, A. B., Babosan, A., Kassis-Chikhani, N., Struve, C., & Decré, D. (2013). Wzi gene sequencing, a rapid method for determination of capsular type for klebsiella strains. *Journal of Clinical Microbiology, 51*(12), 4073-4078. doi:10.1128/JCM.01924-13

Candan, E. D., & Aksöz, N. (2015). Klebsiella pneumoniae: Characteristics of carbapenem resistance and virulence factors. *Acta Biochimica Polonica, 62*(4), 867-874. doi:10.18388/abp.2015_1148

Cantón, R., González-Alba, J. M., & Galán, J. C. (2012). CTX-M enzymes: Origin and diffusion. *Frontiers in Microbiology, 3*, 110. doi:10.3389/fmicb.2012.00110

Centers for Disease Control and Prevention. (2013). Standard operating procedure for PulseNet PFGE of escherichia coli O157: H7, escherichia coli non-O157 (STEC), salmonella serotypes, shigella sonnei and shigella flexneri. *Centers for Disease Control and Prevention, Atlanta,*

Cepas, V., López, Y., Munoz, E., Rolo, D., Ardanuy, C., Martí, S., . . . Soto, S. M. (2019). Relationship between biofilm formation and antimicrobial resistance in gram-negative bacteria. *Microbial Drug Resistance*, *25*(1), 72-79.

Chen, A., & Huebschmann, H. (2008). GCMS/MS analysis of the receptor sensitizing natural active spice ingredients capsaicin, piperine and thymol. *Thermo Fisher Scientific,*

Chen, F., Chan, C., Huang, Y., Liu, K., Peng, H., Chang, H., . . . Hsu, L. (2011). Structural and mechanical properties of klebsiella pneumoniae type 3 fimbriae. *Journal of Bacteriology*, *193*(7), 1718-1725. doi:10.1128/JB.01395-10

Chen, P., Sun, J., & Ford, P. (2014). Differentiation of the four major species of cinnamons (C. burmannii, C. verum, C. cassia, and C. loureiroi) using a flow injection mass spectrometric (FIMS) fingerprinting method. *Journal of Agricultural and Food Chemistry, 62*(12), 2516-2521. doi:10.1021/jf405580c

Choby, J. E., Howard-Anderson, J., & Weiss, D. S. (2020). Hypervirulent klebsiella pneumoniae – clinical and molecular perspectives. *Journal of Internal Medicine, 287*(3), 283-300. doi:10.1111/joim.13007

Chong, Y., Shimoda, S., & Shimono, N. (2018). Current epidemiology, genetic evolution and clinical impact of extended-spectrum [beta]-lactamase-producing escherichia coli and klebsiella pneumoniae. *Infection, Genetics and Evolution, 61*, 185. doi:10.1016/j.meegid.2018.04.005

Chung, P. Y. (2016). The emerging problems of klebsiella pneumoniae infections: Carbapenem resistance and biofilm formation. *FEMS Microbiology Letters, 363*(20) doi:10.1093/femsle/fnw219

Clegg, S., & Murphy, C. N. (2016). Epidemiology and virulence of klebsiella pneumoniae. *Microbiology Spectrum, 4*(1) doi:10.1128/microbiolspec.UTI-0005-2012

CLSI. (2013). Performance standards for antimicrobial susceptibility testing: CLSI approved standard M100-S23.

Cockerill, F. R., Patel, J., Alder, J., Bradford, P., Dudley, M., & Eliopoulos, G. (2013). Performance standards for antimicrobial susceptibility testing: Twenty-third informational supplement; M100-S23. *Wayne, PA: CLSI,*

Coskun, S., Girisgin, O., Kürkcüoglu, M., Malyer, H., Girisgin, A. O., Kırımer, N., & Baser, K. H. (2008). Acaricidal efficacy of origanum onites L. essential oil against rhipicephalus turanicus (ixodidae). *Parasitology Research, 103*(2), 259-261.

Craig, A. P., Fields, C. C., & Simpson, J. V. (2014). Development of a gas chromatography-mass spectrometry method for the quantification of glucaric acid

derivatives in beverage substrates. *International Journal of Analytical Chemistry, 2014*, 402938-8. doi:10.1155/2014/402938

D'Andrea, M. M., Arena, F., Pallecchi, L., & Rossolini, G. M. (2013). CTX-M-type β-lactamases: A successful story of antibiotic resistance. *International Journal of Medical Microbiology, 303*(6), 305-317. doi:10.1016/j.ijmm.2013.02.008

de Avila, E. D., de Molon, R. S., Vergani, C. E., de Assis Mollo, Jr, Francisco, & Salih, V. (2014). The relationship between biofilm and physical-chemical properties of implant abutment materials for successful dental implants. *Materials (Basel, Switzerland), 7*(5), 3651-3662. doi:10.3390/ma7053651

Desai, S., Sanghrajka, K., & Gajjar, D. (2019). High adhesion and increased cell death contribute to strong biofilm formation in klebsiella pneumoniae. *Pathogens*, *8*(4), 277.

Di Pasqua, R., Betts, G., Hoskins, N., Edwards, M., Ercolini, D., & Mauriello, G. (2007). Membrane toxicity of antimicrobial compounds from essential oils. *Journal of Agricultural and Food Chemistry*, *55*(12), 4863-4870. doi:10.1021/jf0636465

Djeribi, R., Bouchloukh, W., Jouenne, T., & Menaa, B. (2012). Characterization of bacterial biofilms formed on urinary catheters. *American Journal of Infection Control*, *40*(9), 854-859.

Emwas, A. M., Al-Talla, Z. A., Yang, Y., & Kharbatia, N. M. (2015). Gas chromatography–mass spectrometry of biofluids and extracts. *Metabonomics* (pp. 91-112) Springer.

Evrard, B., Balestrino, D., Dosgilbert, A., J. Bouya-Gachancard, J., Charbonnel, N., Forestier, C., & Tridon, A. (2010). Roles of capsule and lipopolysaccharide O antigen in interactions of human monocyte-derived dendritic cells and klebsiella pneumoniae. *Infection and Immunity, 78*(1), 210-219. doi:10.1128/IAI.00864-09

Faleiro, L. (2011). *The mode of antibacterial action of essential oils* FORMATEX.

Feldman, M. F., Mayer Bridwell, A. E., Scott, N. E., Vinogradov, E., McKee, S. R., Chavez, S. M., . . . Harding, C. M. (2019). A promising bioconjugate vaccine against hypervirulent klebsiella pneumoniae. *Proceedings of the National Academy of Sciences of the United States of America, 116*(37), 18655-18663. doi:10.1073/pnas.1907833116

Ferreira, R. L., da Silva, Brenda C M, Rezende, G. S., Nakamura-Silva, R., Pitondo-Silva, A., Campanini, E. B., . . . Pranchevicius, M. d. S. (2019). High prevalence of multidrug-resistant klebsiella pneumoniae harboring several virulence and β-lactamase encoding genes in a brazilian intensive care unit. *Frontiers in Microbiology, 9*, 3198. doi:10.3389/fmicb.2018.03198

Finlay, B. B., & McFadden, G. (2006). Anti-immunology: Evasion of the host immune system by bacterial and viral pathogens. *Cell, 124*(4), 767-782. doi:10.1016/j.cell.2006.01.034

Flemming, H., & Wingender, J. (2010). The biofilm matrix. *Nature Reviews Microbiology, 8*(9), 623-633. doi:10.1038/nrmicro2415

Follador, R., Heinz, E., Wyres, K. L., Ellington, M. J., Kowarik, M., Holt, K. E., & Thomson, N. R. (2016). The diversity of klebsiella pneumoniae surface polysaccharides. *Microbial Genomics, 2*(8), e000073. doi:10.1099/mgen.0.000073

Fong, J. N. C., & Yildiz, F. H. (2015). Biofilm matrix proteins. *Microbiology Spectrum, 3*(2) doi:10.1128/microbiolspec.MB-0004-2014

Founou, R. C., Founou, L. L., & Essack, S. Y. (2018). Extended spectrum beta-lactamase mediated resistance in carriage and clinical gram-negative ESKAPE bacteria: A comparative study between a district and tertiary hospital in south africa. *Antimicrobial Resistance and Infection Control, 7*(1), 134. doi:10.1186/s13756-018-0423-0

Fu, L., Huang, M., Zhang, X., Yang, X., Liu, Y., Zhang, L., . . . Zhou, Y. (2018). Frequency of virulence factors in high biofilm formation blaKPC-2 producing klebsiella pneumoniae strains from hospitals. *Microbial Pathogenesis, 116*, 168-172.

Gharrah, M. M., Mostafa El-Mahdy, A., & Barwa, R. F. (2017). Corrigendum to "association between virulence factors and extended spectrum beta-lactamase producing klebsiella pneumoniae compared to nonproducing isolates". *Interdisciplinary Perspectives on Infectious Diseases, 2018*, 1023076-2. doi:10.1155/2018/1023076

Gomes, A. É I., Stuchi, L. P., Siqueira, N. M. G., Henrique, J. B., Vicentini, R., Ribeiro, M. L., . . . Ferraz, L. F. C. (2018). Selection and validation of reference genes for gene expression studies in klebsiella pneumoniae using reverse transcription quantitative real-time PCR. *Scientific Reports, 8*(1), 9001-14. doi:10.1038/s41598-018-27420-2

Guilhen, C., Miquel, S., Charbonnel, N., Joseph, L., Carrier, G., Forestier, C., & Balestrino, D. (2019). Colonization and immune modulation properties of klebsiella pneumoniae biofilm-dispersed cells. *Npj Biofilms and Microbiomes, 5*(1), 1-11. doi:10.1038/s41522-019-0098-1

Guo, S., Xu, J., Wei, Y., Xu, J., Li, Y., & Xue, R. (2016). Clinical and molecular characteristics of klebsiella pneumoniae ventilator-associated pneumonia in mainland china. *BMC Infectious Diseases, 16*(1), 608-7. doi:10.1186/s12879-016-1942-z

Hadi, M. Y., & Hameed, I. H. (2017). Uses of gas chromatography-mass spectrometry (GC-MS) technique for analysis of bioactive chemical compounds of lepidium sativum: A review. *Research Journal of Pharmacy and Technology, 10*(11), 4039-4042. doi:10.5958/0974-360X.2017.00732.6

Hall-Stoodley, L., Costerton, J. W., & Stoodley, P. (2004). Bacterial biofilms: From the natural environment to infectious diseases. *Nature Reviews Microbiology, 2*(2), 95-108.

Hameed, I. H., Altameme, H. J., & Mohammed, G. J. (2016). Evaluation of antifungal and antibacterial activity and analysis of bioactive phytochemical compounds of cinnamomum zeylanicum (cinnamon bark) using gas chromatography-mass spectrometry. *Oriental Journal of Chemistry, 32*(4), 1769.

Happel, K. I., Dubin, P. J., Zheng, M., Ghilardi, N., Lockhart, C., Quinton, L. J., . . . Kolls, J. K. (2005). Divergent roles of IL-23 and IL-12 in host defense against klebsiella pneumoniae. *The Journal of Experimental Medicine, 202*(6), 761-769. doi:10.1084/jem.20050193

Hassan, A., Usman, J., Kaleem, F., Omair, M., Khalid, A., & Iqbal, M. (2011). Evaluation of different detection methods of biofilm formation in the clinical isolates. *Brazilian Journal of Infectious Diseases, 15*(4), 305-311. doi:10.1016/S1413-8670(11)70197-0

Holden, V. I., Breen, P., Houle, S., Dozois, C. M., & Bachman, M. A. (2016). Klebsiella pneumoniae siderophores induce inflammation, bacterial dissemination, and HIF-1α stabilization during pneumonia. *mBio, 7*(5), 1397. doi:10.1128/mBio.01397-16

Holt, K. E., Wertheim, H., Zadoks, R. N., Baker, S., Whitehouse, C. A., Dance, D., . . . Thomson, N. R. (2015). Genomic analysis of diversity, population structure, virulence, and antimicrobial resistance in klebsiella pneumoniae, an urgent threat to public health. Retrieved from http://eprints.gla.ac.uk/108761

Horan, T., Culver, D., Jarvis, W., Emori, G., Banerjee, S., Martone, W., & Thornsberry, C. (1988). Pathogens causing nosocomial infections preliminary data from the national nosocomial infections surveillance system. *Antimicrobic Newsletter, 5*(9), 65-67.

Hsieh, P., Lin, T., Yang, F., Wu, M., Pan, Y., Wu, S., & Wang, J. (2012). Lipopolysaccharide O1 antigen contributes to the virulence in klebsiella pneumoniae causing pyogenic liver abscess. *PloS One, 7*(3), e33155. doi:10.1371/journal.pone.0033155

Hunt, J. J., Wang, J., & Callegan, M. C. (2011). Contribution of mucoviscosity-associated gene A (magA) to virulence in experimental klebsiella pneumoniae endophthalmitis. *Investigative Ophthalmology & Visual Science, 52*(9), 6860-6866. doi:10.1167/iovs.11-7798

Huynh, D. T. N., Kim, A., & Kim, Y. (2017). Identification of pathogenic factors in klebsiella pneumoniae using impedimetric sensor equipped with biomimetic surfaces. *Sensors, 17*(6), 1406.

Ierardi, V., Domenichini, P., Reali, S., Chiappara, G., Devoto, G., & Valbusa, U. (2017). Klebsiella pneumoniae antibiotic resistance identified by atomic force microscopy. *Journal of Biosciences, 42*(4), 623-636. doi:10.1007/s12038-017-9713-6

Iordache, A., Culea, M., Gherman, C., & Cozar, O. (2009). Characterization of some plant extracts by GC–MS. *Nuclear Inst. and Methods in Physics Research, B, 267*(2), 338-342. doi:10.1016/j.nimb.2008.10.021

Ismail, A., Hneini, F., & Nawas, T. (2019). Tilia cordata: A potent inhibitor of growth and biofilm formation of bacterial clinical isolates.

Jamila, K., Naima, S., Farida, L., saadia, Z., saâdia, N., Mohammed, E., & Mohamed, O. (2018). COMPARATIVE STUDY OF THE ANTIBACTERIAL ACTIVITY OF CINNAMON AND ORIGAN ESSENTIAL OILS AND THEIR PRIMARYCOMPONENTS ON AVIAN escherichia coli STRAINS. *International Journal of Advanced Research, 6*(9), 373-381. doi:10.21474/IJAR01/7688

Jun, J. (2018). Klebsiella pneumoniae liver abscess. *Infection & Chemotherapy, 50*(3), 210-218.

Kaskatepe, B., Yildiz, S., Kiymaci, M., Yazgan, A., Cesur, S., & Erdem, S. (2017). Chemical composition and antimicrobial activity of the commercial origanum onites L. oil against nosocomial carbapenem resistant extended spectrum beta lactamase producer escherichia coli isolates. *Acta Biologica Hungarica, 68*(4), 466-476. doi:10.1556/018.68.2017.4.11

Kawasaki, T., & Kawai, T. (2014). Toll-like receptor signaling pathways. *Frontiers in Immunology, 5*(461)

Kerekes, E., Vidács, A., Török Jenei, J., Gömöri, C., Takó, M., Chandrasekaran, M., . . . Vágvölgyi, C. (2015). Essential oils against bacterial biofilm formation and quorum sensing of food-borne pathogens and spoilage microorganisms.

Keyrouz, E., Abou Raji El Feghali, P, Jaafar, M., & Nawas, T. (2017). Abou raji el feghali P, jaafar M, et al. malva neglecta: A natural inhibitor of bacterial growth and biofilm formation. *Journal of Medicinal Plants Research, 11*(24), 380-386.

Khaertynov, K. S., Anokhin, V. A., Rizvanov, A. A., Davidyuk, Y. N., Semyenova, D. R., Lubin, S. A., & Skvortsova, N. N. (2018). Virulence factors and antibiotic resistance of klebsiella pneumoniae strains isolated from neonates with sepsis. *Frontiers in Medicine, 5*, 225. doi:10.3389/fmed.2018.00225

Kim, J., Jo, A., Chukeatirote, E., & Ahn, J. (2016). Assessment of antibiotic resistance in klebsiella pneumoniae exposed to sequential in vitro antibiotic treatments. *Annals of Clinical Microbiology and Antimicrobials, 15*(1), 60. doi:10.1186/s12941-016-0173-x

Krapp, F., Morris, A. R., Ozer, E. A., & Hauser, A. R. (2017). Virulence characteristics of carbapenem-resistant klebsiella pneumoniae strains from patients with necrotizing skin and soft tissue infections. *Scientific Reports, 7*(1), 13533-14. doi:10.1038/s41598-017-13524-8

Kristo, M. J. (2012). Nuclear forensics. *Handbook of radioactivity analysis (third edition)* (pp. 1281-1304) Elsevier.

Kumar, D., Singh, A. K., Ali, M. R., & Chander, Y. (2014). Antimicrobial susceptibility profile of extended spectrum [beta]-lactamase producing escherichia coli from various clinical samples. *Infectious Diseases: Research and Treatment, 7*, 1. doi:10.4137/IDRT.S13820

Kumar, V., Sun, P., Vamathevan, J., Li, Y., Ingraham, K., Palmer, L., . . . Brown, J. R. (2011). Comparative genomics of klebsiella pneumoniae strains with different antibiotic resistance profiles. *Antimicrobial Agents and Chemotherapy, 55*(9), 4267-4276. doi:10.1128/AAC.00052-11

Kwasny, S. M., & Opperman, T. J. (2010). Static biofilm cultures of Gram-Positive pathogens grown in a microtiter format used for Anti-Biofilm drug discovery. *Current Protocols in Pharmacology, 50*(1), 13A.8.1-13A.8.23. doi:10.1002/0471141755.ph13a08s50

Lam, M. M. C., Wyres, K. L., Judd, L. M., Wick, R. R., Jenney, A., Brisse, S., & Holt, K. E. (2018). Tracking key virulence loci encoding aerobactin and salmochelin siderophore synthesis in klebsiella pneumoniae. *Genome Medicine, 10*(1), 77. doi:10.1186/s13073-018-0587-5

Lawlor, M. S., O'Connor, C., & Miller, V. L. (2007). Yersiniabactin is a virulence factor for klebsiella pneumoniae during pulmonary infection. *Infection and Immunity, 75*(3), 1463-1472. Retrieved from https://search.proquest.com/docview/20986082

Lee, C., Lee, J. H., Park, K. S., Jeon, J. H., Kim, Y. B., Cha, C., . . . Lee, S. H. (2017). Antimicrobial resistance of hypervirulent klebsiella pneumoniae: Epidemiology, hypervirulence-associated determinants, and resistance mechanisms. *Frontiers in Cellular and Infection Microbiology, 7*, 483. doi:10.3389/fcimb.2017.00483

Li, B., Zhao, Y., Liu, C., Chen, Z., & Zhou, D. (2014). Molecular pathogenesis of klebsiella pneumoniae. *Future Microbiology, 9*(9), 1071-1081. doi:10.2217/fmb.14.48

Li, G., Sun, S., Zhao, Z. Y., & Sun, Y. (2019). The pathogenicity of rmpA or aerobactin-positive klebsiella pneumoniae in infected mice. *Journal of International Medical Research, 47*(9), 4344-4352. doi:10.1177/0300060519863544

Lin, J., Chang, F., Fung, C., Xu, J., Cheng, H., Wang, J., . . . Siu, L. K. (2004). High prevalence of phagocytic-resistant capsular serotypes of klebsiella pneumoniae in liver abscess. *Microbes and Infection, 6*(13), 1191-1198. doi:10.1016/j.micinf.2004.06.003

Liu, C., & Guo, J. (2019). Hypervirulent klebsiella pneumoniae (hypermucoviscous and aerobactin positive) infection over 6 years in the elderly in china: Antimicrobial resistance patterns, molecular epidemiology and risk factor. *Annals of Clinical Microbiology and Antimicrobials, 18*(1), 4. doi:10.1186/s12941-018-0302-9

Llobet, E., Martínez-Moliner, V., Moranta, D., Dahlström, K. M., Regueiro, V., Tomás, A., . . . Bengoechea, J. A. (2015). Deciphering tissue-induced klebsiella pneumoniae lipid A structure. *Proceedings of the National Academy of Sciences of the United States of America, 112*(46), E6369. Retrieved from https://search.proquest.com/docview/1736918503

Magill, S. S., Edwards, J. R., Bamberg, W., Beldavs, Z. G., Dumyati, G., Kainer, M. A., . . . Fridkin, S. K. (2014). Multistate point-prevalence survey of health Care–Associated infections. *The New England Journal of Medicine, 370*(13), 1198-1208. doi:10.1056/NEJMoa1306801

Mallavarapu, G., & Rao, B. (2007). Chemical constituents and uses of cinnamomum zeylanicum blume. *Aromatic Plants from Asia their Chemistry and Application in Foof and Therapy.Har.Krishan Bhalla & Sons.Dehradun.India,*

Mallhi, T. H., Abbas, K., Ali, M., Qadir, M. I., Saleem, M., & Khan, Y. H. (2014). Hepatoprotective activity of methanolic extract of malva parviflora against paracetamol-induced hepatotoxicity in mice. *Bangladesh Journal of Pharmacology, 9*(3) doi:10.3329/bjp.v9i3.19105

Marr, C. M., & Russo, T. A. (2019). Hypervirulent klebsiella pneumoniae: A new public health threat. *Expert Review of Anti-Infective Therapy, 17*(2), 71-73. doi:10.1080/14787210.2019.1555470

Martin, R. M., & Bachman, M. A. (2018). Colonization, infection, and the accessory genome of klebsiella pneumoniae. *Frontiers in Cellular and Infection Microbiology, 8*, 4. doi:10.3389/fcimb.2018.00004

Martin, R. M., Cao, J., Brisse, S., Passet, V., Wu, W., Zhao, L., . . . Bachman, M. A. (2016). Molecular epidemiology of colonizing and infecting isolates of klebsiella pneumoniae. *mSphere, 1*(5), 261. doi:10.1128/mSphere.00261-16

Mazzariol, A., Bazaj, A., & Cornaglia, G. (2017). Multi-drug-resistant gram-negative bacteria causing urinary tract infections: A review. *Journal of Chemotherapy: Actual Role of Older Oral Antibiotics in the Treatment of Multidrug Resistant UTI Infections, 29*(sup1), 2-9. doi:10.1080/1120009X.2017.1380395

Merino, S., Camprubi, S., Alberti, S., Benedi, V., & Tomas, J. M. (1992). Mechanisms of klebsiella pneumoniae resistance to complement-mediated killing. *Infection and Immunity, 60*(6), 2529-2535. Retrieved from https://search.proquest.com/docview/16322286

Merritt, J. H., Kadouri, D. E., & O'Toole, G. A. (2011). Growing and analyzing static biofilms. *Current Protocols in Microbiology, 22*(1), 1B.1.1-1B.1.18. doi:10.1002/9780471729259.mc01b01s22

Millezi, A. F., Costa, K. A. D., Oliveira, J. M., Lopes, S. P., Pereira, M. O., & Piccoli, R. H. (2019). Antibacterial and anti-biofilm activity of cinnamon essential oil and eugenol. *Ciencia Rural, 49*(1) doi:10.1590/0103-8478cr20180314

Milovanović, I. L., Mišan, A. Č, Sakač, M. B., Čabarkapa, I. S., Šarić, B. M., Matić, J. J., & Jovanov, P. T. (2009). Evaluation of a GC-MS method for the analysis of oregano essential oil composition. *Food and Feed Research, 36*(3-4), 75-79.

Mohammed, A., Seid, M. E., Gebrecherkos, T., Tiruneh, M., & Moges, F. (2017). Bacterial isolates and their antimicrobial susceptibility patterns of wound infections among inpatients and outpatients attending the university of gondar referral hospital, northwest ethiopia. *International Journal of Microbiology, 2017*, 8953829-10. doi:10.1155/2017/8953829

Murphy, C. N., Mortensen, M. S., Krogfelt, K. A., & Clegg, S. (2013). Role of klebsiella pneumoniae type 1 and type 3 fimbriae in colonizing silicone tubes implanted into the bladders of mice as a model of catheter-associated urinary tract infections. *Infection and Immunity, 81*(8), 3009-3017. doi:10.1128/IAI.00348-13

Murphy, C. N., & Clegg, S. (2012). Klebsiella pneumoniae and type 3 fimbriae: Nosocomial infection, regulation and biofilm formation. *Future Microbiology, 7*(8), 991-1002. doi:10.2217/fmb.12.74

Nandakumar, V., Chittaranjan, S., Kurian, V. M., & Doble, M. (2013). Characteristics of bacterial biofilm associated with implant material in clinical practice. *Polymer Journal, 45*(2), 137-152. doi:10.1038/pj.2012.130

Navon-Venezia, S., Kondratyeva, K., & Carattoli, A. (2017). Klebsiella pneumoniae: A major worldwide source and shuttle for antibiotic resistance. *FEMS Microbiology Reviews, 41*(3), 252-275. doi:10.1093/femsre/fux013

Nirwati, H., Sinanjung, K., Fahrunissa, F., Wijaya, F., Napitupulu, S., Hati, V. P., . . . Nuryastuti, T. (2019). Biofilm formation and antibiotic resistance of klebsiella

pneumoniae isolated from clinical samples in a tertiary care hospital, klaten, indonesia. *BMC Proceedings, 13*(S11), 1-20. doi:10.1186/s12919-019-0176-7

Ojdana, D., Sacha, P., Wieczorek, P., Czaban, S., Michalska, A., Jaworowska, J., . . . Tryniszewska, E. (2014). The occurrence of blaCTX-M, blaSHV, and blaTEM genes in extended-spectrum β-lactamase-positive strains of klebsiella pneumoniae, escherichia coli, and proteus mirabilis in poland. doi:10.1155/2014/935842

Okshevsky, M., Regina, V. R., & Meyer, R. L. (2014). Extracellular DNA as a target for biofilm control. *Current Opinion in Biotechnology, 33*, 73-80. doi:10.1016/j.copbio.2014.12.002

Opoku-Temeng, C., Kobayashi, S. D., & DeLeo, F. R. (2019). Klebsiella pneumoniae capsule polysaccharide as a target for therapeutics and vaccines. *Computational and Structural Biotechnology Journal, 17*, 1360-1366. doi:10.1016/j.csbj.2019.09.011

Özkan, A., & Erdoğan, A. (2011). A comparative evaluation of antioxidant and anticancer activity of essential oil from origanum onites (lamiaceae) and its two major phenolic components. *Turkish Journal of Biology, 35*(6), 735-742.

Ozkan, G., Baydar, H., & Erbas, S. (2010). The influence of harvest time on essential oil composition, phenolic constituents and antioxidant properties of turkish oregano (origanum onites L.). *Journal of the Science of Food and Agriculture, 90*(2), 205-209. doi:10.1002/jsfa.3788

Paczosa, M. K., & Mecsas, J. (2016). Klebsiella pneumoniae: Going on the offense with a strong defense. *Microbiology and Molecular Biology Reviews : MMBR, 80*(3), 629-661. doi:10.1128/MMBR.00078-15

Padmini, N., Ajilda, A. A. K., Sivakumar, N., & Selvakumar, G. (2017). Extended spectrum β-lactamase producing escherichia coli and klebsiella pneumoniae: Critical tools for antibiotic resistance pattern. *Journal of Basic Microbiology, 57*(6), 460-470. doi:10.1002/jobm.201700008

Palacios, M., Miner, T. A., Frederick, D. R., Sepulveda, V. E., Quinn, J. D., Walker, K. A., & Miller, V. L. (2018). Identification of two regulators of virulence that are conserved in klebsiella pneumoniae classical and hypervirulent strains. *mBio, 9*(4), 1443. doi:10.1128/mBio.01443-18

Palzkill, T. (2013). Metallo-β-lactamase structure and function. *Annals of the New York Academy of Sciences, 1277*, 91.

Pendleton, J. N., Gorman, S. P., & Gilmore, B. F. (2013). Clinical relevance of the ESKAPE pathogens. *Expert Review of Anti-Infective Therapy, 11*(3), 297-308. doi:10.1586/eri.13.12

Piperaki, E., Syrogiannopoulos, G., Tzouvelekis, L., & Daikos, G. (2017). Klebsiella pneumoniae: Virulence, biofilm and antimicrobial resistance. *The Pediatric Infectious Disease Journal, 36*(10), 1002-1005. doi:10.1097/INF.0000000000001675

Podschun, R., Pietsch, S., Höller, C., & Ullmann, U. (2001). Incidence of klebsiella species in surface waters and their expression of virulence factors. *Applied and Environmental Microbiology, 67*(7), 3325-3327. doi:10.1128/AEM.67.7.3325-3327.2001

Podschun, R., & Ullmann, U. (1998). Klebsiella spp. as nosocomial pathogens: Epidemiology, taxonomy, typing methods, and pathogenicity factors. *Clinical Microbiology Reviews, 11*(4), 589-603. doi:10.1128/CMR.11.4.589

Pomakova, D., Pomakova, D., Hsiao, C., Hsiao, C., Beanan, J., Beanan, J., . . . Russo, T. (2012). Clinical and phenotypic differences between classic and hypervirulent klebsiella pneumonia: An emerging and under-recognized pathogenic variant. *European Journal of Clinical Microbiology & Infectious Diseases, 31*(6), 981-989. doi:10.1007/s10096-011-1396-6

Prabuseenivasan, S., Jayakumar, M., & Ignacimuthu, S. (2006). In vitro antibacterial activity of some plant essential oils. *BMC Complementary and Alternative Medicine, 6*(1), 39. doi:10.1186/1472-6882-6-39

Rabin, N., Zheng, Y., Opoku-Temeng, C., Du, Y., Bonsu, E., & Sintim, H. O. (2015). Biofilm formation mechanisms and targets for developing antibiofilm agents. *Future Medicinal Chemistry, 7*(4), 493-512.

Ramos-Vivas, J., Chapartegui-González, I., Fernández-Martínez, M., González-Rico, C., Fortún, J., Escudero, R., . . . Fariñas, M. C. (2019). Biofilm formation by multidrug resistant enterobacteriaceae strains isolated from solid organ transplant recipients. *Scientific Reports, 9*(1), 8928-10. doi:10.1038/s41598-019-45060-y

Rao, P. V., & Gan, S. H. (2014). Cinnamon: A multifaceted medicinal plant. *Evidence-Based Complementary and Alternative Medicine : eCAM, 2014*, 642942-12. doi:10.1155/2014/642942

Regueiro, V., Moranta, D., Frank, C. G., Larrarte, E., Margareto, J., March, C., . . . Bengoechea, J. A. (2011). Klebsiella pneumoniae subverts the activation of inflammatory responses in a NOD1-dependent manner. *Cellular Microbiology, 13*(1), 135-153. doi:10.1111/j.1462-5822.2010.01526.x

Ribeiro, S. M., Cardoso, M. H., Cândido, E. d. S., & Franco, O. L. (2016). Understanding, preventing and eradicating klebsiella pneumoniae biofilms. *Future Microbiology, 11*(4), 527-538. doi:10.2217/fmb.16.7

Rodrigues, C., Passet, V., Rakotondrasoa, A., Diallo, T. A., Criscuolo, A., & Brisse, S. (2019). Description of klebsiella africanensis sp. nov., klebsiella variicola subsp. tropicalensis subsp. nov. and klebsiella variicola subsp. variicola subsp. nov. *Research in Microbiology, 170*(3), 165-170. doi:10.1016/j.resmic.2019.02.003

Roy, R., Tiwari, M., Donelli, G., & Tiwari, V. (2018). Strategies for combating bacterial biofilms: A focus on anti-biofilm agents and their mechanisms of action. *Virulence, 9*(1), 522-554. doi:10.1080/21505594.2017.1313372

Russo, T. A., & Marr, C. M. (2019). Hypervirulent klebsiella pneumoniae. *Clinical Microbiology Reviews, 32*(3) doi:10.1128/CMR.00001-19

Russo, T. A., Olson, R., Macdonald, U., Metzger, D., Maltese, L. M., Drake, E. J., & Gulick, A. M. (2014). Aerobactin mediates virulence and accounts for increased siderophore production under iron-limiting conditions by hypervirulent (hypermucoviscous) klebsiella pneumoniae. *Infection and Immunity, 82*(6), 2356-2367. doi:10.1128/IAI.01667-13

Saga, T., & Yamaguchi, K. (2009). History of antimicrobial agents and resistant bacteria. *Jmaj, 52*(2), 103-108.

Sahly, H., Keisari, Y., & Ofek, I. (2009). Manno(rhamno)biose-containing capsular polysaccharides of klebsiella pneumoniae enhance opsono-stimulation of human polymorphonuclear leukocytes. *Journal of Innate Immunity, 1*(2), 136-144. doi:10.1159/000154812

Sakkas, H., Bozidis, P., Ilia, A., Mpekoulis, G., & Papadopoulou, C. (2019). Antimicrobial resistance in bacterial pathogens and detection of carbapenemases in klebsiella pneumoniae isolates from hospital wastewater. *Antibiotics (Basel, Switzerland), 8*(3), 85. doi:10.3390/antibiotics8030085

Schembri, M. A., Blom, J., Krogfelt, K. A., & Klemm, P. (2005). Capsule and fimbria interaction in klebsiella pneumoniae. *Infection and Immunity, 73*(8), 4626-4633. doi:10.1128/IAI.73.8.4626-4633.2005

Schroll, C., Barken, K. B., Krogfelt, K. A., & Struve, C. (2010). Role of type 1 and type 3 fimbriae in klebsiella pneumoniae biofilm formation. *BMC Microbiology, 10*(1), 179. doi:10.1186/1471-2180-10-179

Seifi, K., Kazemian, H., Heidari, H., Rezagholizadeh, F., Saee, Y., Shirvani, F., & Houri, H. (2016). Evaluation of biofilm formation among klebsiella pneumoniae isolates and molecular characterization by ERIC-PCR. *Jundishapur Journal of Microbiology, 9*(1), e30682. doi:10.5812/jjm.30682

Sharifi-Rad, M., Varoni, E. M., Iriti, M., Martorell, M., Setzer, W. N., del Mar Contreras, M., . . . Sharifi-Rad, J. (2018). Carvacrol and human health: A

comprehensive review. *Phytotherapy Research, 32*(9), 1675-1687. doi:10.1002/ptr.6103

Shon, A. S., Bajwa, R. P. S., & Russo, T. A. (2013). Hypervirulent (hypermucoviscous) klebsiella pneumoniae. *Virulence, 4*(2), 107-118. doi:10.4161/viru.22718

Shu, H., Fung, C., Liu, Y., Wu, K., Chen, Y., Li, L., . . . Tsai, S. (2009). Genetic diversity of capsular polysaccharide biosynthesis in klebsiella pneumoniae clinical isolates. *Microbiology, 155*(12), 4170-4183. doi:10.1099/mic.0.029017-0

Singla, S., Harjai, K., & Chhibber, S. (2013). Susceptibility of different phases of biofilm of klebsiella pneumoniae to three different antibiotics. *The Journal of Antibiotics, 66*(2), 61-66. doi:10.1038/ja.2012.101

Spyridopoulou, K., Fitsiou, E., Bouloukosta, E., Tiptiri-Kourpeti, A., Vamvakias, M., Oreopoulou, A., . . . Chlichlia, K. (2019). Extraction, chemical composition, and anticancer potential of origanum onites L. essential oil. *Molecules (Basel, Switzerland), 24*(14), 2612. doi:10.3390/molecules24142612

Stahlhut, S. G., Struve, C., Krogfelt, K. A., & Reisner, A. (2012). Biofilm formation of klebsiella pneumoniae on urethral catheters requires either type 1 or type 3 fimbriae. *FEMS Immunology & Medical Microbiology, 65*(2), 350-359.

Struve, C., & Krogfelt, K. A. (2004). Pathogenic potential of environmental klebsiella pneumoniae isolates. *Environmental Microbiology, 6*(6), 584-590. doi:10.1111/j.1462-2920.2004.00590.x

Struve, C., Roe, C. C., Stegger, M., Stahlhut, S. G., Hansen, D. S., Engelthaler, D. M., . . . Krogfelt, K. A. (2015). Mapping the evolution of hypervirulent klebsiella pneumoniae. *mBio, 6*(4), e00630. doi:10.1128/mBio.00630-15

Surgers, L., Boyd, A., Girard, P., Arlet, G., & Decré, D. (2019). Biofilm formation by ESBL-producing strains of escherichia coli and klebsiella pneumoniae. *International Journal of Medical Microbiology, 309*(1), 13-18. doi:10.1016/j.ijmm.2018.10.008

Swamy, M. K., Akhtar, M. S., & Sinniah, U. R. (2016). Antimicrobial properties of plant essential oils against human pathogens and their mode of action: An updated review. *Evidence-Based Complementary and Alternative Medicine : eCAM, 2016,* 3012462-21. doi:10.1155/2016/3012462

Szczepanski, S., & Lipski, A. (2014). Essential oils show specific inhibiting effects on bacterial biofilm formation. *Food Control, 36*(1), 224-229.

Tamang, M. D., Seol, S. Y., Oh, J., Kang, H. Y., Lee, J. C., Lee, Y. C., . . . Kim, J. (2008). Plasmid-mediated quinolone resistance determinants qnrA, qnrB, and qnrS

among clinical isolates of enterobacteriaceae in a korean hospital. *Antimicrobial Agents and Chemotherapy, 52*(11), 4159-4162.

Thieme, L., Hartung, A., Tramm, K., Klinger-Strobel, M., Jandt, K. D., Makarewicz, O., & Pletz, M. W. (2019). MBEC versus MBIC: The lack of differentiation between biofilm reducing and inhibitory effects as a current problem in biofilm methodology. *Biological Procedures Online, 21*(1) doi:10.1186/s12575-019-0106-0

Türkel, İ, Yıldırım, T., Yazgan, B., Bilgin, M., & Başbulut, E. (2018). Relationship between antibiotic resistance, efflux pumps, and biofilm formation in extended-spectrum β-lactamase producing klebsiella pneumoniae. *Journal of Chemotherapy, 30*(6-8), 354-363. doi:10.1080/1120009X.2018.1521773

Unlu, M., Ergene, E., Unlu, G. V., Zeytinoglu, H. S., & Vural, N. (2010). Composition, antimicrobial activity and in vitro cytotoxicity of essential oil from cinnamomum zeylanicum blume (lauraceae). *Food and Chemical Toxicology, 48*(11), 3274-3280.

Vading, M., Nauclér, P., Kalin, M., & Giske, C. G. (2018). Invasive infection caused by klebsiella pneumoniae is a disease affecting patients with high comorbidity and associated with high long-term mortality. *PloS One, 13*(4), e0195258. doi:10.1371/journal.pone.0195258

Wang, H., Wilksch, J., Strugnell, R., & Gee, M. (2015). Role of capsular polysaccharides in biofilm formation: An AFM nanomechanics study. Retrieved from http://researchbank.rmit.edu.au/view/rmit:49293

Wasfi, R., Elkhatib, W. F., & Ashour, H. M. (2016). Molecular typing and virulence analysis of multidrug resistant klebsiella pneumoniae clinical isolates recovered from egyptian hospitals. *Scientific Reports, 6*(1), 38929. doi:10.1038/srep38929

Whitchurch, C. B., Tolker-Nielsen, T., Ragas, P. C., & Mattick, J. S. (2002). Extracellular DNA required for bacterial biofilm formation. *Science, 295*(5559), 1487.

Wu, C., Huang, Y., Fung, C., & Peng, H. (2010). Regulation of the klebsiella pneumoniae kpc fimbriae by the site-specific recombinase KpcI. *Microbiology (Reading, England), 156*(Pt 7), 1983-1992. doi:10.1099/mic.0.038158-0

Wu, K., Li, L., Yan, J., Tsao, N., Liao, T., Tsai, H., . . . Tsai, S. (2009). Genome sequencing and comparative analysis of klebsiella pneumoniae NTUH-K2044, a strain causing liver abscess and meningitis. doi:10.1128/JB.00315-09

Wyres, K. L., & Holt, K. E. (2016). Klebsiella pneumoniae population genomics and antimicrobial-resistant clones. *Trends in Microbiology, 24*(12), 944-956. doi:10.1016/j.tim.2016.09.007

Wyres, K. L., & Holt, K. E. (2018). Klebsiella pneumoniae as a key trafficker of drug resistance genes from environmental to clinically important bacteria. *Current Opinion in Microbiology, 45*, 131-139. doi:10.1016/j.mib.2018.04.004

Wyres, K. L., Lam, M. M. C., & Holt, K. E. (2020). Population genomics of klebsiella pneumoniae. *Nature Reviews. Microbiology,* doi:10.1038/s41579-019-0315-1

Yeh, K., Kurup, A., Siu, L. K., Koh, Y. L., Fung, C., Lin, J., . . . Koh, T. (2007). Capsular serotype K1 or K2, rather than magA and rmpA, is a major virulence determinant for klebsiella pneumoniae liver abscess in singapore and taiwan. *Journal of Clinical Microbiology, 45*(2), 466-471. doi:10.1128/JCM.01150-06

Yu, V. L., Hansen, D. S., Ko, W. C., Sagnimeni, A., Klugman, K. P., von Gottberg, A., . . . Benedi, V. J. (2007). Virulence characteristics of klebsiella and clinical manifestations of K. pneumoniae bloodstream infections. *Emerging Infectious Diseases, 13*(7), 986-993. doi:10.3201/eid1307.070187

Zeynudin, A., Pritsch, M., Schubert, S., Messerer, M., Liegl, G., Hoelscher, M., . . . Wieser, A. (2018). Prevalence and antibiotic susceptibility pattern of CTX-M type extended-spectrum β-lactamases among clinical isolates of gram-negative bacilli in jimma, ethiopia. *BMC Infectious Diseases, 18*(1), 524. doi:10.1186/s12879-018-3436-7

Zheng, J., Lin, Z., Chen, C., Chen, Z., Lin, F., Wu, Y., . . . Deng, Q. (2018). Biofilm formation in klebsiella pneumoniae bacteremia strains was found to be associated with CC23 and the presence of wcaG. *Frontiers in Cellular and Infection Microbiology, 8*, 21. doi:10.3389/fcimb.2018.00021

Zodrow, K. R., Schiffman, J. D., & Elimelech, M. (2012). Biodegradable polymer (PLGA) coatings featuring cinnamaldehyde and carvacrol mitigate biofilm formation. *Langmuir, 28*(39), 13993-13999. doi:10.1021/la303286v

Appendix

Appendix Tables

Table A1. Biofilm forming capacity of non-ESBL *K. pneumoniae* isolates used in this study.

Table A2. Biofilm forming capacity of ESBL *K. pneumoniae* isolates used in this study.

Table A3. OD_{570} values of the biofilm formed by non-ESBL *K. pneumoniae* isolates with and without cinnamon methanolic extract.

Table A4. OD_{570} values of the biofilm formed by ESBL *K. pneumoniae* isolates with and without cinnamon methanolic extract.

Table A5. OD_{570} values of the biofilm formed by non-ESBL *K. pneumoniae* isolates with and without oregano methanolic extract.

Table A6. OD_{570} values of the biofilm formed by ESBL *K. pneumoniae* isolates with and without oregano methanolic extract.

Table A7. OD_{570} values of the biofilm formed by non-ESBL *K. pneumoniae* isolates with and without cinnamaldehyde (CA).

Table A8. OD_{570} values of the biofilm formed by ESBL *K. pneumoniae* isolates with and without cinnamaldehyde (CA).

Table A9. OD_{570} values of the biofilm formed by non-ESBL *K. pneumoniae* isolates with and without eugenol (EG).

Table A10. OD_{570} values of the biofilm formed by ESBL *K. pneumoniae* isolates with and without eugenol (EG).

Table A11. OD_{570} values of the biofilm formed by non-ESBL *K. pneumoniae* isolates with and without thymol (TH).

Table A12. OD_{570} values of the biofilm formed by ESBL *K. pneumoniae* isolates with and without thymol (TH).

Table A13. OD_{570} values of the biofilm formed by non-ESBL *K. pneumoniae* isolates with and without carvacrol (CR).

Table A14. OD_{570} values of the biofilm formed by ESBL *K. pneumoniae* isolates with and without carvacrol (CR).

Table A15. OD_{570} values of the biofilm formed by non-ESBL *K. pneumoniae* isolates with and without cinnamaldehyde and eugenol mixture (CA&EG).

Table A16. OD_{570} values of the biofilm formed by ESBL *K. pneumoniae* isolates with and without cinnamaldehyde and eugenol mixture (CA&EG).

Table A17. OD_{570} values of the biofilm formed by non-ESBL *K. pneumoniae* isolates with and without thymol and carvacrol mixture (TH&CR).

Table A18. OD_{570} values of the biofilm formed by ESBL *K. pneumoniae* isolates with and without thymol and carvacrol mixture (TH&CR).

Table A1: Biofilm forming capacity of non-ESBL *K. pneumoniae* isolates used in this study. The OD_{570} value are represented as means of the triplicate assays (n=3). (-) the negative control. AVG: Average.

	-	KP1	-	KP2	-	KP3	-	KP4	-	KP5
N1	0.320212	0.421336	0.300348	0.366263	0.307385	0.431567	0.306685	0.533289	0.332503	0.521083
N2	0.34178	0.552964	0.138343	0.24394	0.225443	0.325071	0.332424	0.538607	0.327743	0.470278
N3	0.320212	0.421336	0.375338	0.455553	0.213879	0.336534	0.339124	0.650368	0.255104	0.353561
AVG	**0.327401**	**0.465212**	**0.271343**	**0.355252**	**0.248902**	**0.364391**	**0.326078**	**0.574088**	**0.305117**	**0.448307**

	-	KP6	-	KP7	-	KP8	-	KP9	-	KP10
N1	0.24396	0.301682	0.307806	0.57115	0.337864	0.517224	0.332862	0.555741	0.221003	0.401019
N2	0.263316	0.325056	0.274433	0.521991	0.360743	0.573696	0.313072	0.526358	0.255619	0.400681
N3	0.272347	0.333406	0.298147	0.624689	0.310069	0.446919	0.324252	0.601384	0.306275	0.484966
AVG	**0.259874**	**0.320048**	**0.293462**	**0.57261**	**0.336225**	**0.512613**	**0.323395**	**0.561161**	**0.260966**	**0.428888**

	-	KP11	-	KP12	-	KP13
N1	0.283857	0.434975	0.343438	0.631513	0.303768	0.625911
N2	0.273655	0.513734	0.279564	0.461906	0.305676	0.573204
N3	0.222594	0.529836	0.231224	0.399212	0.383581	0.609464
AVG	**0.260035**	**0.492848**	**0.284742**	**0.497544**	**0.331008**	**0.602859**

Table A2: Biofilm forming capacity of ESBL *K. pneumoniae* isolates used in this study. The OD_{570} value are represented as means of the triplicate assays (n=3). (-) the negative control. AVG: Average.

	-	KP14	-	KP15	-	KP16	-	KP17	-
N1	0.218744	0.338861	0.22557	0.333355	0.264541	0.394264	0.336418	0.463142	0.297882
N2	0.125325	0.3195	0.244842	0.359737	0.249826	0.321977	0.309451	0.433778	0.285634
N3	0.280032	0.534385	0.263409	0.502542	0.307625	0.392893	0.207394	0.436661	0.236223
AVG	**0.208034**	**0.397582**	**0.244607**	**0.398545**	**0.273998**	**0.369711**	**0.284421**	**0.444527**	**0.273246**

	-	KP19	-	KP20	-	KP21	-	KP22	-
N1	0.153984	0.368826	0.177005	0.614939	0.204848	0.379628	0.187921	0.259421	0.23136
N2	0.186917	0.320527	0.209717	0.757841	0.259553	0.495704	0.241185	0.329117	0.185468
N3	0.360112	0.51856	0.326072	0.779831	0.205479	0.4459	0.143815	0.222879	0.155985
AVG	**0.233671**	**0.402638**	**0.237598**	**0.717537**	**0.223293**	**0.440411**	**0.190973**	**0.270472**	**0.190938**

	-	KP24	-	KP25	-	KP26
N1	0.18155	0.346911	0.290449	0.584979	0.222391	0.391716
N2	0.188885	0.381831	0.269767	0.599751	0.248469	0.403369
N3	0.243918	0.437649	0.249826	0.552339	0.374052	0.505896
AVG	**0.204784**	**0.388797**	**0.270014**	**0.579023**	**0.281637**	**0.43366**

Table A3: OD_{570} values of the biofilm formed by non-ESBL *K. pneumoniae* isolates with and without cinnamon methanolic extract (C). The OD_{570} values are represented as means of triplicate assays (n=3). -: Negative control, B: Bacteria, B+C: Bacteria and cinnamon extract, AVG: Average.

	KP1				KP2				KP3			
	-	C	B	B + C	-	C	B	B + C	-	C	B	B + C
N1	0.337755	0.819463	0.606582	1.282933	0.343639	0.715384	1.006746	0.768773	0.349877	0.738364	0.536575	0.738498333
N2	0.366504	1.300956	0.586946	0.778368429	0.374619	1.311806	0.648704	0.886674714	0.365661	1.281475	0.63054	1.159457286
N3	0.353155	1.101153	0.610593	0.654271286	0.367597	1.109191	0.726506	0.677362625	0.361598	1.165991	0.601598	0.594844286
AVG	**0.352471**	**1.073857**	**0.601374**	**0.905190905**	**0.361952**	**1.045461**	**0.793985**	**0.777603446**	**0.359045**	**1.061943**	**0.589571**	**0.830933302**

	KP4				KP5				KP6			
	-	C	B	B + C	-	C	B	B + C	-	C	B	B + C
N1	0.3459	0.616959	0.652818	0.722708	0.346351	0.78605	1.214997	0.719670667	0.347606	0.748402	0.383896	0.970250714
N2	0.370834	1.232964	0.691775	0.841919857	0.363655	1.251355	0.883704	0.648265125	0.366073	1.372092	0.363629	0.8781755
N3	0.35801	1.00581	0.547219	0.559050125	0.363014	0.927362	0.6924	0.4768305	0.357207	1.008728	0.370098	0.712185
AVG	**0.358248**	**0.951911**	**0.630604**	**0.707892661**	**0.357673**	**0.988255**	**0.930367**	**0.614922097**	**0.356962**	**1.043074**	**0.372541**	**0.853537071**

	KP7				KP8				KP9			
	-	C	B	B + C	-	C	B	B + C	-	C	B	B + C
N1	0.340764	0.67834	0.700841	0.739231286	0.344312	0.898567	0.576787	0.734661	0.343271	0.745743	0.958686	0.69281225
N2	0.375971	1.314993	0.715558	0.6691075	0.367945	1.276143	0.544054	0.587035143	0.373368	1.331157	0.723422	0.742658875
N3	0.364146	0.913873	0.696433	0.47848725	0.368128	1.190069	0.554914	0.565752	0.368395	1.186047	0.630258	0.465564375
AVG	**0.360294**	**0.969069**	**0.704277**	**0.628942012**	**0.360128**	**1.121593**	**0.558585**	**0.629149381**	**0.361678**	**1.087649**	**0.770789**	**0.6336785**

	KP10				KP11				KP12			
	-	C	B	B + C	-	C	B	B + C	-	C	B	B + C
N1	0.341402	0.729265	1.044843	0.741215286	0.34091	0.662135	0.832421	0.675152571	0.349662	0.849171	1.081103	0.84143925
N2	0.364252	1.271271	1.071124	0.717708	0.375558	1.222836	0.916941	0.63530675	0.375965	1.335344	0.871792	0.665889875
N3	0.359841	1.119645	0.668393	0.541898375	0.356503	0.958743	0.644952	0.40396975	0.365738	1.077415	0.649379	0.485479375
AVG	**0.355165**	**1.04006**	**0.92812**	**0.666940554**	**0.357657**	**0.947905**	**0.798105**	**0.571476357**	**0.363788**	**1.08731**	**0.867425**	**0.6642695**

	KP13			
	-	C	B	B + C
N1	0.343855	0.672522	0.877684	0.837348
N2	0.367967	1.296401	0.866954	0.9473925
N3	0.367277	1.119552	0.658707	0.683855
AVG	**0.3597**	**1.029492**	**0.801115**	**0.822865167**

Table A4: OD_{570} values of the biofilm formed by ESBL *K. pneumoniae* isolates with and without cinnamon methanolic extract (C). The OD_{570} values are represented as means of triplicate assays (n=3). -: Negative control, B: Bacteria, B+C: Bacteria and cinnamon extract, AVG: Average.

	KP14				KP15				KP16			
	-	C	B	B + C	-	C	B	B + C	-	C	B	B + C
N1	0.349025	0.744884	0.556638	0.720374	0.348739	0.799701	0.714006	0.589378	0.345792	0.683339	0.672985	0.591248
N2	0.379048	1.314681	1.004165	0.738184	0.36693	1.21051	0.864258	0.759533	0.365844	1.296537	0.728812	0.874139
N3	0.367333	1.152191	0.883961	0.684709	0.359618	1.033054	0.687558	0.547298	0.362728	0.937259	0.518004	0.568974
AVG	**0.365135**	**1.070585**	**0.814922**	**0.714422**	**0.358429**	**1.014421**	**0.755274**	**0.632069**	**0.358121**	**0.972378**	**0.639934**	**0.67812**

	KP17				KP18				KP19			
	-	C	B	B + C	-	C	B	B + C	-	C	B	B + C
N1	0.352691	0.738553	0.574706	0.667	0.344276	0.765331	0.869751	0.614831	0.343673	0.726904	0.583736	0.63364
N2	0.372447	1.312654	0.921819	0.637636	0.369831	1.34393	0.895915	1.219546	0.370991	1.237995	0.97692	0.914713
N3	0.374209	1.233457	0.933055	0.643834	0.362819	1.073253	0.571336	0.669145	0.359423	0.970136	0.893932	0.48523
AVG	**0.366449**	**1.094888**	**0.80986**	**0.64949**	**0.358975**	**1.060838**	**0.779**	**0.834507**	**0.358029**	**0.978345**	**0.818196**	**0.677861**

	KP20				KP21				KP22			
	-	C	B	B + C	-	C	B	B + C	-	C	B	B + C
N1	0.344555	0.775985	0.779831	0.803313	0.354604	0.608115	0.790541	0.632367	0.348897	0.75533	0.605306	0.672013
N2	0.365805	1.392178	1.06522	0.728552	0.377352	1.245189	0.65366	0.638107	0.370948	1.311311	0.966137	0.819048
N3	0.370616	1.238608	0.762189	0.524819	0.369821	1.219715	0.495859	0.522069	0.365424	1.20255	0.751483	0.701201
AVG	**0.360326**	**1.13559**	**0.86908**	**0.685561**	**0.367259**	**1.024339**	**0.646687**	**0.597514**	**0.361756**	**1.089731**	**0.774308**	**0.730754**

	KP23				KP24				KP25			
	-	C	B	B + C	-	C	B	B + C	-	C	B	B + C
N1	0.353562	0.664819	0.279481	0.771493	0.350744	0.821906	0.50509	0.799465	0.353024	0.810201	0.368884	0.660683
N2	0.363638	1.318078	0.695879	0.896187	0.373432	1.22527	0.785666	0.839577	0.373331	1.242159	0.629113	1.065
N3	0.371951	0.954146	0.741448	0.605805	0.371579	1.021418	0.904396	0.737193	0.368211	1.045274	0.781754	0.646588
AVG	**0.36305**	**0.979014**	**0.572269**	**0.757828**	**0.365252**	**1.022865**	**0.731717**	**0.792078**	**0.364855**	**1.032545**	**0.59325**	**0.790757**

	KP26			
	-	C	B	B + C
N1	0.345463	0.738234	0.518863	0.963088
N2	0.367961	1.264667	0.736897	1.023372
N3	0.373214	0.913305	0.543147	0.790006
AVG	**0.362213**	**0.972069**	**0.599635**	**0.925489**

Table A5: OD_{570} values of the biofilm formed by non-ESBL *K. pneumoniae* isolates with and without oregano methanolic extract (O). The OD_{570} values are represented as means of triplicate assays (n=3). -: Negative control, B: Bacteria, B+O: Bacteria and oregano extract, AVG: Average.

	KP1				KP2				KP3			
	-	O	B	B + O	-	O	B	B + O	-	O	B	B + O
N1	0.350344	1.161255	0.654565	2.123154	0.350704	1.130024	0.819832	2.206899	0.346454	1.082297	0.538231	1.876323
N2	0.370567	1.271609	0.576119	1.69761	0.362299	1.255353	0.722322	1.554264	0.375525	1.106925	0.675259	1.118635
N3	0.357042	1.236069	0.518839	0.914875	0.371555	1.286529	0.621492	1.028685	0.35516	1.249735	0.478378	0.715603
AVG	**0.359318**	**1.222978**	**0.583174**	**1.578547**	**0.361519**	**1.223968**	**0.721216**	**1.596616**	**0.359046**	**1.146319**	**0.563956**	**1.236854**

	KP4				KP5				KP6			
	-	O	B	B + O	-	O	B	B + O	-	O	B	B + O
N1	0.349451	1.150825	0.666981	1.488871	0.353049	1.235535	0.809548	1.812039	0.345255	1.112813	0.445	1.256896
N2	0.370768	1.21609	0.74215	1.101078	0.362807	1.288912	0.823075	1.286948	0.383177	1.364415	0.40687	1.034965
N3	0.367703	1.191696	0.572038	1.08135	0.355797	1.265376	0.712812	0.864281	0.355071	1.31865	0.511601	0.700897
AVG	**0.362641**	**1.186204**	**0.66039**	**1.223766**	**0.357218**	**1.263274**	**0.781812**	**1.321089**	**0.361167**	**1.265293**	**0.45449**	**0.997586**

	KP7				KP8				KP9			
	-	O	B	B + O	-	O	B	B + O	-	O	B	B + O
N1	0.342214	1.126649	0.739289	2.021491	0.350864	1.178686	0.457954	1.896565	0.360705	1.166921	0.765934	1.337255
N2	0.367308	1.25769	0.737527	1.129647	0.359986	1.14613	0.477727	1.301275	0.368956	1.114034	0.671099	0.988201
N3	0.352625	1.267742	0.640214	0.839958	0.37547	1.258958	0.531578	1.011931	0.350889	1.147444	0.572366	0.764232
AVG	**0.354049**	**1.21736**	**0.705677**	**1.330365**	**0.362107**	**1.194591**	**0.489086**	**1.403257**	**0.360183**	**1.1428**	**0.669799**	**1.029896**

	KP10				KP11				KP12			
	-	O	B	B + O	-	O	B	B + O	-	O	B	B + O
N1	0.353897	1.216689	1.164033	1.445152	0.359277	1.177439	0.809377	1.688993	0.359554	1.288079	1.222908	1.848821
N2	0.373123	1.277959	0.879742	1.467111	0.369622	1.191745	0.897545	1.03254	0.380506	1.216003	0.924479	1.077879
N3	0.35603	1.137161	0.572921	0.688672	0.348932	1.143699	0.645989	0.864703	0.351896	1.09562	0.554545	0.747253
AVG	**0.361017**	**1.210603**	**0.872232**	**1.200312**	**0.359277**	**1.170961**	**0.784304**	**1.195412**	**0.363985**	**1.1999**	**0.900644**	**1.224651**

	KP13			
	-	O	B	B + O
N1	0.368927	1.167805	0.725893	1.646027
N2	0.378786	1.343148	1.083918	1.750321
N3	0.363345	1.209216	0.519901	0.907565
AVG	**0.370353**	**1.240056**	**0.776571**	**1.434638**

Table A6: OD_{570} values of the biofilm formed by ESBL *K. pneumoniae* isolates with and without oregano methanolic extract (O). The OD_{570} values are represented as means of triplicate assays (n=3). -: Negative control, B: Bacteria, B+O: Bacteria and oregano extract, AVG: Average.

	KP14				KP15				KP16			
	-	O	B	B + O	-	O	B	B + O	-	O	B	B + O
N1	0.367251	1.179434	0.57206	2.191	0.362972	1.327291	1.036154	1.747574	0.368331	1.28197	0.711064	1.561545
N2	0.373192	1.342298	0.885468	1.560614	0.386969	1.310421	0.83818	1.404151	0.361061	1.086797	0.709625	1.033864
N3	0.35431	1.262846	0.761854	1.002757	0.371684	1.225821	0.687134	0.761373	0.357667	1.120333	0.518888	0.70358
AVG	**0.364917**	**1.261526**	**0.739794**	**1.58479**	**0.373875**	**1.287845**	**0.853823**	**1.304366**	**0.362353**	**1.163033**	**0.646526**	**1.099663**

	KP17				KP18				KP19			
	-	O	B	B + O	-	O	B	B + O	-	O	B	B + O
N1	0.354854	1.163031	0.62741	1.653244	0.365462	1.182001	0.755261	1.242579	0.365319	1.264613	0.51856	1.473821
N2	0.375266	1.391968	0.894985	1.163279	0.370517	1.365535	0.886805	1.320234	0.372572	1.267176	0.899038	1.208194
N3	0.376759	1.383936	0.839753	0.908502	0.372709	1.417583	0.575495	1.010436	0.366117	1.215154	0.992373	0.809675
AVG	**0.36896**	**1.312978**	**0.787383**	**1.241675**	**0.369562**	**1.321706**	**0.739187**	**1.191083**	**0.368003**	**1.248981**	**0.803324**	**1.163897**

	KP20				KP21				KP22			
	-	O	B	B + O	-	O	B	B + O	-	O	B	B + O
N1	0.36548	1.189649	1.213367	1.412201	0.356122	1.283473	0.669287	1.377788	0.36494	1.222871	0.785267	1.611611
N2	0.359952	1.429523	1.110266	1.35936	0.362074	1.266986	0.65542	1.419266	0.381751	1.284844	0.753917	1.217505
N3	0.372445	1.326289	0.799885	0.991468	0.372342	1.316019	0.464921	0.726606	0.378697	1.223774	0.749204	1.043959
AVG	**0.365959**	**1.315153**	**1.041173**	**1.254343**	**0.363513**	**1.288826**	**0.596542**	**1.174553**	**0.375129**	**1.24383**	**0.762796**	**1.291025**

	KP23				KP24				KP25			
	-	O	B	B + O	-	O	B	B + O	-	O	B	B + O
N1	0.344694	1.165736	0.406065	1.778655	0.357408	1.262558	0.661344	1.579383	0.364577	1.221579	0.430768	1.460644
N2	0.360521	1.44469	0.697534	1.162794	0.384147	1.326935	0.874646	1.211137	0.364713	1.322706	0.680719	0.941636
N3	0.360984	1.270374	0.742466	0.900425	0.373544	1.225655	0.794524	0.842597	0.37857	1.224921	0.790289	0.925457
AVG	**0.3554**	**1.2936**	**0.615355**	**1.280625**	**0.3717**	**1.271716**	**0.776838**	**1.211039**	**0.369287**	**1.256402**	**0.633925**	**1.109246**

	KP26			
	-	O	B	B + O
N1	0.360381	1.194435	0.606708	1.220144
N2	0.359977	1.124046	0.663345	0.949907
N3	0.345067	1.404832	0.471874	0.664023
AVG	**0.355142**	**1.241104**	**0.580643**	**0.944691**

Table A7: OD_{570} values of the biofilm formed by non-ESBL *K. pneumoniae* isolates with and without cinnamaldehyde (CA). The OD_{570} values are represented as means of triplicate assays (n=3). -: Negative control, B: Bacteria, B+CA: Bacteria and cinnamaldehyde, AVG: Average.

	KP1				KP2				KP3			
	-	CA	B	B + CA	-	CA	B	B + CA	-	CA	B	B + CA
N1	0.181135	0.174923	0.209062	0.202102	0.180661	0.201067	0.291893	0.294149	0.202803	0.198846	0.378996	0.353474
N2	0.180903	0.174679	0.246329	0.273318	0.189539	0.192478	0.635185	0.419872	0.202532	0.207802	0.395805	0.342428
N3	0.182561	0.210551	0.264484	0.297974	0.199352	0.212457	0.424628	0.347292	0.189289	0.213809	0.407671	0.380601
AVG	**0.181533**	**0.186718**	**0.239958**	**0.257798**	**0.189851**	**0.202**	**0.450569**	**0.353771**	**0.198208**	**0.206819**	**0.394157**	**0.358834**

	KP4				KP5				KP6			
	-	CA	B	B + CA	-	CA	B	B + CA	-	CA	B	B + CA
N1	0.174773	0.181481	0.58773	0.561055	0.174176	0.181358	0.313637	0.330201	0.181808	0.212683	0.469854	0.365277
N2	0.184172	0.180788	0.51774	0.560335	0.184023	0.193281	0.399716	0.317424	0.186317	0.192833	0.366465	0.301529
N3	0.191134	0.208917	0.618611	0.637668	0.190274	0.210531	0.396176	0.40746	0.197773	0.210062	0.47756	0.398699
AVG	**0.183359**	**0.190395**	**0.574694**	**0.586353**	**0.182824**	**0.195057**	**0.369843**	**0.351695**	**0.188632**	**0.205193**	**0.43796**	**0.355168**

	KP7				KP8				KP9			
	-	CA	B	B + CA	-	CA	B	B + CA	-	CA	B	B + CA
N1	0.184589	0.210566	0.377055	0.407663	0.191961	0.212805	0.328859	0.452307	0.197592	0.201364	0.43274	0.447364
N2	0.174306	0.185319	0.288146	0.204364	0.174894	0.181322	0.381274	0.355874	0.176847	0.191474	0.344826	0.313495
N3	0.190664	0.2114	0.40795	0.41808	0.197939	0.215709	0.696954	0.5876	0.190189	0.21202	0.424859	0.386089
AVG	**0.183186**	**0.202428**	**0.357717**	**0.343369**	**0.188265**	**0.203278**	**0.469029**	**0.465261**	**0.188209**	**0.20162**	**0.400808**	**0.382316**

	KP10				KP11				KP12			
	-	CA	B	B + CA	-	CA	B	B + CA	-	CA	B	B + CA
N1	0.17612	0.212971	0.303778	0.396809	0.188715	0.206698	0.332499	0.304183	0.176451	0.207302	0.705903	0.716088
N2	0.188216	0.180078	0.431331	0.272358	0.20145	0.203205	0.370168	0.346502	0.18312	0.22018	0.509548	0.473181
N3	0.191404	0.208713	0.451507	0.435041	0.193239	0.209875	0.310214	0.295734	0.196039	0.203231	0.40382	0.370397
AVG	**0.185247**	**0.200587**	**0.395539**	**0.368069**	**0.194468**	**0.206593**	**0.337627**	**0.315473**	**0.185203**	**0.210238**	**0.539757**	**0.519889**

	KP13			
	-	CA	B	B + CA
N1	0.179849	0.177919	0.241494	0.27034
N2	0.1954	0.197801	0.28953	0.32302
N3	0.196177	0.203867	0.315428	0.36938
AVG	**0.190476**	**0.193196**	**0.282151**	**0.320913**

Table A8: OD_{570} values of the biofilm formed by ESBL *K. pneumoniae* isolates with and without cinnamaldehyde (CA). The OD_{570} values are represented as means of triplicate assays (n=3). -: Negative control, B: Bacteria, B+CA: Bacteria and cinnamaldehyde, AVG: Average.

	KP14				KP15				KP16			
	-	CA	B	B + CA	-	CA	B	B + CA	-	CA	B	B + CA
N1	0.173651	0.188733	0.374135	0.404507	0.175247	0.186942	0.4669	0.43077	0.188933	0.200794	0.221235	0.224793
N2	0.185887	0.191659	0.286135	0.318107	0.195044	0.207544	0.321108	0.360735	0.182556	0.188568	0.283478	0.247331
N3	0.194876	0.208957	0.717273	0.528798	0.200602	0.202656	0.38237	0.353638	0.200549	0.202118	0.354612	0.360351
AVG	**0.184805**	**0.19645**	**0.459181**	**0.417137**	**0.190298**	**0.199047**	**0.390126**	**0.381715**	**0.190679**	**0.19716**	**0.286441**	**0.277492**

	KP17				KP18				KP19			
	-	CA	B	B + CA	-	CA	B	B + CA	-	CA	B	B + CA
N1	0.180334	0.174989	0.47149	0.468495	0.175872	0.19599	0.237128	0.21258	0.180597	0.18634	0.312416	0.307114
N2	0.189777	0.182051	0.696513	0.690289	0.197893	0.211893	0.323014	0.284322	0.153984	0.146165	0.368826	0.490898
N3	0.196174	0.205454	0.92016	0.783762	0.199439	0.211017	0.280096	0.252266	0.202842	0.210932	0.304737	0.353206
AVG	**0.188762**	**0.187498**	**0.696054**	**0.647516**	**0.191068**	**0.2063**	**0.280079**	**0.249723**	**0.179141**	**0.181146**	**0.32866**	**0.38374**

	KP20				KP21				KP22			
	-	CA	B	B + CA	-	CA	B	B + CA	-	CA	B	B + CA
N1	0.192127	0.198858	0.557282	0.529332	0.181531	0.183201	0.312498	0.289853	0.173208	0.173979	0.279784	0.283817
N2	0.177005	0.184061	0.614939	0.578214	0.192383	0.181079	0.544072	0.569341	0.187921	0.185313	0.259421	0.272674
N3	0.206766	0.210407	0.757841	0.761346	0.207655	0.195135	0.273435	0.337289	0.202968	0.209934	0.329117	0.303583
AVG	**0.191966**	**0.197775**	**0.643354**	**0.622964**	**0.193856**	**0.186471**	**0.376668**	**0.398827**	**0.188032**	**0.189742**	**0.28944**	**0.286691**

	KP23				KP24				KP25			
	-	CA	B	B + CA	-	CA	B	B + CA	-	CA	B	B + CA
N1	0.180503	0.195627	0.364192	0.45312	0.182419	0.195407	0.411699	0.545778	0.1701	0.173559	0.349623	0.371999
N2	0.180655	0.18687	0.38371	0.417148	0.190647	0.205826	0.45649	0.534449	0.187631	0.188834	0.298939	0.315968
N3	0.200156	0.206984	0.647622	0.657934	0.199519	0.215754	0.495218	0.487799	0.192123	0.203069	0.385279	0.4169
AVG	**0.187105**	**0.196494**	**0.465175**	**0.509401**	**0.190861**	**0.205662**	**0.454469**	**0.522675**	**0.183285**	**0.188487**	**0.344614**	**0.368289**

	KP6			
	-	CA	B	B + CA
N1	0.175873	0.178369	0.40515	0.328365
N2	0.175726	0.181179	0.278438	0.290658
N3	0.204279	0.218927	0.403369	0.460333
AVG	**0.185293**	**0.192825**	**0.362319**	**0.359785**

Table A9: OD_{570} values of the biofilm formed by non-ESBL *K. pneumoniae* isolates with and without eugenol (EG). The OD_{570} values are represented as means of triplicate assays (n=3). -: Negative control, B: Bacteria, B+EG: Bacteria and eugenol, AVG: Average.

	KP1				KP2				KP3			
	-	EG	B	B + EG	-	EG	B	B + EG	-	EG	B	B + EG
N1	0.173223	0.206836	0.308381	0.437648	0.174724	0.219663	0.313393	0.300809	0.193894	0.220481	0.341863	0.420376
N2	0.178887	0.198073	0.260992	0.266378	0.216758	0.201441	0.427261	0.389047	0.21001	0.177991	0.45064	0.578346
N3	0.161367	0.166357	0.306467	0.30777	0.17721	0.189571	0.482874	0.390678	0.212585	0.204198	0.373703	0.426874
AVG	**0.171159**	**0.190422**	**0.291947**	**0.337265**	**0.189564**	**0.203558**	**0.407843**	**0.360178**	**0.205496**	**0.20089**	**0.388736**	**0.475199**

	KP4				KP5				KP6			
	-	EG	B	B + EG	-	EG	B	B + EG	-	EG	B	B + EG
N1	0.167977	0.185981	0.471731	0.464735	0.185233	0.177073	0.308435	0.290299	0.180681	0.2225	0.305779	0.28441
N2	0.159328	0.162751	0.464777	0.493382	0.184038	0.221807	0.333771	0.30619	0.195757	0.217246	0.378207	0.37523
N3	0.152663	0.17018	0.561112	0.635223	0.1969	0.199386	0.45124	0.31078	0.192584	0.193759	0.423994	0.413231
AVG	**0.159989**	**0.172971**	**0.499207**	**0.531113**	**0.188723**	**0.199422**	**0.364482**	**0.302423**	**0.189674**	**0.211168**	**0.369327**	**0.357623**

	KP7				KP8				KP9			
	-	EG	B	B + EG	-	EG	B	B + EG	-	EG	B	B + EG
N1	0.154526	0.18402	0.252578	0.288319	0.159484	0.175175	0.349561	0.376484	0.17663	0.22039	0.505899	0.461213
N2	0.150371	0.169619	0.284788	0.2715	0.180657	0.184475	0.424965	0.458074	0.205479	0.190351	0.410539	0.465458
N3	0.191179	0.227659	0.440933	0.479923	0.203029	0.177528	0.761647	0.703002	0.192182	0.212687	0.698598	0.601137
AVG	**0.165358**	**0.193766**	**0.326099**	**0.346581**	**0.181057**	**0.179059**	**0.512058**	**0.51252**	**0.19143**	**0.207809**	**0.538345**	**0.509269**

	KP10				KP11				KP12			
	-	EG	B	B + EG	-	EG	B	B + EG	-	EG	B	B + EG
N1	0.166326	0.202662	0.213517	0.230932	0.155734	0.178636	0.235393	0.265154	0.164978	0.201835	0.519849	0.527344
N2	0.169148	0.188006	0.29068	0.366939	0.196476	0.188409	0.402918	0.384807	0.194577	0.226167	0.600774	0.688877
N3	0.17911	0.183873	0.485122	0.339883	0.163524	0.159843	0.333788	0.279458	0.175575	0.170088	0.441392	0.392549
AVG	**0.171528**	**0.191513**	**0.329773**	**0.312585**	**0.171911**	**0.175629**	**0.324033**	**0.309806**	**0.178377**	**0.199363**	**0.520671**	**0.536257**

	KP13			
	-	EG	B	B + EG
N1	0.159497	0.170794	0.199333	0.258026
N2	0.183735	0.173402	0.325865	0.356199
N3	0.152566	0.176113	0.433125	0.373781
AVG	**0.165266**	**0.173436**	**0.319441**	**0.329336**

Table A10: OD_{570} values of the biofilm formed by ESBL *K. pneumoniae* isolates with and without eugenol (EG). The OD_{570} values are represented as means of triplicate assays (n=3). -: Negative control, B: Bacteria, B+EG: Bacteria and eugenol, AVG: Average.

	KP14				KP15				KP16			
	-	EG	B	B + EG	-	EG	B	B + EG	-	EG	B	B + EG
N1	0.178903	0.188962	0.416582	0.37966	0.200054	0.209009	0.436735	0.461931	0.138294	0.191001	0.184927	0.197484
N2	0.182678	0.23337	0.342489	0.365581	0.198119	0.193886	0.36915	0.280506	0.165748	0.16736	0.311258	0.289798
N3	0.204169	0.201044	0.526008	0.367007	0.209219	0.242475	0.341888	0.306022	0.169493	0.16799	0.260927	0.284595
AVG	**0.188583**	**0.207792**	**0.42836**	**0.370749**	**0.202464**	**0.215123**	**0.382591**	**0.349486**	**0.157845**	**0.17545**	**0.252371**	**0.257292**

	KP17				KP18				KP19			
	-	EG	B	B + EG	-	EG	B	B + EG	-	EG	B	B + EG
N1	0.178594	0.177769	0.593919	0.504049	0.195535	0.196031	0.233131	0.225892	0.114332	0.171274	0.284427	0.215416
N2	0.194445	0.172137	0.731649	0.610633	0.20881	0.215133	0.262893	0.306207	0.154629	0.147773	0.316639	0.336435
N3	0.191688	0.181375	0.436661	0.440159	0.18451	0.202002	0.24508	0.236582	0.192949	0.176325	0.239447	0.317725
AVG	**0.188242**	**0.177094**	**0.58741**	**0.51828**	**0.196285**	**0.204388**	**0.247035**	**0.256227**	**0.15397**	**0.165124**	**0.280171**	**0.289859**

	KP20				KP21				KP22			
	-	EG	B	B + EG	-	EG	B	B + EG	-	EG	B	B + EG
N1	0.144246	0.150634	0.534944	0.448819	0.171055	0.179521	0.380356	0.252919	0.167255	0.176835	0.23882	0.236611
N2	0.154334	0.166479	0.442041	0.40633	0.169014	0.178332	0.4459	0.45433	0.16831	0.153816	0.249939	0.27505
N3	0.206596	0.204769	0.686989	0.591074	0.207394	0.201164	0.277148	0.26133	0.123767	0.18723	0.220894	0.226323
AVG	**0.168392**	**0.173961**	**0.554658**	**0.482075**	**0.182488**	**0.186339**	**0.367801**	**0.32286**	**0.153111**	**0.172627**	**0.236551**	**0.245995**

	KP23				KP24				KP25			
	-	EG	B	B + EG	-	EG	B	B + EG	-	EG	B	B + EG
N1	0.163251	0.181738	0.373793	0.357303	0.180041	0.221723	0.350288	0.51813	0.182161	0.166116	0.310345	0.292754
N2	0.166322	0.166225	0.368599	0.35912	0.159101	0.225477	0.380193	0.341537	0.131824	0.147931	0.385953	0.36924
N3	0.168453	0.195672	0.468255	0.391526	0.188885	0.200025	0.381831	0.407681	0.168925	0.174639	0.387065	0.431715
AVG	**0.166009**	**0.181212**	**0.403549**	**0.369316**	**0.176009**	**0.215741**	**0.37077**	**0.422449**	**0.16097**	**0.162895**	**0.361121**	**0.36457**

	KP26			
	-	EG	B	B + EG
N1	0.20691	0.217692	0.323607	0.302989
N2	0.145615	0.161717	0.300701	0.268147
N3	0.16239	0.189371	0.297409	0.322349
AVG	**0.171638**	**0.189593**	**0.307239**	**0.297828**

Table A11: OD_{570} values of the biofilm formed by non-ESBL *K. pneumoniae* isolates with and without thymol (TH). The OD_{570} values are represented as means of triplicate assays (n=3). -: Negative control, B: Bacteria, B+TH: Bacteria and thymol, AVG: Average.

	KP1				KP2				KP3			
	-	TH	B	B + TH	-	TH	B	B + TH	-	TH	B	B + TH
N1	0.159571	0.162884	0.203774	0.247476	0.156697	0.192406	0.316737	0.353089	0.180734	0.184772	0.295417	0.293947
N2	0.159192	0.156821	0.245426	0.251698	0.157521	0.186684	0.314662	0.377356	0.159023	0.167543	0.242822	0.235425
N3	0.174857	0.19435	0.33002	0.283229	0.191905	0.239269	0.473933	0.433366	0.225083	0.220027	0.552389	0.298468
AVG	**0.16454**	**0.171352**	**0.25974**	**0.260801**	**0.168707**	**0.20612**	**0.368444**	**0.387937**	**0.18828**	**0.190781**	**0.363543**	**0.275947**

	KP4				KP5				KP6			
	-	TH	B	B + TH	-	TH	B	B + TH	-	TH	B	B + TH
N1	0.165543	0.191306	0.49206	0.48425	0.155089	0.169607	0.299007	0.356086	0.19214	0.19227	0.332428	0.339158
N2	0.144886	0.155334	0.349352	0.350619	0.145712	0.199667	0.255577	0.255777	0.182235	0.18243	0.313786	0.309996
N3	0.183049	0.173432	0.415623	0.406568	0.194988	0.219245	0.385427	0.29657	0.220158	0.23218	0.515315	0.42633
AVG	**0.164493**	**0.173357**	**0.419011**	**0.413812**	**0.165263**	**0.196173**	**0.313337**	**0.302811**	**0.198178**	**0.202293**	**0.387176**	**0.358495**

	KP7				KP8				KP9			
	-	TH	B	B + TH	-	TH	B	B + TH	-	TH	B	B + TH
N1	0.168772	0.17143	0.260813	0.341594	0.156892	0.190079	0.323706	0.325068	0.168053	0.190926	0.506821	0.490739
N2	0.154502	0.158256	0.243034	0.218042	0.143775	0.201318	0.366361	0.313025	0.174471	0.187862	0.342143	0.333824
N3	0.162834	0.169987	0.353027	0.39888	0.20007	0.223168	0.544359	0.504133	0.219852	0.22296	0.630552	0.524378
AVG	**0.162036**	**0.166558**	**0.285625**	**0.319505**	**0.166912**	**0.204855**	**0.411475**	**0.380742**	**0.187458**	**0.200583**	**0.493172**	**0.449647**

	KP10				KP11				KP12			
	-	TH	B	B + TH	-	TH	B	B + TH	-	TH	B	B + TH
N1	0.157335	0.19566	0.222567	0.349764	0.180577	0.191303	0.302957	0.312768	0.230196	0.212659	0.48495	0.553977
N2	0.193211	0.178511	0.481141	0.426718	0.190486	0.223598	0.572241	0.464727	0.226885	0.221636	0.678438	0.74335
N3	0.154658	0.161224	0.363988	0.41617	0.173453	0.20114	0.48087	0.345453	0.213104	0.225579	0.577156	0.398234
AVG	**0.168401**	**0.178465**	**0.355899**	**0.397551**	**0.181505**	**0.205347**	**0.452022**	**0.374316**	**0.223395**	**0.219958**	**0.580182**	**0.565187**

	KP13			
	-	TH	B	B + TH
N1	0.110418	0.12849	0.193786	0.246421
N2	0.153788	0.155482	0.240477	0.2667
N3	0.19886	0.207389	0.323752	0.378141
AVG	**0.154356**	**0.163787**	**0.252671**	**0.297087**

Table A12: OD_{570} values of the biofilm formed by ESBL *K. pneumoniae* isolates with and without thymol (TH). The OD_{570} values are represented as means of triplicate assays (n=3). -: Negative control, B: Bacteria, B+TH: Bacteria and thymol, AVG: Average.

	KP14				KP15				KP16			
	-	TH	B	B + TH	-	TH	B	B + TH	-	TH	B	B + TH
N1	0.137193	0.174805	0.439545	0.418898	0.187124	0.175783	0.402644	0.411717	0.150437	0.153805	0.224847	0.249589
N2	0.202603	0.234416	0.282494	0.314658	0.180027	0.219938	0.361525	0.357515	0.168362	0.158879	0.188349	0.170991
N3	0.158283	0.222157	0.380743	0.375423	0.217401	0.227831	0.340891	0.326856	0.155782	0.162505	0.293086	0.286329
AVG	**0.166026**	**0.210459**	**0.367594**	**0.36966**	**0.194851**	**0.207851**	**0.368353**	**0.365362**	**0.158194**	**0.158396**	**0.235427**	**0.235636**

	KP17				KP18				KP19			
	-	TH	B	B + TH	-	TH	B	B + TH	-	TH	B	B + TH
N1	0.143265	0.163734	0.480044	0.437779	0.168015	0.185982	0.222332	0.238899	0.144775	0.176976	0.421695	0.32899
N2	0.176218	0.190268	0.545017	0.502319	0.183113	0.216446	0.262369	0.230451	0.155588	0.156341	0.260408	0.299004
N3	0.186699	0.212126	0.555563	0.477242	0.207787	0.226329	0.273262	0.24672	0.138555	0.155839	0.260317	0.269674
AVG	**0.168727**	**0.188709**	**0.526874**	**0.472447**	**0.186305**	**0.209586**	**0.252655**	**0.23869**	**0.146306**	**0.163052**	**0.31414**	**0.299223**

	KP20				KP21				KP22			
	-	TH	B	B + TH	-	TH	B	B + TH	-	TH	B	B + TH
N1	0.2277	0.203987	0.464124	0.522606	0.173126	0.214694	0.266089	0.325612	0.158511	0.179486	0.236451	0.301365
N2	0.16409	0.209638	0.586403	0.485697	0.190722	0.19984	0.570434	0.529864	0.157956	0.176258	0.250109	0.271929
N3	0.167458	0.197299	0.551358	0.567851	0.199785	0.22454	0.40757	0.372344	0.191466	0.222322	0.282928	0.303251
AVG	**0.186416**	**0.203641**	**0.533961**	**0.525385**	**0.187878**	**0.213025**	**0.414698**	**0.409273**	**0.169311**	**0.192689**	**0.256496**	**0.292182**

	KP23				KP24				KP25			
	-	TH	B	B + TH	-	TH	B	B + TH	-	TH	B	B + TH
N1	0.174432	0.181498	0.301341	0.405253	0.180809	0.214374	0.448935	0.445954	0.15077	0.159546	0.196022	0.202492
N2	0.195283	0.235226	0.39862	0.422857	0.200802	0.215153	0.392928	0.468719	0.133304	0.146647	0.248647	0.253917
N3	0.208553	0.221034	0.639116	0.568398	0.209218	0.207512	0.668074	0.662174	0.193878	0.202143	0.350327	0.367302
AVG	**0.192756**	**0.212586**	**0.446359**	**0.465503**	**0.196943**	**0.212346**	**0.503312**	**0.525615**	**0.159317**	**0.169445**	**0.264999**	**0.27457**

	KP26			
	-	TH	B	B + TH
N1	0.167794	0.189563	0.274505	0.310869
N2	0.15356	0.174134	0.248485	0.251277
N3	0.204216	0.218293	0.393654	0.40554
AVG	**0.17519**	**0.193997**	**0.305548**	**0.322562**

Table A13: OD_{570} values of the biofilm formed by non-ESBL *K. pneumoniae* isolates with and without carvacrol (CR). The OD_{570} values are represented as means of triplicate assays (n=3). -: Negative control, B: Bacteria, B+CR: Bacteria and carvacrol, AVG: Average.

	KP1				KP2				KP3			
	-	CR	B	B + CR	-	CR	B	B + CR	-	CR	B	B + CR
N1	0.187011	0.186962	0.201747	0.291661	0.181673	0.18586	0.24394	0.297925	0.1748	0.184971	0.336534	0.256748
N2	0.185633	0.1893	0.213608	0.336793	0.191652	0.192488	0.737216	0.545383	0.185883	0.197728	0.405532	0.430703
N3	0.17592	0.182059	0.207476	0.29107	0.172443	0.181968	0.440537	0.328439	0.179441	0.186972	0.374045	0.391658
AVG	**0.182854**	**0.186107**	**0.20761**	**0.306508**	**0.181923**	**0.186772**	**0.473897**	**0.390582**	**0.180041**	**0.18989**	**0.372037**	**0.359703**

	KP4				KP5				KP6			
	-	CR	B	B + CR	-	CR	B	B + CR	-	CR	B	B + CR
N1	0.181555	0.198767	0.437609	0.449774	0.179581	0.183572	0.265003	0.310193	0.18886	0.188864	0.272853	0.311194
N2	0.185096	0.187575	0.328239	0.389749	0.183587	0.18542	0.366321	0.3625	0.187756	0.187491	0.349033	0.294788
N3	0.182452	0.183409	0.400583	0.432566	0.185624	0.18543	0.381702	0.275505	0.183772	0.192232	0.226148	0.276194
AVG	**0.183034**	**0.189917**	**0.38881**	**0.424029**	**0.182931**	**0.184807**	**0.337675**	**0.316066**	**0.186796**	**0.189529**	**0.282678**	**0.294058**

	KP7				KP8				KP9			
	-	CR	B	B + CR	-	CR	B	B + CR	-	CR	B	B + CR
N1	0.185268	0.196742	0.228551	0.31929	0.180407	0.197654	0.316783	0.335511	0.179087	0.19415	0.273746	0.310154
N2	0.180865	0.18019	0.261732	0.257109	0.180953	0.182727	0.410497	0.380243	0.181826	0.181903	0.441788	0.396837
N3	0.181672	0.18486	0.192164	0.191189	0.183165	0.186943	0.445225	0.348879	0.181658	0.185758	0.25249	0.278776
AVG	**0.182602**	**0.187264**	**0.227482**	**0.255863**	**0.181509**	**0.189108**	**0.390835**	**0.354878**	**0.180857**	**0.18727**	**0.322675**	**0.328589**

	KP10				KP11				KP12			
	-	CR	B	B + CR	-	CR	B	B + CR	-	CR	B	B + CR
N1	0.18994	0.193397	0.317647	0.401473	0.182728	0.19876	0.324234	0.362884	0.182398	0.198754	0.679445	0.600174
N2	0.180226	0.192018	0.461671	0.411906	0.182454	0.203929	0.52931	0.429542	0.186877	0.191063	0.616198	0.741746
N3	0.181074	0.18942	0.400803	0.401943	0.180351	0.181245	0.47091	0.362554	0.180401	0.186788	0.30402	0.380356
AVG	**0.183747**	**0.191612**	**0.393373**	**0.405107**	**0.181844**	**0.194645**	**0.441485**	**0.384994**	**0.183225**	**0.192202**	**0.533221**	**0.574092**

	KP13			
	-	CR	B	B + CR
N1	0.181067	0.183553	0.162178	0.285567
N2	0.182213	0.19882	0.245125	0.226281
N3	0.183506	0.190425	0.279131	0.303185
AVG	**0.182262**	**0.190933**	**0.228811**	**0.271678**

Table A14: OD_{570} values of the biofilm formed by ESBL *K. pneumoniae* isolates with and without carvacrol (CR). The OD_{570} values are represented as means of triplicate assays (n=3). -: Negative control, B: Bacteria, B+CR: Bacteria and carvacrol, AVG: Average.

	K14				K15				K16			
	-	CR	B	B + CR	-	CR	B	B + CR	-	CR	B	B + CR
N1	0.180489	0.188185	0.3195	0.36286	0.184902	0.182732	0.470584	0.415901	0.184985	0.187673	0.191974	0.23404
N2	0.188535	0.197336	0.40357	0.377449	0.184109	0.187922	0.218093	0.242506	0.180038	0.184669	0.270735	0.230186
N3	0.182222	0.189333	0.524945	0.336284	0.181481	0.188929	0.310763	0.283359	0.18123	0.18726	0.237516	0.276951
AVG	**0.183749**	**0.191618**	**0.416005**	**0.358864**	**0.183497**	**0.186528**	**0.333147**	**0.313922**	**0.182084**	**0.186534**	**0.233408**	**0.247059**

	K17				K18				K19			
	-	CR	B	B + CR	-	CR	B	B + CR	-	CR	B	B + CR
N1	0.185951	0.188074	0.383159	0.408657	0.179575	0.185121	0.192163	0.21738	0.186917	0.19847	0.320527	0.311332
N2	0.186582	0.185322	0.509988	0.485629	0.185548	0.180803	0.175325	0.217024	0.184435	0.188121	0.25214	0.238359
N3	0.181242	0.186447	0.39055	0.384488	0.180802	0.188002	0.239326	0.217939	0.181417	0.187976	0.242102	0.233791
AVG	**0.184592**	**0.186614**	**0.427899**	**0.426258**	**0.181975**	**0.184642**	**0.202271**	**0.217448**	**0.184256**	**0.191522**	**0.27159**	**0.261161**

	K20				K21				K22			
	-	CR	B	B + CR	-	CR	B	B + CR	-	CR	B	B + CR
N1	0.192064	0.204247	0.467321	0.440922	0.182171	0.180997	0.379628	0.379462	0.17956	0.184395	0.222879	0.256131
N2	0.187178	0.188971	0.488866	0.45298	0.183901	0.187757	0.530164	0.533876	0.216044	0.220894	0.272078	0.287501
N3	0.18271	0.185221	0.592912	0.465646	0.181165	0.186168	0.33231	0.322468	0.181808	0.183535	0.233188	0.241035
AVG	**0.187317**	**0.192813**	**0.516366**	**0.453183**	**0.182412**	**0.184974**	**0.414034**	**0.411935**	**0.192471**	**0.196274**	**0.242715**	**0.261556**

	K23				K24				K25			
	-	CR	B	B + CR	-	CR	B	B + CR	-	CR	B	B + CR
N1	0.1831	0.18711	0.309608	0.36072	0.183799	0.182804	0.304464	0.282937	0.181147	0.187564	0.259282	0.278608
N2	0.202584	0.245168	0.489433	0.353105	0.187539	0.185337	0.489474	0.470762	0.181357	0.183641	0.371981	0.315288
N3	0.181255	0.189804	0.488513	0.310478	0.188732	0.18788	0.444034	0.437002	0.179413	0.187377	0.270148	0.377381
AVG	**0.18898**	**0.207361**	**0.429184**	**0.341434**	**0.18669**	**0.18534**	**0.412657**	**0.3969**	**0.180639**	**0.186194**	**0.30047**	**0.323759**

	K26			
	-	CR	B	B + CR
N1	0.184774	0.189929	0.365463	0.351725
N2	0.179691	0.189229	0.417158	0.38898
N3	0.180775	0.187067	0.343472	0.308027
AVG	**0.181746**	**0.188742**	**0.375364**	**0.349578**

Table A15: OD_{570} values of the biofilm formed by non-ESBL *K. pneumoniae* isolates with and without cinnamaldehyde and eugenol mixture (CA&EG). The OD_{570} values are represented as means of triplicate assays (n=3). -: Negative control, B: Bacteria, B + CA&EG: Bacteria and cinnamaldehyde + eugenol mixture, AVG: Average.

	KP1				KP2				KP3			
	-	CA&EG	B	B + CA&EG	-	CA&EG	B	B + CA&EG	-	CA&EG	B	B + CA&EG
N1	0.195184	0.182312	0.215892	0.227538875	0.192509	0.192833	0.390582	0.4256382	0.18227	0.205286	0.317276	0.26975075
N2	0.183937	0.19476	0.270851	0.25233475	0.192842	0.20607	0.323052	0.2760255	0.205342	0.207819	0.234262	0.280700875
N3	0.161651	0.158455	0.381424	0.342467333	0.165837	0.172184	0.279967	0.2758085	0.187455	0.199671	0.387415	0.31569
AVG	**0.180258**	**0.178509**	**0.289389**	**0.274113653**	**0.183729**	**0.190362**	**0.3312**	**0.325824067**	**0.191689**	**0.204259**	**0.312984**	**0.288713875**

	KP4				KP5				KP6			
	-	CA&EG	B	B + CA&EG	-	CA&EG	B	B + CA&EG	-	CA&EG	B	B + CA&EG
N1	0.183623	0.216065	0.469848	0.48662025	0.193205	0.208716	0.383821	0.37358425	0.210771	0.20859	0.342782	0.352332286
N2	0.166929	0.182181	0.520312	0.490353125	0.190685	0.205844	0.413406	0.317285125	0.189632	0.197694	0.393267	0.3753
N3	0.146842	0.154384	0.553338	0.5476935	0.160394	0.159229	0.269138	0.234010625	0.17527	0.207247	0.411856	0.346877
AVG	**0.165798**	**0.18421**	**0.5145**	**0.508222292**	**0.181428**	**0.191263**	**0.355455**	**0.308293333**	**0.191891**	**0.20451**	**0.382635**	**0.358169762**

	KP7				KP8				KP9			
	-	CA&EG	B	B + CA&EG	-	CA&EG	B	B + CA&EG	-	CA&EG	B	B + CA&EG
N1	0.15185	0.15115	0.233614	0.277959375	0.155765	0.172686	0.443278	0.424194875	0.200998	0.227064	0.354305	0.363529429
N2	0.171139	0.177899	0.264771	0.28848125	0.190026	0.202985	0.556788	0.529386714	0.198367	0.19096	0.471532	0.463099667
N3	0.173103	0.185211	0.266325	0.2686735	0.19282	0.202074	0.490104	0.448368625	0.192365	0.205141	0.519605	0.483253625
AVG	**0.165364**	**0.17142**	**0.254903**	**0.278371375**	**0.179537**	**0.192582**	**0.496723**	**0.467316738**	**0.197243**	**0.207722**	**0.448481**	**0.436627573**

	KP10				KP11				KP12			
	-	CA&EG	B	B + CA&EG	-	CA&EG	B	B + CA&EG	-	CA&EG	B	B + CA&EG
N1	0.142444	0.145148	0.366303	0.3478895	0.160118	0.169564	0.235736	0.2251915	0.147569	0.154548	0.287213	0.285153714
N2	0.169463	0.208587	0.336458	0.3649195	0.200665	0.207712	0.298546	0.317053833	0.203517	0.204816	0.407134	0.366203333
N3	0.16854	0.169296	0.327086	0.286821571	0.171874	0.185654	0.301613	0.299413375	0.195069	0.19859	0.404651	0.39361975
AVG	**0.160149**	**0.174343**	**0.343283**	**0.33321019**	**0.177552**	**0.187643**	**0.278632**	**0.280552903**	**0.182051**	**0.185985**	**0.366333**	**0.348325599**

	KP13			
	-	CA&EG	B	B + CA&EG
N1	0.165154	0.168077	0.220483	0.218732375
N2	0.145836	0.162033	0.295316	0.290397143
N3	0.163369	0.165379	0.293401	0.259315
AVG	**0.158119**	**0.165163**	**0.269733**	**0.256148173**

Table A16: OD_{570} values of the biofilm formed by ESBL *K. pneumoniae* isolates with and without cinnamaldehyde and eugenol mixture (CA&EG). The OD_{570} values are represented as means of triplicate assays (n=3). -: Negative control, B: Bacteria, B + CA&EG: Bacteria and cinnamaldehyde + eugenol mixture, AVG: Average.

	KP14				KP15				KP16			
	-	CA&EG	B	B + CA&EG	-	CA&EG	B	B + CA&EG	-	CA&EG	B	B + CA&EG
N1	0.208973	0.189776	0.32536	0.272792875	0.187397	0.208077	0.310202	0.33192	0.204438	0.200089	0.368649	0.391883143
N2	0.160208	0.186722	0.3695	0.294625286	0.167083	0.168017	0.297789	0.2912225	0.201716	0.194985	0.318583	0.322274286
N3	0.166603	0.189203	0.259494	0.328604167	0.20936	0.202857	0.267255	0.256263	0.154105	0.184242	0.309788	0.32730425
AVG	**0.178595**	**0.188567**	**0.318118**	**0.298674109**	**0.187946**	**0.192984**	**0.291749**	**0.293135167**	**0.186753**	**0.193105**	**0.33234**	**0.347153893**

	KP17				KP18				KP19			
	-	CA&EG	B	B + CA&EG	-	CA&EG	B	B + CA&EG	-	CA&EG	B	B + CA&EG
N1	0.173309	0.150673	0.434056	0.4275265	0.171707	0.184275	0.249016	0.245609	0.189992	0.19279	0.435446	0.351624429
N2	0.19281	0.180563	0.59712	0.716668333	0.178719	0.195936	0.242485	0.306465125	0.192146	0.17662	0.28878	0.290055
N3	0.184258	0.182257	0.516856	0.489297143	0.153068	0.177321	0.213289	0.232663	0.178779	0.196572	0.285733	0.316720286
AVG	**0.183459**	**0.171164**	**0.516011**	**0.544497325**	**0.167831**	**0.185844**	**0.23493**	**0.261579042**	**0.186972**	**0.188661**	**0.336653**	**0.319466571**

	KP20				KP21				KP22			
	-	CA&EG	B	B + CA&EG	-	CA&EG	B	B + CA&EG	-	CA&EG	B	B + CA&EG
N1	0.133802	0.146827	0.453138	0.430941714	0.197122	0.197985	0.244161	0.281531375	0.151409	0.16734	0.274819	0.22326925
N2	0.18001	0.193664	0.474141	0.461936875	0.187147	0.202265	0.246106	0.279227875	0.185469	0.196088	0.275251	0.286925875
N3	0.161184	0.153213	0.360908	0.39862525	0.163273	0.158436	0.306942	0.287224875	0.191916	0.198663	0.253292	0.237758375
AVG	**0.158332**	**0.164568**	**0.429396**	**0.43050128**	**0.182514**	**0.186229**	**0.265736**	**0.282661375**	**0.176264**	**0.187363**	**0.267787**	**0.249317833**

	KP23				KP24				KP25			
	-	CA&EG	B	B + CA&EG	-	CA&EG	B	B + CA&EG	-	CA&EG	B	B + CA&EG
N1	0.179394	0.182079	0.392665	0.3947225	0.201512	0.204221	0.391549	0.325049875	0.156745	0.16292	0.319708	0.28045925
N2	0.160739	0.161332	0.524254	0.570771	0.160222	0.189722	0.456404	0.606794667	0.197481	0.199409	0.353861	0.330124375
N3	0.197602	0.198699	0.370282	0.42465025	0.198239	0.208738	0.31739	0.287514714	0.178425	0.209004	0.274003	0.332643
AVG	**0.179245**	**0.180704**	**0.429067**	**0.46338125**	**0.186658**	**0.200894**	**0.388448**	**0.406453085**	**0.17755**	**0.190444**	**0.315857**	**0.314408875**

	KP26			
	-	CA&EG	B	B + CA&EG
N1	0.154876	0.169205	0.281307	0.271984375
N2	0.192764	0.191943	0.314307	0.416430429
N3	0.207597	0.20982	0.316367	0.446378125
AVG	**0.185079**	**0.190322**	**0.303994**	**0.37826431**

Table A17: OD_{570} values of the biofilm formed by non-ESBL *K. pneumoniae* isolates with and without thymol and carvacrol mixture (TH&CR). The OD_{570} values are represented as means of triplicate assays (n=3). -: Negative control, B: Bacteria, B + TH&CR: Bacteria and thymol + carvacrol mixture, AVG: Average.

	KP1				KP2				KP3			
	-	TH&CR	B	B + TH&CR	-	TH&CR	B	B + TH&CR	-	TH&CR	B	B + TH&CR
N1	0.182725	0.185785	0.191985	0.247424875	0.199797	0.224558	0.415053	0.3668716	0.198878	0.221268	0.367278	0.296854429
N2	0.19154	0.187354	0.293634	0.404007667	0.183324	0.188607	0.376841	0.33391075	0.18231	0.181909	0.556214	0.403981
N3	0.190338	0.199724	0.271711	0.411032143	0.191055	0.194625	0.327112	0.260127	0.19216	0.206619	0.47974	0.4754142
AVG	**0.188201**	**0.190954**	**0.252443**	**0.354154895**	**0.191392**	**0.202597**	**0.373002**	**0.320303117**	**0.191116**	**0.203266**	**0.467744**	**0.39208321**

	KP4				KP5				KP6			
	-	TH&CR	B	B + TH&CR	-	TH&CR	B	B + TH&CR	-	TH&CR	B	B + TH&CR
N1	0.200692	0.179279	0.380355	0.43252175	0.21448	0.227144	0.395589	0.410075625	0.213604	0.226561	0.398565	0.352585286
N2	0.208665	0.191081	0.488521	0.431293375	0.182463	0.18609	0.661878	0.460430857	0.180477	0.196352	0.608448	0.5559175
N3	0.199327	0.215231	0.415439	0.34463825	0.201321	0.21607	0.298475	0.27332175	0.19823	0.20018	0.318855	0.256449375
AVG	**0.202895**	**0.195197**	**0.428105**	**0.402817792**	**0.199421**	**0.209768**	**0.451981**	**0.381276077**	**0.197437**	**0.207698**	**0.441956**	**0.388317387**

	KP7				KP8				KP9			
	-	TH&CR	B	B + TH&CR	-	TH&CR	B	B + TH&CR	-	TH&CR	B	B + TH&CR
N1	0.190681	0.188142	0.252322	0.283280625	0.191584	0.216227	0.35872	0.3292995	0.204344	0.225318	0.370498	0.36466725
N2	0.209541	0.212875	0.407994	0.319823286	0.208434	0.218725	0.445556	0.507022571	0.197642	0.196069	0.483223	0.409061857
N3	0.204445	0.209725	0.366738	0.337054875	0.200951	0.208798	0.469732	0.432599625	0.209728	0.21859	0.438983	0.395003857
AVG	**0.201556**	**0.203581**	**0.342351**	**0.313386262**	**0.200323**	**0.214583**	**0.424669**	**0.422973899**	**0.203905**	**0.213325**	**0.430901**	**0.389577655**

	KP10				KP11				KP12			
	-	TH&CR	B	B + TH&CR	-	TH&CR	B	B + TH&CR	-	TH&CR	B	B + TH&CR
N1	0.193953	0.191331	0.25016	0.266678875	0.188388	0.199746	0.255385	0.258288	0.19013	0.202867	0.25137	0.268055
N2	0.18822	0.188095	0.333806	0.322670625	0.189514	0.188113	0.407647	0.372630286	0.180498	0.184458	0.628362	0.467819375
N3	0.191335	0.19462	0.322606	0.289212333	0.194532	0.205285	0.28825	0.2981985	0.202481	0.206943	0.478857	0.457157
AVG	**0.191169**	**0.191348**	**0.302191**	**0.292853944**	**0.190811**	**0.197715**	**0.317094**	**0.309705595**	**0.191036**	**0.198089**	**0.452863**	**0.397677125**

	KP13			
	-	Thy+Car	Bacteria	T+C&Bct
N1	0.191457	0.190982	0.214858	0.22610975
N2	0.210458	0.213966	0.275001	0.293958875
N3	0.20554	0.205254	0.251695	0.276223
AVG	**0.202485**	**0.2034**	**0.247184**	**0.265430542**

Table A18: OD_{570} values of the biofilm formed by ESBL *K. pneumoniae* isolates with and without thymol and carvacrol mixture (TH&CR). The OD_{570} values are represented as means of triplicate assays (n=3). -: Negative control, B: Bacteria, B + TH&CR: Bacteria and thymol + carvacrol mixture, AVG: Average.

	KP14				KP15				KP16			
	-	TH&CR	B	B + TH&CR	-	TH&CR	B	B + TH&CR	-	TH&CR	B	B + TH&CR
N1	0.188472	0.176595	0.237604	0.279369125	0.163696	0.193824	0.284575	0.33206075	0.211327	0.202051	0.322744	0.238997
N2	0.197216	0.205896	0.273781	0.240734333	0.199788	0.197209	0.30178	0.261480125	0.200624	0.201854	0.271971	0.40422575
N3	0.203557	0.209692	0.292065	0.305671167	0.209314	0.209797	0.295525	0.36864425	0.199474	0.209494	0.356881	0.366743833
AVG	**0.196415**	**0.197394**	**0.267817**	**0.275258208**	**0.190933**	**0.200277**	**0.29396**	**0.320728375**	**0.203809**	**0.204466**	**0.317199**	**0.336655528**

	KP17				KP18				KP19			
	-	TH&CR	B	B + TH&CR	-	TH&CR	B	B + TH&CR	-	TH&CR	B	B + TH&CR
N1	0.179267	0.17272	0.396996	0.414971	0.175874	0.179191	0.214692	0.252312	0.17305	0.194944	0.315519	0.32285125
N2	0.206354	0.218803	0.61314	0.566495714	0.228608	0.208913	0.236659	0.22105625	0.187283	0.196057	0.310013	0.25507375
N3	0.203955	0.215864	0.5879	0.548333625	0.1962	0.210217	0.407552	0.445761286	0.192832	0.193713	0.242611	0.258010375
AVG	**0.196525**	**0.202462**	**0.532679**	**0.509933446**	**0.200227**	**0.19944**	**0.286301**	**0.306376512**	**0.184388**	**0.194904**	**0.289381**	**0.278645125**

	KP20				KP21				KP22			
	-	TH&CR	B	B + TH&CR	-	TH&CR	B	B + TH&CR	-	TH&CR	B	B + TH&CR
N1	0.17979	0.183308	0.332599	0.416191714	0.181948	0.188977	0.40462	0.319809375	0.177173	0.184839	0.20042	0.241456375
N2	0.194451	0.207486	0.475171	0.46191775	0.19126	0.203768	0.476193	0.312237625	0.187916	0.189228	0.287057	0.284117429
N3	0.199226	0.199567	0.453035	0.436921375	0.189358	0.219324	0.316192	0.39153825	0.194467	0.204693	0.27462	0.28150175
AVG	**0.191156**	**0.196787**	**0.420268**	**0.438343613**	**0.187522**	**0.204023**	**0.399002**	**0.341195083**	**0.186519**	**0.19292**	**0.254032**	**0.269025185**

	KP23				KP24				KP25			
	-	TH&CR	B	B + TH&CR	-	TH&CR	B	B + TH&CR	-	TH&CR	B	B + TH&CR
N1	0.178164	0.169844	0.294053	0.256439857	0.18155	0.183295	0.346911	0.346579	0.182427	0.185405	0.294318	0.31069175
N2	0.180497	0.180051	0.440238	0.33068375	0.194552	0.188685	0.50506	0.455339857	0.190055	0.196358	0.408106	0.471895
N3	0.208402	0.209135	0.394666	0.309516375	0.20643	0.205572	0.548645	0.450407333	0.193014	0.205559	0.350079	0.320921125
AVG	**0.189021**	**0.186343**	**0.376319**	**0.298879994**	**0.194177**	**0.192517**	**0.466872**	**0.417442063**	**0.188499**	**0.195774**	**0.350834**	**0.367835958**

	KP26			
	-	TH&CR	B	B + TH&CR
N1	0.186749	0.213854	0.331942	0.340202875
N2	0.204756	0.215415	0.414922	0.35906875
N3	0.205575	0.207682	0.287225	0.3695065
AVG	**0.199026**	**0.212317**	**0.344696**	**0.356259375**